



Universität für Bodenkultur Wien

# Influence of Surface Curvature on Unfolding of Proteins on Nanoparticles

**Dissertation zur Erlangung des Doktorgrades an der  
Universität für Bodenkultur Wien**

**Department für Biotechnologie**

**Institut für angewandte Mikrobiologie (IAM)**

Vorstand: Florian Rümer, Ao.Univ.Prof. Dipl.-Ing. Dr.nat.techn.

Betreuer: Alois Jungbauer, Ao.Univ.Prof. Dipl.-Ing. Dr.nat.techn.

Eingereicht von **Peter Satzer, Dipl.-Ing.**

Wien, Oktober 2015

# Danksagung

Während meiner Arbeit genoss ich die Unterstützung meiner Arbeitsgruppe, und ich möchte jedem von ihnen danken, für viele fruchtbare Diskussionen, für fröhliche Abende, für die Unterstützung bei Problemen und die Unterstützung in jeder Phase dieser Arbeit. Ich habe in dieser Arbeitsgruppe nicht nur gute Arbeitskollegen und ein angenehmes Arbeitsklima gefunden, sondern auch viele neue Freunde.

Besonders möchte ich mich bei Prof. Alois Jungbauer für seine Unterstützung bedanken, ohne ihn wäre diese Arbeit nicht zustande gekommen und ich bedanke mich für die wissenschaftliche Hilfestellung und für das angenehme Arbeitsklima. Bedanken möchte ich mich auch bei Prof. Paul Messner für seine bereitwillige Hilfe und sein Interesse an der Arbeit sowie bei Dr. Frantisek Svec für wissenschaftliche Diskussionen, Hilfe beim Verfassen von Publikationen und die Chance in Berkeley sechs Monate wissenschaftlich zu arbeiten.

Bedanken möchte ich mich auch bei meiner Freundin Claudia, die mich auch wenn es nicht immer leicht war immer bei dieser Arbeit unterstützt hat, viele Diskussionen durchgestanden hat, und doch nie den Glauben an mich verloren hat. Dank gilt auch meinem Bruder Manfred und seiner Frau Daniela für ihre Unterstützung und ihrer Tochter Sophia, die mit einem kindlichen Lächeln alle Sorgen wegzaubern kann.

Zu guter Letzt möchte ich meinen Eltern Erwin und Eva dafür danken, schon in jungen Jahren ein Interesse an der Wissenschaft gefördert zu haben, und für ihre Unterstützung während all meiner Lebenslagen. Sie haben diese Arbeit durch ihre Unterstützung vor, während und nach dem Studium erst möglich gemacht.

# Abstract

The future use of nanoparticle-protein conjugates requires new methods for purification of the complex as well as detailed understanding of the interaction of proteins and nanoparticles. In this doctoral work, a solution to the problem of purification of nanoparticle-protein conjugates from any other non-particular substance in solution was achieved by size exclusion chromatography. This approach was then transferred to a continuous operation mode by using a 4 zone closed loop simulated moving bed technique to achieve pilot scale productivities in the range of 0.25 g /h /L chromatography medium. This purification method was then used in combination with classical approaches like centrifugation and filtration to obtain samples for the investigation of the specific interaction of proteins and nanoparticles. Silica nanoparticles of sizes ranging from 30 nm to 1000 nm obtained by a commercial manufacturer were intensively characterized to get high quality data on the surface properties (zeta-potential and roughness) and particle properties (size, size distribution and porosity) of the nanoparticle material. Nine model proteins, selected to span a wide variety of different protein characteristics like size, charge and thermal stability, were investigated on how they interact with these particles. Structural changes in the conformation of these model proteins were monitored by circular dichroism and related to the particle size at which they occurred. Two model proteins (bovine serum albumin and myoglobin) showed structural changes, and both also showed nanoparticle size dependent structural changes. With small particle size (< 100 nm), the protein conformation remains unchanged while on larger particles (> 300nm) significant conformational changes occur. The range in which these structural changes occurred was the same for both proteins, in both cases the structural ordering of the proteins was reduced when interacting with large particles. In addition to the qualitative assessment of the interaction in regards to the particle size, also kinetics of this conformational changes were investigated. Myoglobin and BSA showed significantly different kinetics: While myoglobin immediately changes its conformation upon adsorption, albumin first adsorbs, and then slowly changes its conformation in a timeframe of hours.

While some cases of conformational changes of proteins were already reported in the literature, only the conclusive and extended dataset created in this study allowed to assess commonly used explanations for this phenomena. This study proofed that none of the explanations proposed in any literature till now is able to fit the data. Especially the commonly used explanation of a direct influence of the surface curvature on the structural changes of the proteins is not applicable for particles between 30 and 1000 nm while it may still be able to explain some phenomena for very small particles (below 20 nm).

# Zusammenfassung

Das Aufkommen von Nanopartikel-Konjugaten als Arznei hat dazu geführt, dass an Mess- und Aufreinigungsmethoden zusätzliche Anforderungen gestellt werden. Im Rahmen dieser Dissertation wurde eine solche Aufreinigungsmethode entwickelt, die dazu geeignet ist, Nanopartikel, die mit einem Arzneistoff beschichtet wurden in industriell relevanten Mengen aufzureinigen. Größenausschluss-Chromatographie wurde dazu in einem kontinuierlichen Modus mit der „Simulated Moving Bed“-Technologie verwendet und erreichte eine Produktivität von 0.25g / h / L Chromatographie-Material. Diese Methode ergänzt traditionelle Ansätze die auf Zentrifugation oder Filtration basieren um eine Methode die kontinuierlich und großtechnologisch eingesetzt werden kann.

Für die Untersuchung der Interaktion zwischen Proteinen und Nanopartikeln verwendeten wir 9 Modell-Proteine und Silikat-Nanopartikeln in den Größen 30-1000 nm. Die Charakterisierung der Nanopartikel mit dynamischer Lichtstreuung, Stickstoff-Adsorption und Elektronenmikroskopie zeigte, dass sie sehr homogen, glatt und nicht-porös waren und damit für unsere Zwecke geeignet waren. Von neun Modellproteinen zeigten zwei (BSA und Myoglobin) eine Konformationsänderung bei der Bindung an Nanopartikel, und in beiden Fällen war diese Konformationsänderung abhängig von der Größe der Nanopartikel: kleinere Nanopartikel (<100nm) führten zu keiner Konformationsänderung, während größere Nanopartikel (>300nm) zu signifikanter Änderung der Sekundärstruktur dieser zwei Modellproteine führte. Die Konformationsänderung bei beiden Proteinen fand bei ähnlicher Partikelgröße statt. Beide Proteine verloren wenn sie an größere Nanopartikel adsorbiert waren einen Teil ihrer Sekundärstruktur. Bei BSA führte die Bindung an Nanopartikel zu einer sehr langsamen Abnahme der alpha-Helix-Struktur des Proteins über Stunden, während bei Myoglobin die alpha-helikale Struktur sehr schnell nach der Adsorption an das Partikel abnahm.

Diese Daten, in Zusammenhang mit der Modellierung der gängigen Erklärungstheorien ermöglichte es uns zu zeigen dass diese Theorien nicht in der Lage sind dieses Phänomen zu erklären, es handelt sich also nicht wie oft behauptet um einen direkten Einfluss der Krümmung der Nanopartikel.

# Table of Contents

Danksagung .....	i
Abstract .....	ii
Zusammenfassung .....	iv
Introduction .....	1
Nanoparticles .....	1
Metal particles .....	2
Metal oxide nanoparticles .....	3
Organic nanoparticles .....	3
Silica nanoparticles .....	4
Protein corona .....	5
Protein conformational changes upon adsorption to nanomaterials .....	7
Objectives .....	14
Results and discussion .....	15
Methods for separation .....	15
Batch separation .....	15
Continuous separation .....	19
Protein structure determination .....	21
UV-VIS .....	21
ATR-FT-IR .....	22
NMR .....	23
CD .....	25
Small angle X-ray scattering (SAXS) .....	28
Conclusion .....	29
Lists .....	32
References .....	32
List of figures .....	38
Publications .....	40

# Introduction

## Nanoparticles

In the last two decades nanomaterials have emerged to be a major player in almost every scientific field. Although already described in the famous talk of Richard Feynman “There’s Plenty of Room at the Bottom” in 1959 it took almost 50 years for the idea to be developed for the use in the human body. Nowadays suppliers of nanoparticles are able to produce an enormous variety of different kinds of nanomaterials but we still do not understand much about the interaction of nanomaterials with living matter. Although we have known for years that certain nanomaterials, such as silver nanoparticles can be cytotoxic not only to bacteria, they are still used in cosmetics [1]. We still do not know what is going on the molecular level. This investigation on the molecular level was the scope of this work.

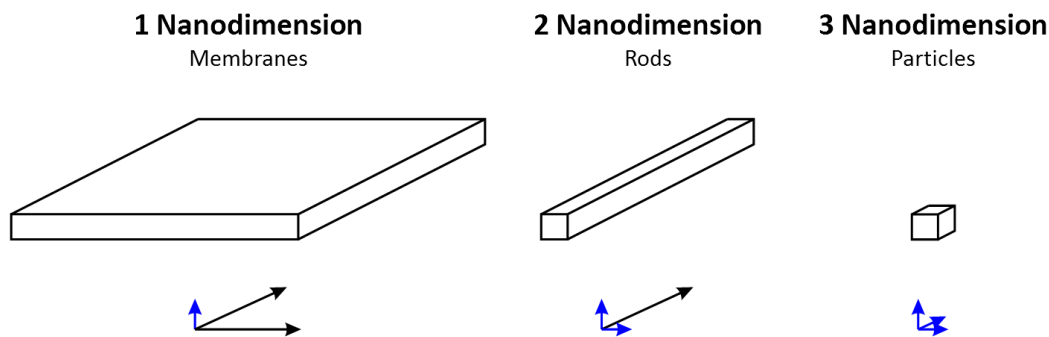


***Figure 1 – Typical Characterization of Nanomaterials depending on the number of nanodimensions.***

Usually nanomaterials are categorized by how many nano-dimensions they have (Figure 1). Nano-membranes, which only possess one nano-scale dimension, are under heavy investigation for separation purposes especially for nano-sensors in medical and non-medical applications [2-5]. A few groups deal with nano-rods [6-8], but besides the huge interest for carbon nanotubes for their unique electrical and mechanical characteristics, nano-rods are usually not the focus of research in biorelated fields. Nanomaterials with 3 nanodimensions (nanoparticles) are under investigation in many fields, in and outside of the body because of their unique features (see reviews [9-15]).

Many different formats and materials ranging from metal and metal-oxide particles to silica and organic materials are being used. The most promising nanomaterials used in bio-applications are gold nanoparticles, silica nanoparticles (mesoporous and non-porous), organic nanoparticles like polystyrene and in recent years a growing field of protein nanoparticles emerged (Figure 2).

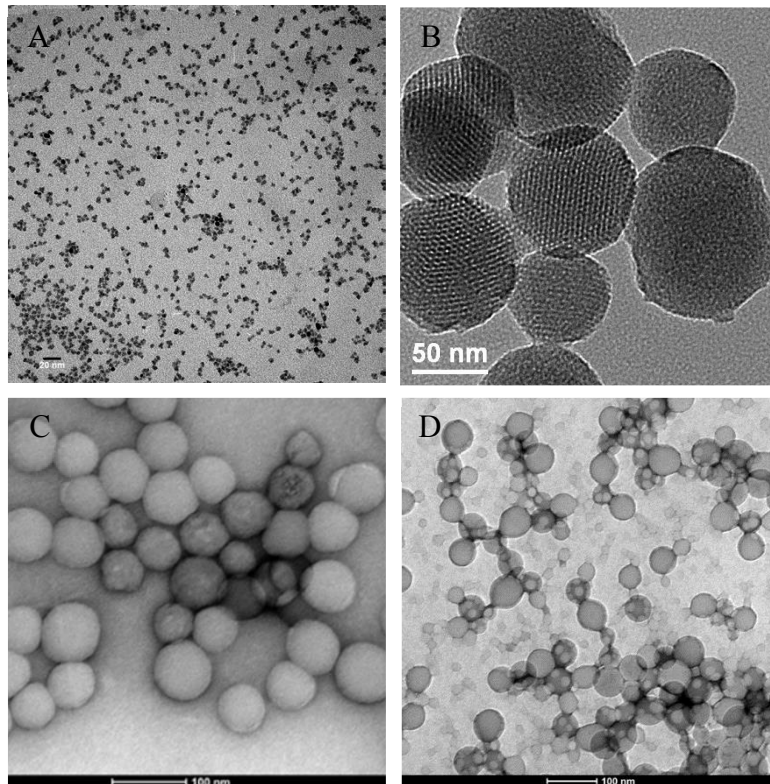


**Figure 2 – 5 nm gold nanoparticles (A [16]), 100 nm mesoporous silica nanoparticles (B [17]), 70 nm solid silica nanoparticles (C [18]), polydisperse organic polystyrene nanoparticles (D).**

## Metal particles

The most prominent metal nanoparticle is the gold nanoparticle [19-22]. Gold nanoparticles have been around for a long time since they can be produced by reducing dissolved gold ions into elemental gold, causing the gold to precipitate, producing gold nanoparticles of various characteristics and sizes. The famous talk of Richard Feynman was inspired by emerging techniques for the production of gold nanoparticles. In the beginning mostly used by sciences that deal with electric devices, nowadays they are also used for analytical purposes, and various other applications [23-26]. The technique of producing gold nanoparticles has been refined to yield highly monodisperse particles of defined size characteristics ranging from single digit nanometers up by using nanotemplates [27-30]. Although gold nanoparticles possess very unique

characteristics, for most applications in biotechnology they are just too expensive to be used in any larger scale than micro-devices or for analytical purposes.

## Metal oxide nanoparticles

There are many different metal oxide nanoparticles under investigation, and many more will be developed in the future [31-34]. As this class of nanoparticles is huge and highly diverse, it is very difficult to pick out the most prominent one, but titanium oxide is for sure one that is often used in studies, also in context of protein-nanomaterial interaction [35-37]. Titanium oxides are especially interesting because titanium has a long history of being used for various applications in the human body without causing any harm. The hope is that nanomaterials based on titanium show good biocompatibility and less side effects in the human body than other metal oxides.

## Organic nanoparticles

Organic nanoparticles can be anything from crude polystyrene to cross-linked BSA, all exhibiting different characteristics. The group of organic nanoparticles is even more diverse than that of metal oxide nanoparticles. As we just started to produce and investigate protein nanoparticles, we still do not know much about how they behave and how they could be used [38-41]. Proteins themselves show good biocompatibility and are perfectly degradable. They are even not foreign to the body as long as the right protein is used for their production, so the hope for biocompatible nanomaterials based on proteins is strong. Nevertheless, at the moment nobody can predict how protein nanoparticles might influence the field in the future. We know much more about other organic particles, for instance about polystyrene nanoparticles, which have been around for a while. A number of cytotoxicity studies have been conducted with polystyrene particles, showing good biocompatibility under the right conditions [42-45]. Organic nanoparticles offer the opportunity to use tools developed by organic chemistry to modify and specifically tailor the surface and interior of the particles to the special need of their intended application. Although we do not know exactly what surfaces we would desire, the tools for obtaining them are readily available.

## Silica nanoparticles

A very interesting, if not the most interesting, group of nanoparticles are the silica particles [46, 47]. Silica is regarded as safe material to be introduced into the human body, and therefore is under heavy investigation for biopharmaceutical applications [48]. Silica is relatively cheap, but suffers from the fact that small nanoparticles (below 30 nm) with uniform characteristics are very difficult to achieve. Especially when talking about different sizes of nanoparticles it can be difficult to obtain the same surface characteristics for differently sized particles. Silica can be readily modified to yield particles of different characteristics, and the biodistribution and possible ways for the body to get rid of them again have already been studied [49]. An interesting subclass of silica nanoparticles are the mesoporous silica particles, which combine nanoscale material properties with an internal surface by providing pores of several nanometer diameter, produced by an organic template used in the production process [27, 50-52]. These nanomaterials have perfect characteristics for drug delivery vehicle, combining an outer surface to be tailored to protect both the body and the drug inside the nanoparticle from each other, and additionally an inner surface to provide an environment for stabilizing the drug. Once this carrier is at its destined target, the cargo can be released, either chemically by the changing environment (e.g. the environment of the liposome) or physically by introducing high frequency magnetic fields (Figure 3) [27, 50-54]. Such applications are especially interesting for cancer treatment, as most of the cancer drugs available today suffer either from low solubility in the human body, or are too destructive to the organism. Both problems could be prevented using silica nanoparticles, separating tissue and drug as long as the drug is not at or inside the cancer cell it is intended to kill.

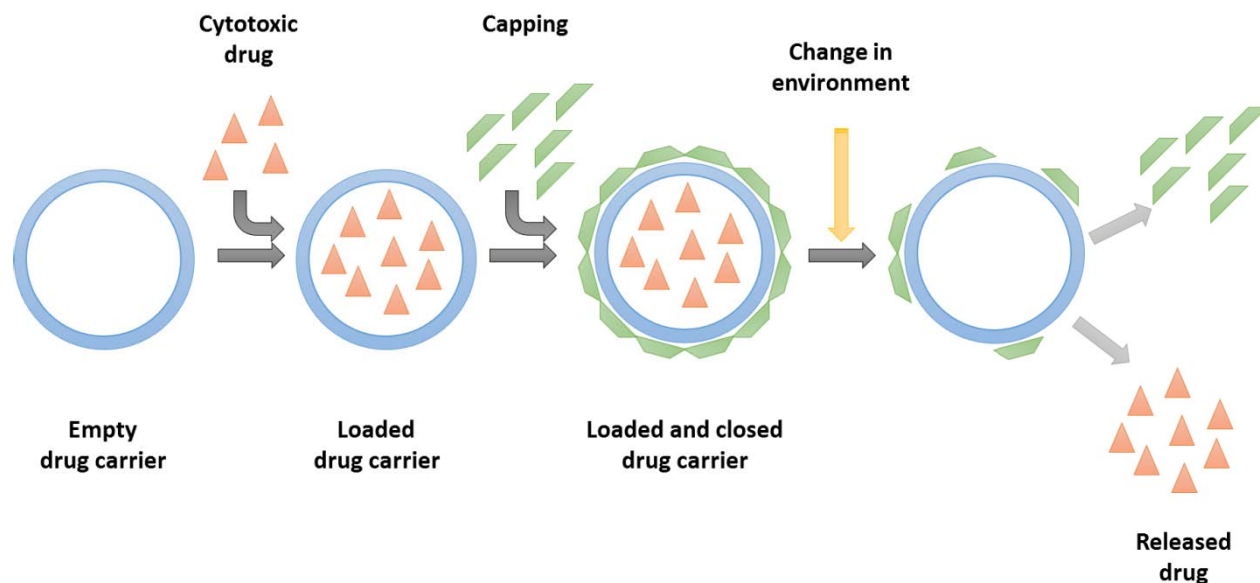


**Figure 3 – Principle of a drug carrier particle, which is loaded with a cytotoxic drug and coated to protect the drug from the body and vice versa. Once the particle is at its desired destination in the body and the environment changes, the drug is released by destroying the bond between the capping agent and the drug carrier.**

## Protein corona

When nanoparticles get introduced into the human body, or for that matter in any complex solution of different proteins, they will get surrounded by proteins that stick to the surface [42, 55, 56]. This protein layer is called protein corona, and consists of two different layers which have been defined in analogy to the double layer theory, and are called the hard and soft protein corona (Figure 4). The hard protein corona is the first layer of proteins bound to the nanoparticle and is usually very tightly bound, so tightly that in most cases this hard corona will not change, even if the protein solution around it is changed [43, 57]. Although other proteins with higher affinity to the surface might be around, the kinetics of desorption are so slow, that affinities do not affect the hard protein corona any more. This innermost layer is usually build up during the first contact of the nanoparticle with the protein corona, and is therefore mostly driven by the abundances of proteins and their kinetics, rather than specific affinities. Around this hard protein corona a soft corona is build up, but this layer is able to change composition depending on the solution surrounding the particle.

At first contact with the complex protein solution, the composition of the soft corona will also be driven by protein abundances rather than affinities, but due to the possibility of proteins desorbing and resorbing, the composition of the corona will then slowly change to proteins of higher affinity [58].

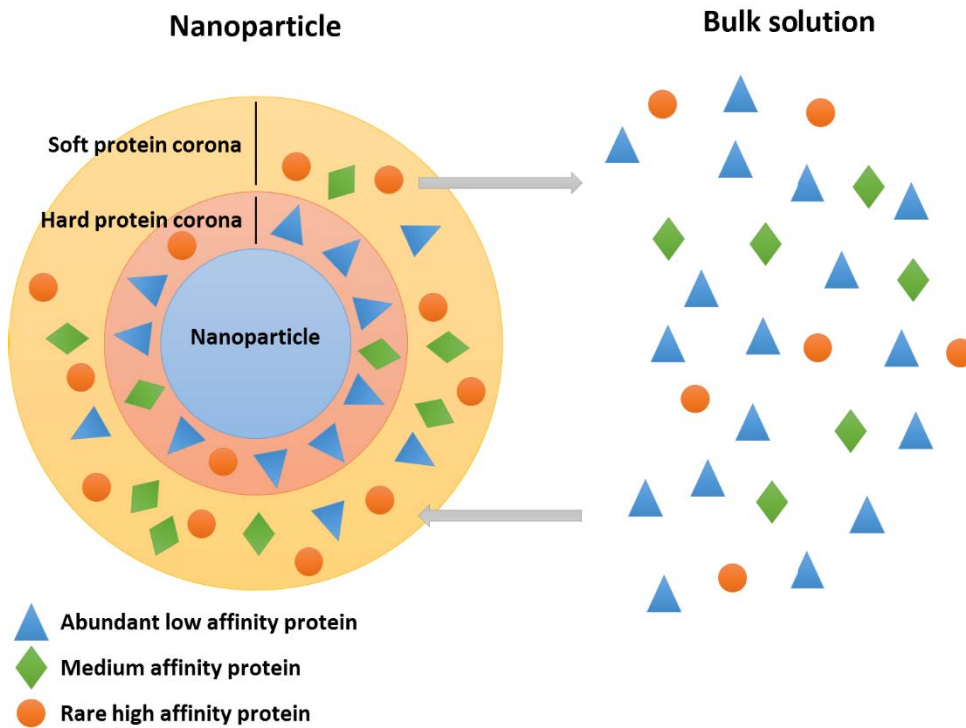


**Figure 4 – Nanoparticles in a protein mixture build up a hard protein corona, which does not interact with the proteins in solution and its composition is mainly dependent on the abundance of individual proteins, and a soft protein corona, which interchanges proteins with the bulk solution by desorption and resorption and is mainly dependent on the affinity of the protein to the surface.**

It is to note while talking about nanoparticles in the human body that the human body and the immune system of the human body is not able to “see” the nanoparticle itself, because of the close coverage of the particle by proteins. What is visible to the immune system is only the protein corona around a relatively small object in the size of a virus. Therefore it is crucial to understand how it comes that the body reacts to different kinds of nanoparticles in a different way [59]. It cannot be a direct assessment of the nanoparticle properties, but rather has to be an indirect assessment mediated through the protein corona (Figure 4).

Understanding how proteins bound to the surface of nanoparticles look like, and how this may influence the reaction of the body to this surface of proteins will lead to better understanding of existing nanoparticle systems and to novel nanoparticles exploiting the features of the protein corona.

## Protein conformational changes upon adsorption to nanomaterials

As we established the importance of the protein corona and the time dependency and complexity of the problem, we find ourselves faced with an additional problem. Reports in literature show that proteins adsorbed to nanoparticles can change their conformation, leading to an additional layer of complexity understanding the problem of nanoparticle-protein interaction. The conformation of the proteins is of great importance, because the particle is only “visible” to the body through information passing through this protein layer. Even more, we find reports of nanoparticle size dependent conformational changes of proteins, which adds even more complexity. A search through the literature reveals an inconclusive view on this subject. A summary of the literature available and relevant to this subject can be found in Table 1. The data not only is inconclusive of the mode of action for conformational changes upon adsorption but it is impossible to deduce any new theories or even test existing ones because of a broad range of different nanoparticle materials, sizes and adsorbed proteins. Each of the studies used a very limited set of nanoparticles and proteins, but different ones from other studies making it practically impossible to get a complete and conclusive picture. This work was focused on silica based nanoparticles as they are obtainable as monodisperse particles with defined surface characteristics over a wide range of sizes. Despite huge development efforts for production methods of nanoparticles it is still a challenge to obtain differently sized nanoparticles with the same surface characteristics. Whenever working with differently sized nanoparticles in such studies, one has extensively characterize the nanoparticles to be sure they have comparable surface characteristics.

One set of studies started 1997 by Billsten et al and dealt with silica nanoparticles of 9 nm size and using the protein human carbonic anhydrase II (HCAII) [60]. A change of secondary structure observed in these studies pointed to an unfolding of the protein which could be quite similar to unfolding by chaotropic salts, although detailed information on this matter was missing. The employed methods, circular dichroism and fluorescence, were not able to provide data at the atomic

level. This work was picked up by Lundqvist et al [61-63], who completed the studies with silica nanoparticles in the size range from 6 to 15 nm and with the protein human carbonic anhydrase I (HCAI) and HCAII. In this study NMR was used to investigate the structure of proteins both in solution and adsorbed to nanoparticles. The small nanoparticle size facilitated the use of NMR for structure determination of the proteins, but rendered it not comparable to many studies. Using nanoparticles below 20 nm is very unusual for studies done for drug delivery vehicles for pharmaceutical use, which are usually in the range of 100 nm size. Nevertheless this study gave a deep insight into the interaction of human carbonic anhydrase variants with silica nanoparticles of small size. The work indicated that the rather soft structure of HCAII and the more rigid structure of HCAI can make a difference in how the protein reacts to adsorption [62]. The rather soft protein HCAII seems to alter its structure rather radically to find an energy minimum while adsorbed on the surface of the nanoparticle, while the hard protein HCAI seems to preserve its structure with only little structural perturbation. The data suggests a time dependency of this conformational change in the range of hours, leading to more and more change for longer incubation times. Additional studies on the nature of this conformational change revealed a metastable conformation of HCAI resembling a near native molten globular-like structure, while retaining its enzymatic capabilities [63]. It seems that this transition state of near-native conformation can be the starting point for the subsequent conformational change and irreversible binding which have been seen for the less stable HCAII. These changes were also proven to be nanoparticle size dependent [61] as more conformational change was observed when adsorbed to 15 nm nanoparticles in comparison to adsorption on 6 nm nanoparticles. The work of Lundqvist et al showed such conformational changes only for these very small nanoparticle sizes and tried to relate this to the surface curvature of the nanoparticle. In this work they speculated that this change could be due to the change in the interaction area between proteins and nanoparticles with regards to different nanoparticle sizes, but calculations to prove the plausibility of this hypothesis were never presented. It seems to be a reasonable explanation for very small particles which are roughly the same size of the protein under investigation. This study of Lundqvist et al, although only dealing with two different proteins and three different very small nanoparticles, are at present the most thorough study of nanoparticle-protein interaction investigating the phenomenon of size dependent conformational changes.

Two studies describe adsorption of lysozyme onto silica nanoparticles. One of them presented by Tian et al. deals with lysozyme after contact with nanoparticles [64], which means proteins were investigated not while being bound to the nanoparticles, but after desorption from the nanoparticles. This study indicated a change of lysozyme activity after contact with 9 nm silica nanoparticles. The change of lysozyme variants activity after contact with nanoparticles was proportional to the thermal stability of the protein variants, indicating that variants with less structural stability are more prone to denature on the nanoparticle surface, which is in agreement to the findings of Lundqvist et al [61, 62]. Further studies on lysozyme were done by Vertegel et al, not only on a single nanoparticle size, but on three differently sized nanoparticles, 4, 20 and 100 nm [65]. Circular dichroism data and lysozyme activity showed a size dependency of the conformational change of adsorbed lysozyme, leading to more conformational change on bigger particles than on smaller particles which again is in line with the findings of Lundqvist et al. In this work the authors hypothesized that a different surface potential calculated by the double layer theory could be an explanation for the phenomenon of size dependent conformational change. Both works which hypothesize on the reason for nanoparticle size dependent conformational changes do not provide explicit data to support one or the other theory.

Additionally to these studies, some smaller studies dealing with only two sizes of nanoparticles and dealing with different proteins have been published. Two studies deal with different proteins, but a similar size range to the studies done by Lundqvist et al and Vertegel et al. Shrivastava et al presented the adsorption of acylphosphatase adsorbed to 4 and 15 nm silica nanoparticles investigated by NMR [66]. Like the HCAI investigated by Lundqvist et al, the acylphosphatase showed more conformational changes adsorbed to 15 nm in comparison to 4 nm, but also showed different attachment sites for the protein while binding to the differently sized nanoparticles. The explanation presented by Shrivastava et al was the same used by Lundqvist et al: bigger nanoparticles provide more surface area for interaction because of the decreased curvature. The second publication dealing with particles of very small size is presented by Shang et al dealing with ribonuclease A adsorbed to either 4 or 15 nm silica nanoparticles [67]. In this work circular dichroism was used to follow the structural changes of ribonuclease A, showing no substantial change of the secondary structure of ribonuclease A upon adsorption to either 4 or 15 nm silica nanoparticles.

However urea denaturation studies done in this work showed different denaturation energies for proteins adsorbed to either 4 or 15 nm nanoparticles, showing more change to the free state in solution for 15 nm silica nanoparticles. Also in this study the explanation used for this phenomenon was the one presented by Lundqvist [42, 55, 61-63].

Two of the studies deal with only a single nanoparticle size, a study done by Wang et al dealt with butyrylcholinesterase adsorbed to 20 nm non-porous and 30 nm mesoporous silica nanoparticles also reported a decrease in activity of butyrylcholinesterase upon adsorption to nanoparticles [68]. The reported data suggested also a different impact of 20 nm and 30 nm silica nanoparticles, but whether this was due to the different size of the particles or due to the different structure and surface characteristics is not possible to tell. A study done by Wu et al on 90 nm silica nanoparticles with beta-lactalbumin showed conformational changes upon adsorption and was able to follow this denaturation in time by using fluorescence and infrared spectroscopy [69]. The conformational change was characterized by a quick conformational change in the beginning upon adsorption followed by a much slower change over a timespan of hours. In this publication also the influence of the surface coverage was taken into account and it was shown that a lower surface coverage leads to a more rapid and stronger conformational change in beta-lactalbumin.

One study in literature dealing with size dependency related issues for nanoparticles highlights the importance of these studies for bio-related applications. Tenzer et al. [70] describe the composition of the protein corona, which build up on the surface of differently sized silica nanoparticles in the sizes of 25, 120 and 140 nm. This study did not address conformational changes of proteins upon adsorption, but rather addressed which proteins adsorb to which particles out of blood plasma. The strong dependency of the corona composition on the nanoparticle size indicated that the protein corona is not only dictated by the nanoparticle material and surface modification, but also by its size. This fact is very important, especially when thinking about the reaction of the human body on differently sized nanoparticles in the bloodstream and how the human body is able to get information on the nanoparticle surface and nanoparticle size through the protein corona which is rapidly build up once a nanoparticles enters the human blood stream.

Although there are many groups working on this problem, the real cause for size dependent conformational changes of proteins is still missing. Furthermore, existing theories were never critically investigated for their plausibility because of the lack of a sufficient data set. The assessment of the data presented in the literature is complicated by the fact that different groups deal with different proteins and nanoparticle sizes, some of them only dealing with one nanoparticle size. To tackle this problem was the aim of this work, by first providing the preparative methods to purify protein loaded nanoparticles and the analytical tools to investigate the structure of adsorbed proteins; second to follow conformational changes on nanoparticles for a wide range of nanoparticle sizes and third to check the hypothesis for the cause of conformational changes for their plausibility and their ability to fit the data.

**Table 1 – Relevant publications dealing with denaturation of proteins upon adsorption to nanoparticles**

Type	Dimension	Protein	Material	Conformational Change?	Size dependency	Group	Methods	Reference
Particle	9 nm	Lysozyme	Silica	Yes	ND	1998, Tian	Circular dichroism	[64]
Particle	5-100 nm	Histone, albumin, insulin, globulin, fibrinogen	Gold	Yes	Yes	2009, Lacerda	Circular dichroism, Fluorescence	[71]
Particle	25 nm	Apolipoprotein, HDL, HAS	Polystyrene	Yes	ND	2011, Cukalevski	Circular dichroism, Fluorescence, Limited proteolysis	[72]
Crystal	unknown	Myoglobine	Hydrotalcite (NiAl)	Yes	Yes	2009, Bellezza	FT-IR, Fluorescence, Raman, Activity	[73]
Particle	100-200 nm	Lysozyme	Polystyrene +polylactic acid	ND	ND	2008, Cai	TEM, SEM, AFM, DSC	[74]
Particle	20, 30 nm	butyrylcholineste rase	Silica	Yes	Yes	2010, Wang	Activity	[68]
Particle	10-60 nm	butyrylcholineste rase	Metal	Yes	Yes	2010, Wang	Activity	[68]
Particle	60-600 nm	Blood plasma proteins	Polystyrene	ND	Yes	1998, Lück	2D-DIGE	[75]
Particle	90 nm	Beta-lactoglobulin	Silica	Yes	ND	2008, Wu	Fluorescence, FTIR, CD	[69]
Surface	-	Human carbonic anhydrase II	Functionalized thiols	Yes	ND	2005, Karlsson	Surface plasmon resonance	[76]
Particle	35, 120, 140 nm	Blood plasma proteins	Silica	ND	Yes	2013, Tenzer	SDS-PAGE,	[70]
Particle	4, 15 nm	Ribonuclease A	Silica	Yes	Yes	2007, Shang	Circular Dichroism	[67]
Particle	4, 20, 100 nm	Lysozyme	Silica	Yes	Yes	2004, Vertegel	Circular Dichroism, Activity	[65]
Particle	4, 15 nm	Acylphosphatase	Silica	Yes	Yes	2013, Shrivastava	Activity, Circular dichroism, NMR	[66]
Particle	6, 9, 15 nm	Human carbonic anhydrase I and II	Silica	Yes	Yes	2004, Lundqvist	Circular dichroism, NMR	[61]

Type	Dimension	Protein	Material	Conformational Change?	Size dependency	Group	Methods	Reference
Particle	9 nm	Human carbonic anhydrase II	Silica	Yes	ND	1997, Billsten	Circular dichroism, Fluorescence	[60]
Particle	9 nm	Human carbonic anhydrase I	Silica	Yes	ND	2005, Lundqvist	NMR	[63]
Particle	6, 9 nm	Human carbonic anhydrase I and II	Silica	Yes	No	2005, Lundqvist	NMR	[62]
Particle	6 nm	Chymotrypsin	Functionalized gold	Yes	ND	2002, Fischer	Circular dichroism, Activity	[77]
Particle	9 nm	Lysozyme	Silica	Yes	ND	1999, Bower	Circular dichroism, Activity	[78]
Particle	4.5 nm	Human carbonic anhydrase XII	Quantum dot	Yes	ND	2010, Manokaran	Fluorescence, Activity	[79]
Particle	<50nm	Bovine serum albumin	Al <sub>2</sub> O <sub>3</sub>	Yes	ND	2014, Rajeshwari	FT-IR, Circular dichroism, Fluorescence, UV-VIS	[80]
Particle	15, 260nm	TNF- $\alpha$ , IL-8	Carbon black	ND	Yes	2010, Brown	Cellular uptake	[81]
Particle	10 kDa	Lysozyme, IgG	Fullerol	Yes	ND	2014, Chen	Circular Dichroism, Fluorescence, DSC	[82]
Particle	8, 45 nm	Plants	Silver	ND	Yes	2014, Syu	Plant growth	[83]
Particle	30. 200. 400 nm	Blood plasma proteins	Fe <sub>3</sub> O <sub>4</sub>	ND	Yes	2014, Hu	2D DIGE	[84]
Particle	5-50	Ovalbumin	Silver	Yes	ND	2014, Joshi	UV-VIS, Raman Spectroscopy	[85]
Particle	20, 40, 80 nm	Tetanus Oxois	Gold	Yes	Yes	2014, Barhate	Circular Dichroism, Thermodynamic studies	[86]

# Objectives

The behavior of proteins bound to surfaces, especially surfaces with two or more nano-dimensions, for example nanoparticles, is still not very well characterized. This is due to a lack of methods as well as a lack of data available on this phenomenon in the literature. Tools for separation and analysis of proteins bound onto nanoparticles are not readily available and reports in the literature about conformational changes of proteins bound to nanoparticles are indecisive and incomplete. Data in the literature does not allow the formulation and evaluation of possible mechanisms for nanoparticle induced structural changes in proteins. Furthermore, reports on nanoparticle size dependent conformational changes are inconclusive, and no thorough study of model proteins and differently sized and well characterized nanoparticles was made.

Therefore this study had three main objectives:

- *Development of new purification methods for protein loaded nanoparticles with good upscale characteristics for industrial use as a model for drug covered particles.*
- *Characterization of protein conformational changes on nanoparticles with different size.*
- *Formulate possible hypotheses for the cause of size dependent conformational changes and test them for their plausibility.*

## Results and discussion

Results of this work have been summarized in this doctoral thesis and in 2 publications: one published in Journal of Chromatography A with the title “Continuous separation of protein loaded nanoparticles by simulated moving bed chromatography” [18] and one accepted for publication in Engineering in Life Sciences with the title “Protein adsorption onto nanoparticles induces conformational changes: Particle size dependency, kinetics and mechanisms”.

## Methods for separation

Separating protein and particles is essential for the production of nanoparticle based therapeutics. Once the drug has been applied to the nanoparticle usually there is a lot of the drug left in the supernatant during the process. The two species of small drug and big nanoparticle have to be separated before using them in a pharmaceutical concept. Free drug which gets injected with the nanoparticle bound drug can have a number of adverse effects, like unwanted side effects because of toxicity, or waste of potentially expensive drug if only the substance on the particle is effective in the intended use.

### Batch separation

Centrifugation is the commonly used tool to separate particles. It is well understood, characterized and predictable through the Stokes-Einstein-Equation. But although it is fairly common to use centrifugation as a tool to separate nanoparticles at lab scale, it is sometimes difficult to transfer centrifugation or ultracentrifugation to large scale applications. In lab scale applications it is easy to separate particles from supernatant by decanting and suspending them by vortexing, but in large scale these two operations can be difficult, especially because the particles are sometimes soft and fragile and can be densely packed after centrifugation. Centrifugation was used in this work for small scale lab experiments, where centrifugation, separation and suspension of particles was easily possible by desk-centrifuges, decanting and vortexing.

A different method for separation of nanoparticles from other non-particular substances in solution is filtration and ultrafiltration, where particles can be specifically separated from other substances if the size difference is big enough. Filtration is already in use in large scale downstream processes for pharmaceuticals, but usually used as ultrafiltration to concentrate proteins or to exchange buffers via diafiltration.

This work presents a novel alternative and easily scalable method: the use of size exclusion chromatography for separation of particles and suspended proteins. The challenges for the development of such a separation is the selection of the right buffer and stationary phase, the choice of column housing, the choice of nanoparticle and unspecific adsorption of the nanoparticle to the stationary phase. All these problems arise from the fact that the method has to deal with particles and the fact that we do not want to lose the binding of nanoparticle adsorbed proteins. Particles can be a problem for chromatographic steps and can lead to clogging of the stationary phase as well as clogging of the frit in the housing. Because of that they are usually removed from any stream that goes into the chromatographic step by filtration. By choosing the right frit and housing one can avoid clogging and loss of the particle in the chromatographic step. The fact that proteins are bound to the nanoparticle prohibits high salt buffers usually used in size exclusion chromatography, because this could disrupt the binding of the proteins and would result in the loss of protein coverage on the particle. The method developed in this work solved these problems by a number of modifications to the standard size exclusion method. The principle of the new method is that (unlike the common use of size exclusion chromatography) the particles are not able to penetrate into the size exclusion beads at all, are therefore not retained by the chromatography material and leave the column in the so called void volume (which means they leave the column after applying a buffer volume to the column which is the void fraction of the packed bed). Such approach was also shown for other large biomolecules like plasmids or viruses [87-89]. This method is in theory applicable to all dual- or multicomponent systems with one species that is not able to penetrate into the size exclusion material (the particles) and all other impurities and buffer compounds that are able to penetrate into the material, regardless of the detailed particle properties (size or material) or the specific impurity retention factor in the column. In addition the method is easily scalable to production scale, widely used in the industry for various purposes including pharmaceuticals, allows for buffer exchange and can be used in a continuous fashion in a simulated moving bed mode. Although the principle behind size exclusion as separation tool is simple and straight

forward, many different problems arose during the development of the method. In this work polystyrene and silica nanoparticles in the size range of 30 to 1000 nm were used (detailed characterization of silica nanoparticles can be found in Publication 2 – Protein adsorption onto nanoparticles induces conformational changes: Particle size dependency, kinetics and mechanism. To make the process also applicable for drugs bound by electrostatic interaction high salt concentrations have to be avoided in the setup, but are usually used to reduce nonspecific interactions. Additionally, the hydrophobic nature of polystyrene leads to a loss of particles in the column due to hydrophobic interactions between the column material and the nanoparticles. Usual approaches like adding a less polar modifier to the mobile phase like methanol or ethanol could not be used in this work, because a potential drug based on proteins can be damaged when using these non-polar modifiers. A novel approach used in this work was to overcome this problem by completely covering the nanoparticle with protein, which leads to a shielding of the hydrophobic surface of the nanoparticle against the surface of the chromatography material (Figure 5 Panel A). A method which is in theory also applicable to drug-nanoparticle combinations that do not contain any protein, because one can always use human serum albumin to cover the particle if necessary. Using this approach it was able to separate a mixture of bovine serum albumin from completely covered 60 nm polystyrene nanoparticles without any significant loss of material in the column (Figure 5 Panel B). To demonstrate that the goal for a separation method that is versatile and applicable to a wide variety of nanoparticle materials was reached the experiment was repeated using 70 nm silica nanoparticles and bovine serum albumin (Figure 5 Panel C). The result is reproducible, and this work shows the applicability of the method to both hydrophobic (polystyrene) and hydrophilic (silica) particles making the process highly stable and suitable as a platform process.

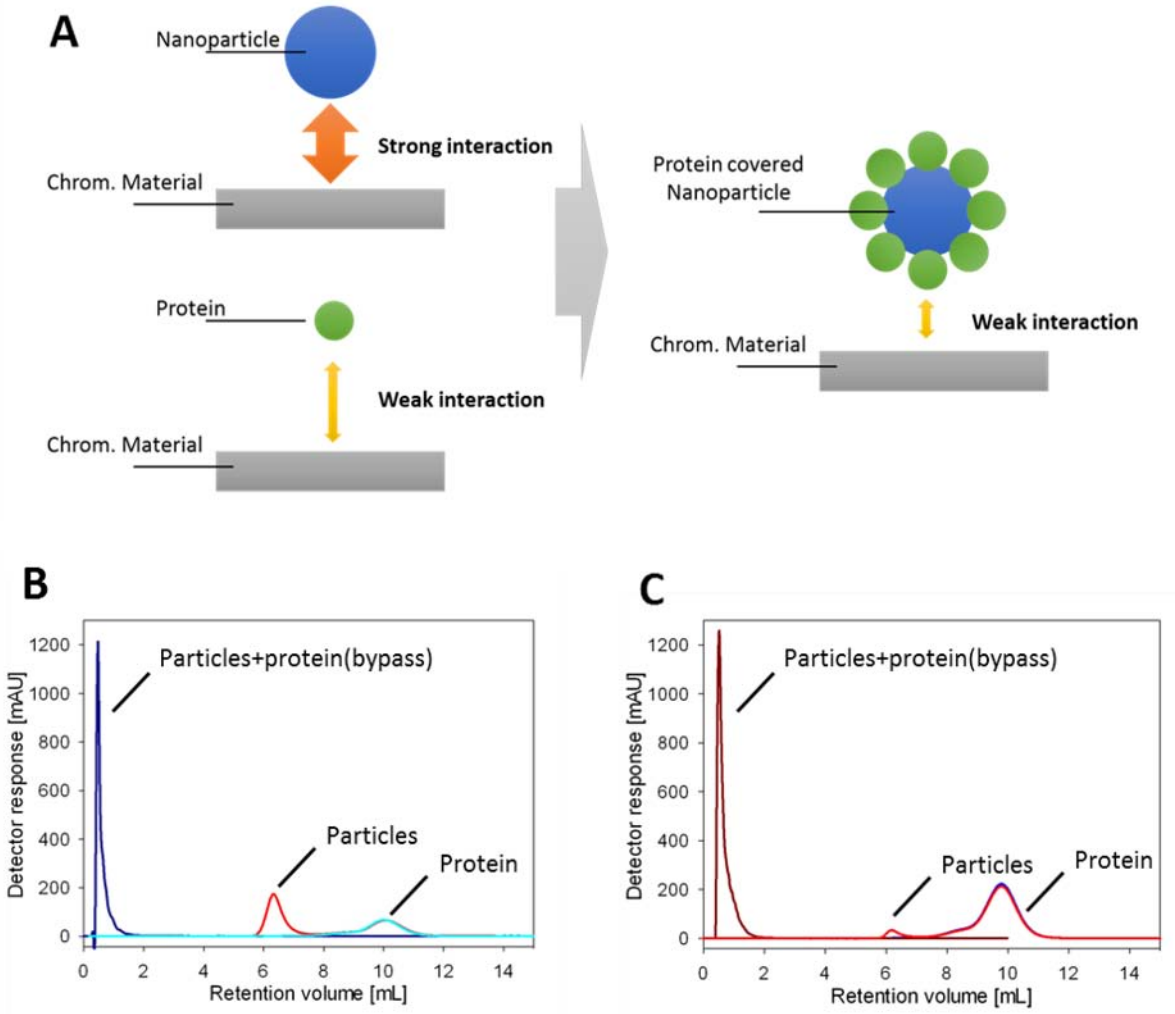


**Figure 5 – Use of a full coverage protein layer to prevent hydrophobic interactions of polystyrene nanoparticles and size exclusion chromatography media (A) and the separation of bovine serum albumin covered 60 nm polystyrene (B) and 70 nm silica (C) nanoparticles from free bovine serum albumin by low salt size exclusion chromatography.**

## Continuous separation

Size exclusion chromatography usually suffers from two major drawbacks when used in a batch-wise system: i) high buffer consumption, ii) dilution of the sample. As the particles are eluting in the void volume, we have as little sample dilution as possible, only caused by the axial diffusion of the particles in the column. A more significant problem for this application of size exclusion chromatography is the high buffer consumption. To avoid high buffer consumption, a continuous operation using a closed loop simulated moving bed with an included recycling of buffer can be used. This possibility was demonstrated using particles and proteins for pilot scale (0.25 g /h /L chromatography resin) for small (beta casein) and larger (bovine serum albumin) proteins. Both proteins were easily separated from the particle fraction (the case of beta casein is presented in Figure 6). Additional detailed information can be found in Publication 1 - Continuous separation of protein loaded nanoparticles by simulated moving bed chromatography

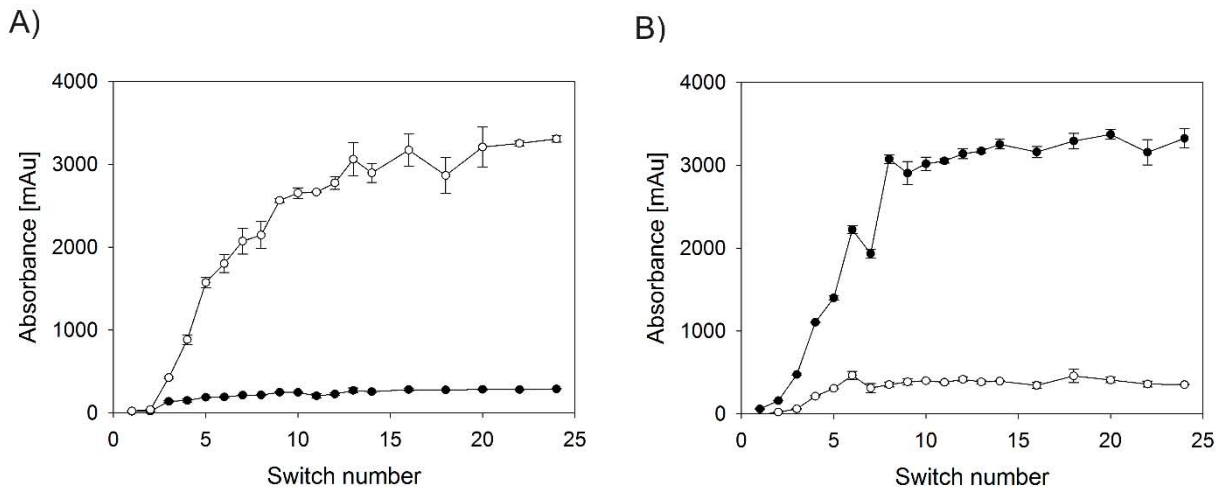


**Figure 6 – Concentrations of 70 nm silica nanoparticles (●) and beta casein (○) in the Extract (Panel A) and Raffinate (Panel B) of the closed loop SEC-SMB [18].**

In addition in this study the possibility to concentrate the protein fraction by tangential flow filtration and recycle it in the system was tested, a possibility especially appealing for expensive drugs which have to be adsorbed to nanoparticles to be most effective. In such a system one would only want to apply the drug in its high-efficacy form (adsorbed to the nanoparticle) to the patient, and want to recycle the rest of the drug which was not bound to the particle back into the system.

How such a system might look like is illustrated in Figure 7 which utilizes not only the continuous feature of simulated moving bed chromatography, but also the possibility of recycling, taking as input only uncovered particles and the drug, and producing no byproducts (like unbound drug), only yielding drug covered nanoparticles in a continuous fashion

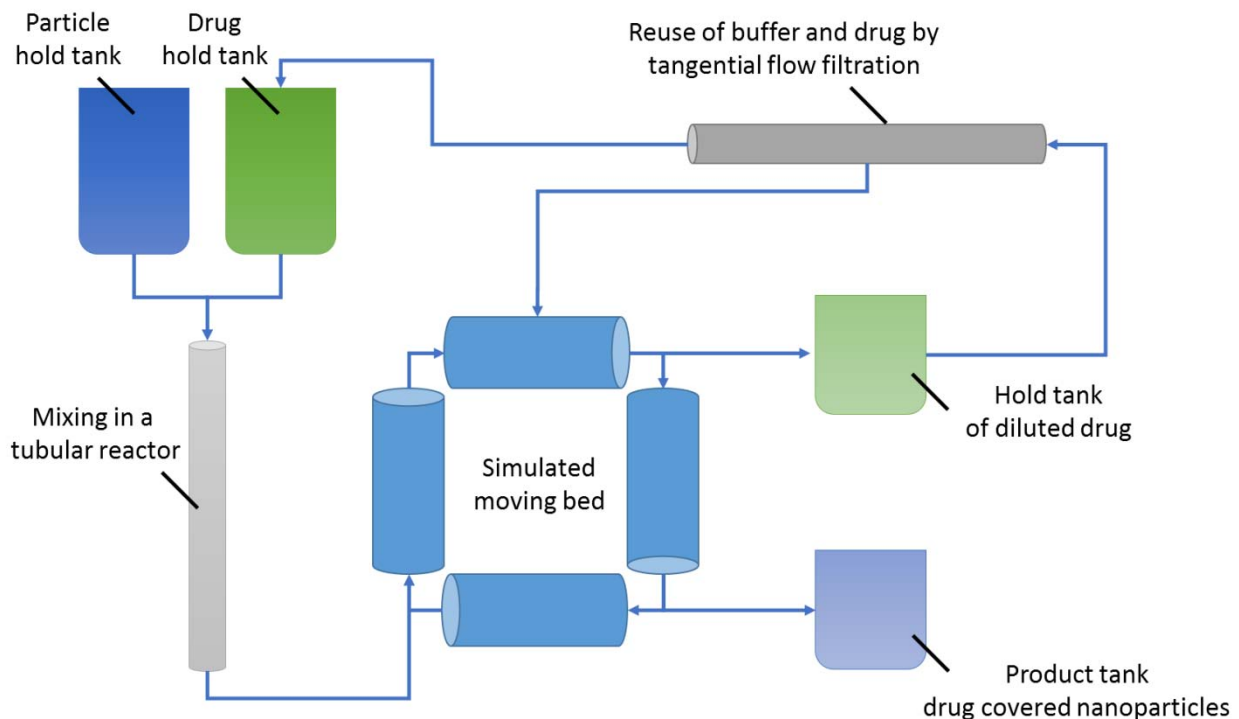


**Figure 7 – Proposed process for a continuous production of drug covered nanoparticles by the use of a simulated moving bed system for separation and a tangential flow filtration for concentration.**

## Protein structure determination

The main objective of this work was the investigation of the structural properties of proteins adsorbed to nanoparticles. A number of possible analytical tools to assess the structure of proteins were investigated for their suitability. Mentioned in the introduction were some reports of proteins measured after contact with nanomaterials [64], for such experiments the whole set of analytical tools available for protein characterization can be used, as the only species in the sample is soluble protein and no particles are present that could interfere with the measurements. Such an approach has its limitations, as the structure of the protein is not measured while having contact with the nanoparticle, but after contact and release of the protein. Although such an experiment yields important data for the use of nanoparticles in the body, it is not suitable to get insight into the particle-protein interaction, and also no data can be collected for the case of protein covered nanoparticles. An item especially interesting in terms of the surface visible to the human body under physiological conditions.

In this study a different approach was selected by measuring the proteins while still adsorbed to the surface. For this, the protein-particle conjugate had to be separated from unbound protein to avoid disturbances of the signal by free protein, and available tools for protein characterization had to be re-evaluated for their suitability to measure protein conformations in the presence of nanoparticles.

### UV-VIS

UV-VIS spectroscopy is one of the basic tools for protein characterization, although it gives only limited information, it is widespread because of its ease of use and cheap equipment. The suitability of UV-VIS spectroscopy was tested, but found that it can only be used with inorganic nanoparticles, as many organic particles (like polystyrene) contain aromatic groups and therefore influence the UV-VIS spectra gained.

## ATR-FT-IR

Infrared spectroscopy yields information about the backbone angles through infrared vibrations of the backbone bonds. Transmission infrared spectroscopy would suffer from the same limitations as UV-VIS spectroscopy, being limited to small nanoparticle sizes because of the strong scattering of light by larger particles. For that reason attenuated total reflection (ATR) Fourier transformed (FT) infrared spectroscopy (IR) was used. By employing a crystal, the light never passes through the sample itself, but is reflected at the surface of the crystal (Figure 8). Although the light never has direct contact to the sample, evanescent fields propagate into the sample and lead to a characteristic absorption much like in transmission spectroscopy.

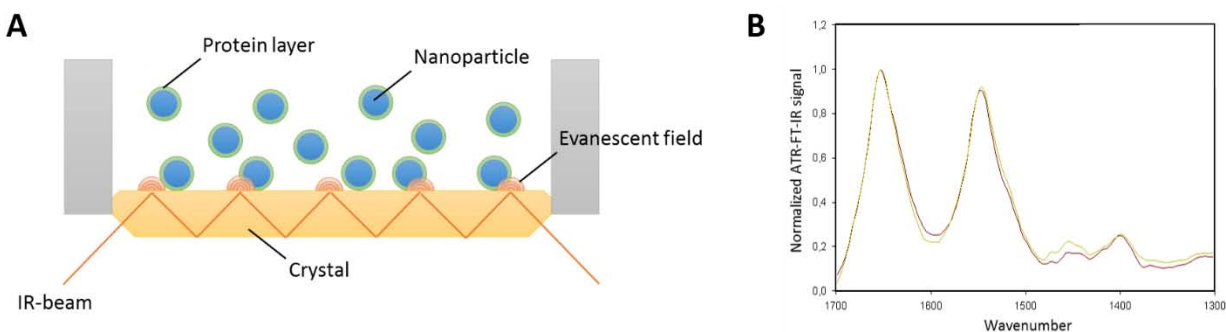


**Figure 8 – Principle of ATR-FT-IR spectroscopy, showing the total reflection of the IR-beam and the evanescent field which propagates into the sample (A) spectra of bovine serum albumin showing the amide I and amide II bands, and bovine serum albumin free in solution (red curve) and adsorbed to particles (green curve) (B)**

The resulting spectra show two characteristic peaks, the amide I and amide II band, located at about wavenumber 1700-1600 and 1600-1500 respectively. These bands are a convolution of a number of vibrations, all associated with the backbone of the protein. By deconvolution of these two bands (sometimes only the amide I band is used for this purpose) one can estimate the overall secondary structure, more precise the overall bond angles in the backbone of the protein. The spectra of bovine serum albumin in Figure 8B shows slight differences between bound and unbound bovine serum albumin, not only in the amide I and amide II region, but also in the region between wavenumber 1500 and 1300, the so called fingerprint-region. This region is very sensitive to changes, although it is impossible to deconvolute it and correlate it to a secondary structure element composition.

Although the obtained spectra looked reasonably well, it was very complicated to gather spectra of high quality by this method. ATR-FT-IR is very surface sensitive, as it only probes the first 20-100 nm of the sample, but bigger particles (above 100 nm) show significant sedimentation over the timespan of the experiments. That would not be a major problem if it were only for the particle, as the resulting peak from the silica is near a wavenumber of 1100, and therefore does not interfere with the protein measurements, but the particle displaces water on the surface, and the water stretching vibration is overlapping with both amide I and amide II band. Sedimentation of particles and displacement of water during the measurement interferes with the measurement by distorting the signal. While measuring small nanoparticles below 100 nm would be possible using this method, larger particles would still have to be measured with a different method. Therefore ATR-FT-IR is not suited for the study intended because it is not able to span the complete range of particles under investigation.

## NMR

In comparison to the spectroscopic methods discussed above, which only give overall structure estimation of the protein, nuclear magnetic resonance (NMR) can be used for detailed structure determination. It gives exact positions for each atom in the structure, and can be used to determine minute changes in the protein conformation which may be missed by UV-VIS spectroscopy or ATR-FT-IR. The measurement principle of NMR is the orientation of atoms in a magnetic field, and the response to the change of this field. Depending on the environment of the atom, the resonance frequency changes, and information can be gained from this change. Only active nuclei can be used for this measurement, which means that they have to have an odd atomic number. In the experiments the effort was concentrated on hydrogen, because the first results indicated that carbon and nitrogen would have to be replaced by their isotope  $C^{13}$  and  $N^{15}$  to yield reasonable results.

NMR can be further divided into one dimensional and two dimensional NMR. 1-dimensional NMR is the method usually used in synthetic chemistry, where simple molecules are investigated and strong signals can be expected. It uses the instrument in the classical way, applying a magnetic field to align the molecules, releasing them from this magnetic field and observing the reorientation into a different field, recording the signal and assessing it after fourier transformation. 2-dimensional NMR is used to obtain results for complex molecules such as proteins, where peaks in the resulting one dimensional spectra overlap and make data interpretation impossible. In this case additional pulses orient and mix spins to assess the coupling of atoms to one another (Figure 9). The evolution time ( $t_1$ ) is changed to obtain the second dimension, which means significantly more spectra have to be collected for a two dimensional spectrum; a time consuming process.

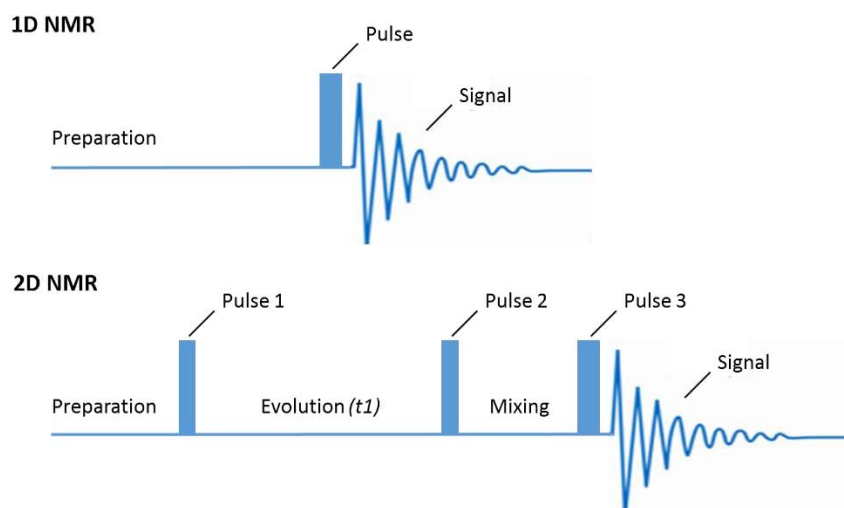


**Figure 9 – Pulse sequences for one dimensional and two dimensional NMR**

The collection and interpretation of one dimensional spectra is usually straight forward for small chemical molecules. The data collection for biological samples like proteins is also straight forward, but the data interpretation is not. An additional problem is that for a signal to give clear results, the whole complex under investigation (in this case the particle-protein aggregate) has to be mobile enough to rotate in the magnetic field. To test if this is the case for samples used in this study it was tried to obtain 1- and 2 dimensional spectra of proteins in solution and adsorbed to 70 nm silica nanoparticles. Although the method is perfectly able to produce reasonable one- and two dimensional spectra of beta casein (Figure 10), bovine serum albumin and myoglobin, it is not able to obtain spectra for adsorbed proteins. Although some publications report investigations of proteins adsorbed to very small particles [62, 66], it seems that it is impossible to collect

reasonable data once the particle-protein complex is bigger than large proteins currently under investigation (around 100 kDa). The complex is not able to change orientation quickly enough in the magnetic field leading to very broad peaks if any. In this study it was not possible to collect any meaningful spectra for particles of 70 nm size and therefore NMR was not investigated any further. It had to be concluded that the employed 700 Mhz NMR is not able to resolve big complexes such as the protein-nanoparticle complex used in this study, even if advanced automation and acquisition-strategies over 24 hours were used.

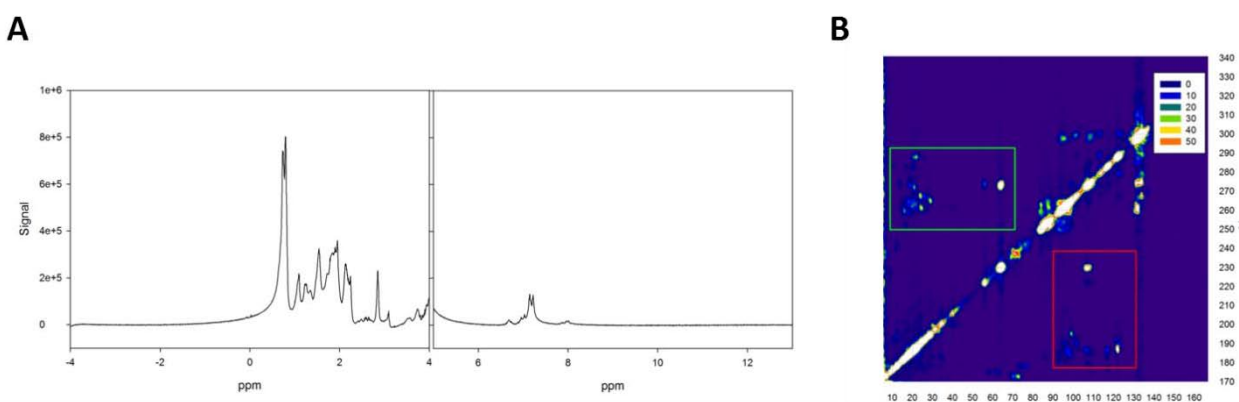


**Figure 10 – One dimensional (A) and two dimensional (B) proton NMR spectra of beta casein. The solvent peak has been cut out in the one dimensional spectra and interesting areas in the two dimensional spectra are marked with red and green rectangles.**

## CD

Another method for determining the protein structure is circular dichroic spectroscopy (CD), usually used for clear solutions of proteins in high concentration. In circular dichroic spectroscopy the optical active chiral center of amino acids are investigated at wavelengths ranging from 190 to 240 nm. Circular polarized light is sent through the sample and distorted by the chirality of the sample, resulting in an elliptically polarized light, which is measured at the outlet. The resulting signal of proteins (Figure 11A) look characteristic and is highly dependent on the secondary structure of the protein. Using theoretical curves of complete alpha-helical, complete beta-sheet and complete random coil proteins, the spectra of any single protein can be estimated by deconvolution of the spectra (Figure 11B). In the scope of this study it was also necessary to test the limitations and possibilities of this method in the presence of particles of various sizes.

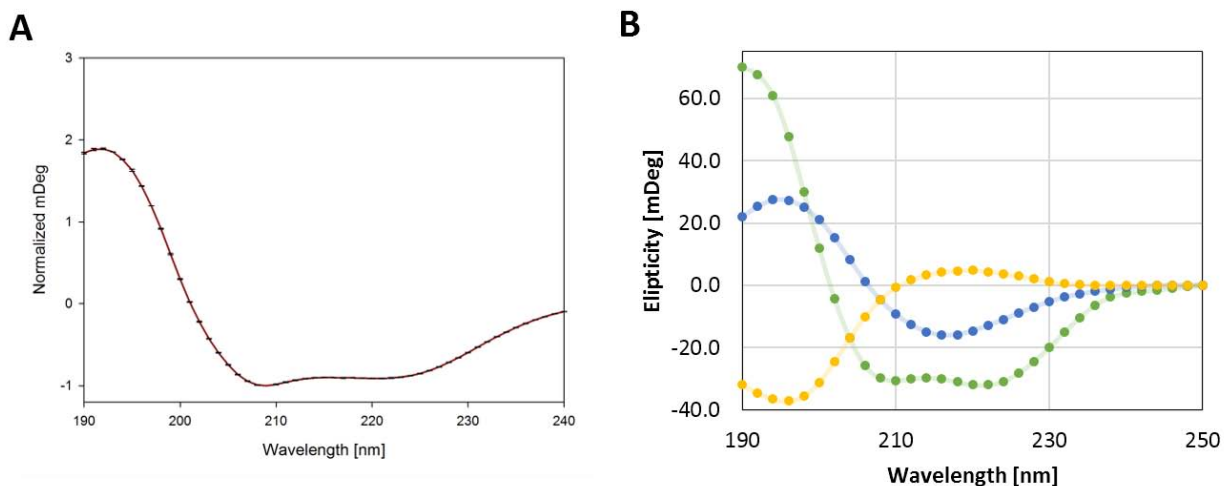


**Figure 11 – Circular dichroic spectra of bovine serum albumin (A) and the principle curves behind the deconvolution of the spectra into a structural composition (B) where blue is a complete random coil protein, yellow is a complete beta sheet protein and green is a complete alpha helical protein.**

For this method the protein concentration is of great importance, but this parameter was not available for many of the samples, as the exact amount of protein adsorbed to the particles was not known for many proteins and for a fast screening the determination of adsorption isotherms of all protein-particle combinations was not feasible. Therefore a different method, but based on the same idea, presented by Raussens [90], was used additionally. Detailed information about the method and the results can be found in Publication 2 – Protein adsorption onto nanoparticles induces conformational changes: Particle size dependency, kinetics and mechanism. In short, the study presents a CD method capable of providing good quality CD data on adsorbed proteins for particle sizes of 30 to 1000 nm size. This method was also adopted to be able to record kinetic data for the conformational change of particle bound proteins.

Using this methods significant conformational differences between proteins adsorbed to differently sized nanoparticles for two model proteins was shown: myoglobin and BSA. This behavior showed a sigmoidal relationship between the particle size and the conformational change (Figure 12). All surface parameters which are usually used to characterize surfaces (like porosity and zeta potential) are the same for all particle sizes, but nevertheless the protein conformation changes. All current explanations which have been developed for very small nanoparticles (below 10 nm) are unable to explain this phenomenon. The study was also able to proof significant differences in the kinetics

of the conformational change after adsorption for both proteins. Myoglobin seems to change its conformation rapidly after adsorption whereas BSA takes hours to reach equilibrium.

All this data leaves us with the conclusion that current theories used to describe nanoparticle size dependent conformational changes during adsorption of proteins fall short in explaining almost all aspects of the phenomenon investigated, and completely new theories and solutions have to be derived in the future. It also points out the importance of producing comprehensive data sets to be able to investigate proposed mechanisms in the first place. Without such comprehensive data sets there is no possibility to test theories for their plausibility, and even ideas that seem obvious and plausible may fall apart once critically investigated.

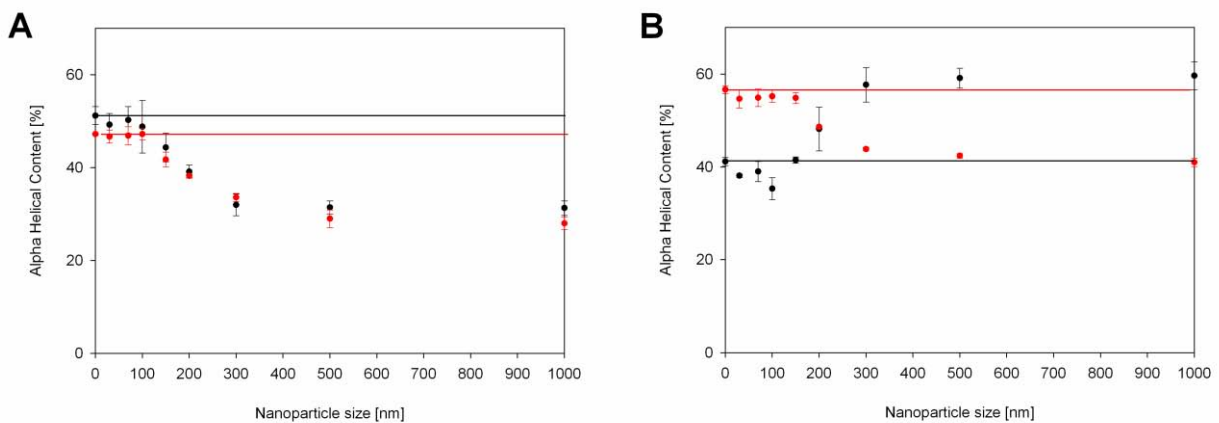


**Figure 12 – alpha helical content of myoglobin (A) and BSA (B) adsorbed on nanoparticles varying in size. The red curve shows the concentration dependent structure prediction by Lois Jeune et al [91], the black curve shows the concentration independent structure prediction by Raussens et al [90]. Horizontal lines represent the structure of the protein in solution. A clear difference between the two methods in the structure prediction for BSA is observable, whereas both methods are in excellent agreement for myoglobin. 10 individual spectra were condensed into one before structure determination. 3 of such sets were used to calculate standard deviations shown in the figure. Reproduced from [92].**

## Small angle X-ray scattering (SAXS)

SAXS is using X-ray scattering to investigate structures in the nanometer range. It lacks the atomic resolution provided by other methods like NMR or classical X-ray diffraction, but has certain advantages. First of all it is able to measure structures while they are in solution and non-crystalline and second it is not limited to dissolved or very small aggregates, but is able to handle bigger particles as well. Using X-ray in general has the advantage that many substances are to a certain degree transparent to X-ray, making it possible to measure samples that are not transparent to UV-VIS. Under certain circumstances SAXS can yield information that no other method is able to provide. Giving the right conditions for investigation as well as the right methods to evaluate the resulting raw data, SAXS can give not only a rough estimate of protein conformation, but it also possible to get information about the protein structure, orientation of proteins and the structure of the adsorbed layer [93-96]. Using SAXS it was possible to determine the layered structure of BSA adsorbed to nanoparticles demonstrating multilayer adsorption in a kind of ordered way. Distinct layers can be observed in the density profile between two particles (Figure 13) suggesting an ordered layer by layer accumulation during adsorption. Understanding not only simple mono-layer adsorption is a critical point in understanding the protein layer build up once particles enter the body, because in biological conditions multilayer adsorption of a mixture of proteins dominates the behavior of the nanoparticle in the body.

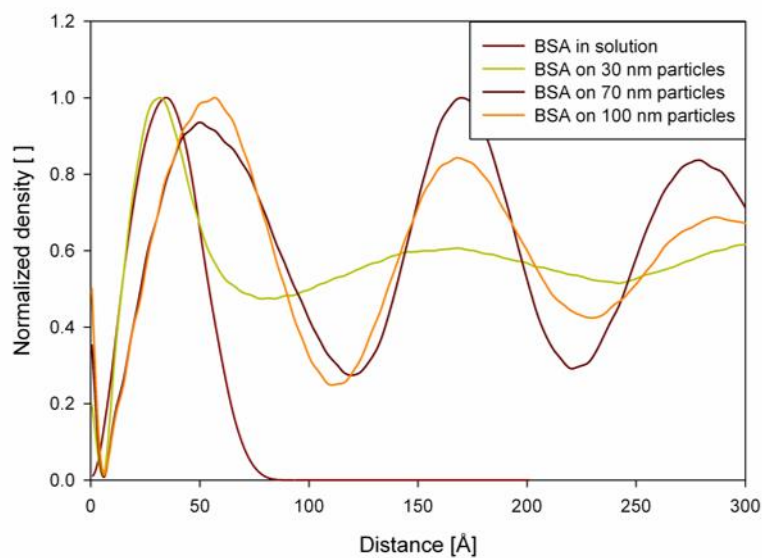


**Figure 13 – Density distribution on the surface of differently sized nanoparticles.**

## Conclusion

In this work a novel continuous purification method for drug covered nanoparticles was developed, based on a size exclusion chromatography in a closed loop simulated moving bed set-up. This technique is easy to scale up and simulated moving bed technology is widely used in small molecules industry to the very large scale. Even non-optimized Space-Time-Yields of  $0.25 \text{ g h}^{-1} \text{ L}^{-1}$  chromatography resin achieved in lab scale experiments are high enough for industrial applications to purify drug covered nanoparticles for pharmaceutical application. This novel purification strategy will facilitate the use of drug-nanoparticle-conjugates in bio-related fields. Using this purification strategy in conjunction with traditional methods such as centrifugation allowed to assess a pending problem in protein-nanoparticle conjugates: the conformational change of protein upon adsorption. Adsorption-based conformational changes could be demonstrated in the experiments in two out of nine model proteins, namely myoglobin and BSA. The literature is not conclusive if adsorption of proteins to nanoparticles has a stabilizing or destabilizing effect on the secondary structure elements of proteins. Our study was the first in this field to assess a complete range of nanoparticles instead of only one or two nanoparticle sizes. This comprehensive data set showed a decrease in alpha helical structure upon adsorption for both proteins. Both proteins share a conformational change dependent on the size of the nanoparticle to which they are adsorbed. This phenomenon has been suggested in the literature, but never investigated in detail in regards to the nanoparticle size. Both proteins show no conformational change upon adsorption to small particles below 100 nm, increasing conformational change in a transition region ranging from 100 to 300 nm, and a steady conformation above 300 nm. The change from one structure in solution and on small nanoparticles to a structure while adsorbed on big nanoparticles seems to have a sigmoidal shape. The collected data regarding the size dependent conformational changes of myoglobin and BSA allowed the assessment of theories currently under discussion about the driving force for nanoparticle size dependent conformational changes of proteins adsorbed to nanoparticles.

Using model calculations the implications of the two theories which are currently discussed in the literature were calculated: (i) the direct impact of the curvature on either the interaction area or the nature of the curved surface and (ii) the double layer potential building up at the interface is geometry dependent and different for different sizes of nanoparticles. Only the double layer potential based theory is somewhat compatible with the size range in which we detected changes, as the interaction area of protein and nanoparticle as well as the curvature visible for the protein does not change any more above 100 nm particle size, suggesting an essentially flat surface from the viewpoint of the protein. We therefore conclude that the first theory, based on the direct influence of the curvature, can be excluded for explaining the size dependent conformation changes of proteins adsorbed nanoparticles. Although the formation of the double layer potential is roughly compatible with the data set experiments on the nature of interaction between particle and protein determined hydrophobicity to be the main driving force for binding of BSA. So either the double layer potential has no influence at all and some other fundamental impact is missing about nanoparticle-protein interactions, or it is at least not the whole story.

This result will allow the scientific community to focus on providing additional insight into the influence of surface potential on protein conformational changes. Further still, it is not explained yet why certain proteins change their conformation upon adsorption and others do not. A simple correlation with known protein parameters like size, charge or thermal stability was not possible, suggesting missing fundamental puzzle pieces in the understanding of protein-nanoparticle interaction. As in the study NMR was not able to provide atomic information on the interaction of nanoparticles larger than proteins (above 10 nm) the only investigation tool which is nowadays available to provide atomic information on this scale is molecular dynamics simulation studies. Such studies have to have starting points for their simulation and need a rather well defined system before starting the simulation, so surface characteristics, protein structure and protein orientation on the surface.

The only other experimental way of assessing something this small is small angle x-ray scattering, which was also employed in this study to get information on the layering on multilayer adsorption onto nanoparticles. Distinct layers were observed that each corresponds to the thickness of one protein molecule suggesting an ordered layer by layer structure of the multilayer adsorption. This may provide a starting point for future studies using molecular dynamics simulations. In conclusion this work suggests to carefully consider nanoparticle size for bio-related applications. A factor which is sometimes neglected or thought of as unimportant in the context of nanoparticle applications which usually concentrate on particle material or surface modification.

According to the objective of the thesis:

- a scalable purification method fit for industrial use has been developed to separate protein loaded nanoparticles from residual protein and other compounds and
- protein conformational changes that happen upon adsorption to nanoparticles have been shown to be size dependent and consistent between different proteins and
- the existing hypothesis for the cause of this phenomenon have been evaluated. It was possible to dismiss all but one mechanisms completely and that the remaining one is not able to account for all aspects seen in the data and therefore has to be either modified or complimented by a different mechanism.

# Lists

## References

- [1] R. de Lima, A. B. Seabra, and N. Durán, "Silver nanoparticles: a brief review of cytotoxicity and genotoxicity of chemically and biogenically synthesized nanoparticles," *Journal of Applied Toxicology*, vol. 32, pp. 867-879, 2012.
- [2] S. E. Albo, L. J. Broadbelt, and R. Q. Snurr, "Multiscale modeling of transport and residence times in nanostructured membranes," *AIChE Journal*, vol. 52, pp. 3679-3687, 2006.
- [3] F. N. Crespilho, M. E. Ghica, C. Gouveia-Caridade, O. N. Oliveira Jr, and C. M. A. Brett, "Enzyme immobilisation on electroactive nanostructured membranes (ENM): Optimised architectures for biosensing," *Talanta*, vol. 76, pp. 922-928, 8/15/ 2008.
- [4] J. R. Siqueira Jr, F. N. Crespilho, V. Zucolotto, and O. N. Oliveira Jr, "Bifunctional electroactive nanostructured membranes," *Electrochemistry Communications*, vol. 9, pp. 2676-2680, 11// 2007.
- [5] M. Tsuchiya, B.-K. Lai, and S. Ramanathan, "Scalable nanostructured membranes for solid-oxide fuel cells," *Nat Nano*, vol. 6, pp. 282-286, 05//print 2011.
- [6] L. Yang, R. Xing, Q. Shen, K. Jiang, F. Ye, J. Wang, et al., "Fabrication of Protein-Conjugated Silver Sulfide Nanorods in the Bovine Serum Albumin Solution," *The Journal of Physical Chemistry B*, vol. 110, pp. 10534-10539, 2006/06/01 2006.
- [7] T. S. Hauck, A. A. Ghazani, and W. C. W. Chan, "Assessing the Effect of Surface Chemistry on Gold Nanorod Uptake, Toxicity, and Gene Expression in Mammalian Cells," *Small*, vol. 4, pp. 153-159, 2008.
- [8] A. M. Alkilany, P. K. Nagaria, C. R. Hexel, T. J. Shaw, C. J. Murphy, and M. D. Wyatt, "Cellular Uptake and Cytotoxicity of Gold Nanorods: Molecular Origin of Cytotoxicity and Surface Effects," *Small*, vol. 5, pp. 701-708, 2009.
- [9] A. E. Nel, L. Mädler, D. Velegol, T. Xia, E. M. V. Hoek, P. Somasundaran, et al., "Understanding biophysicochemical interactions at the nano-bio interface," *Nature Materials*, vol. 8, pp. 543-557, 2009.
- [10] I. Lynch, T. Cedervall, M. Lundqvist, C. Cabaleiro-Lago, S. Linse, and K. A. Dawson, "The Nanoparticle-Protein Complex as a Biological Entity; A Complex Fluids and Surface Science Challenge for the 21st Century," *Advances in Colloid and Interface Science*, vol. 134-135, pp. 167-174, 10/31/ 2007.
- [11] A. A. Shemetov, I. Nabiev, and A. Sukhanova, "Molecular Interaction of Proteins and Peptides with Nanoparticles," *ACS Nano*, vol. 6, pp. 4585-4602, 2012/06/26 2012.
- [12] N. Welsch, Y. Lu, J. Dzubiella, and M. Ballauff, "Adsorption of proteins to functional polymeric nanoparticles," *Polymer*, vol. 54, pp. 2835-2849, 5/24/ 2013.
- [13] Z. Wu, B. Zhang, and B. Yan, "Regulation of Enzyme Activity through Interactions with Nanoparticles," *International Journal of Molecular Sciences*, vol. 10, pp. 4198-4209, 2009.
- [14] I. Fenoglio, B. Fubini, E. M. Ghibaudi, and F. Turci, "Multiple Aspects of the Interaction of Biomacromolecules with Inorganic Surfaces," *Advanced Drug Delivery Reviews*, vol. 63, pp. 1186-1209, 10// 2011.
- [15] J. C. Y. Kah, E. L. L. Yeo, W. L. Koh, B. E. A. Poinard, and D. J. H. Neo, "Nanoparticle interface to biology: Applications in probing and modulating biological processes," *Critical Reviews in Biomedical Engineering*, vol. 41, pp. 323-341, 2013.
- [16] V. Reddy, E. Lymar, M. Hu, and J. F. Hainfeld, "5 nm Gold-Ni-NTA Binds His Tags," *Microscopy and Microanalysis*, vol. 11, pp. 1118-1119, 2005.

- [17] V. Lin, "TEM of mesoporous silica," ed. Wiki Commons: Wiki Commons, 2008.
- [18] P. Satzer, M. Wellhoefer, and A. Jungbauer, "Continuous separation of protein loaded nanoparticles by simulated moving bed chromatography," *Journal of Chromatography A*, vol. 1349, pp. 44-49, 7/4/ 2014.
- [19] M.-C. Daniel and D. Astruc, "Gold Nanoparticles: Assembly, Supramolecular Chemistry, Quantum-Size-Related Properties, and Applications toward Biology, Catalysis, and Nanotechnology," *Chemical Reviews*, vol. 104, pp. 293-346, 2004/01/01 2003.
- [20] P. K. Jain, K. S. Lee, I. H. El-Sayed, and M. A. El-Sayed, "Calculated Absorption and Scattering Properties of Gold Nanoparticles of Different Size, Shape, and Composition: Applications in Biological Imaging and Biomedicine," *The Journal of Physical Chemistry B*, vol. 110, pp. 7238-7248, 2006/04/01 2006.
- [21] P. Ghosh, G. Han, M. De, C. K. Kim, and V. M. Rotello, "Gold nanoparticles in delivery applications," *Advanced Drug Delivery Reviews*, vol. 60, pp. 1307-1315, 8/17/ 2008.
- [22] F. H. a. F. A. D. a. Z. Z. a. D. N. S. a. J. A. K.-E. a. H. M. S. James, "Gold nanoparticles enhance the radiation therapy of a murine squamous cell carcinoma," *Physics in Medicine and Biology*, vol. 55, p. 3045, 2010.
- [23] F. Arduini, C. Zanardi, S. Cinti, F. Terzi, D. Moscone, G. Palleschi, et al., "Effective electrochemical sensor based on screen-printed electrodes modified with a carbon black-Au nanoparticles composite," *Sensors and Actuators B: Chemical*, vol. 212, pp. 536-543, 6// 2015.
- [24] J. K. Nayak, P. Parhi, and R. Jha, "Graphene oxide encapsulated gold nanoparticle based stable fibre optic sucrose sensor," *Sensors and Actuators B: Chemical*, vol. 221, pp. 835-841, 12/31/ 2015.
- [25] T. Shaikh, A. Nafady, F. N. Talpur, Sirajuddin, M. H. Agheem, M. R. Shah, et al., "Tranexamic acid derived gold nanoparticles modified glassy carbon electrode as sensitive sensor for determination of nalbuphine," *Sensors and Actuators B: Chemical*, vol. 211, pp. 359-369, 5// 2015.
- [26] R. H. Vignesh, K. V. Sankar, S. Amaresh, Y. S. Lee, and R. K. Selvan, "Synthesis and characterization of MnFe<sub>2</sub>O<sub>4</sub> nanoparticles for impedometric ammonia gas sensor," *Sensors and Actuators B: Chemical*, vol. 220, pp. 50-58, 12/1/ 2015.
- [27] I. I. Slowing, B. G. Trewyn, S. Giri, and V. S. Y. Lin, "Mesoporous Silica Nanoparticles for Drug Delivery and Biosensing Applications," *Advanced Functional Materials*, vol. 17, pp. 1225-1236, 2007.
- [28] N. Kato and N. Kato, "High-yield hydrothermal synthesis of mesoporous silica hollow capsules," *Microporous and Mesoporous Materials*, vol. 219, pp. 230-239, 1/1/ 2016.
- [29] Z. Zhang, A. Mayoral, and I. Melián-Cabrera, "Protocol optimization for the mild detemplation of mesoporous silica nanoparticles resulting in enhanced texture and colloidal stability," *Microporous and Mesoporous Materials*, vol. 220, pp. 110-119, 1/15/ 2016.
- [30] L. Zhuang, B. Ma, S. Chen, X. Hou, and S. Chen, "Fast synthesis of mesoporous silica materials via simple organic compounds templated sol-gel route in the absence of hydrogen bond," *Microporous and Mesoporous Materials*, vol. 213, pp. 22-29, 9/1/ 2015.
- [31] M. Fernández-García and J. A. Rodriguez, "Metal Oxide Nanoparticles," in *Encyclopedia of Inorganic and Bioinorganic Chemistry*, ed: John Wiley & Sons, Ltd, 2011.
- [32] P. K. Stoimenov, R. L. Klinger, G. L. Marchin, and K. J. Klabunde, "Metal Oxide Nanoparticles as Bactericidal Agents," *Langmuir*, vol. 18, pp. 6679-6686, 2002/08/01 2002.
- [33] M. E. Franke, T. J. Koplin, and U. Simon, "Metal and Metal Oxide Nanoparticles in Chemiresistors: Does the Nanoscale Matter?," *Small*, vol. 2, pp. 36-50, 2006.
- [34] A. A. Keller, H. Wang, D. Zhou, H. S. Lenihan, G. Cherr, B. J. Cardinale, et al., "Stability and Aggregation of Metal Oxide Nanoparticles in Natural Aqueous Matrices," *Environmental Science & Technology*, vol. 44, pp. 1962-1967, 2010/03/15 2010.

- [35] F. Höök, J. Vörös, M. Rodahl, R. Kurrat, P. Böni, J. J. Ramsden, et al., "A comparative study of protein adsorption on titanium oxide surfaces using in situ ellipsometry, optical waveguide lightmode spectroscopy, and quartz crystal microbalance/dissipation," *Colloids and Surfaces B: Biointerfaces*, vol. 24, pp. 155-170, 3/15/ 2002.
- [36] T. F. Keller, J. Reichert, T. P. Thanh, R. Adjiski, L. Spiess, L. Berzina-Cimdina, et al., "Facets of protein assembly on nanostructured titanium oxide surfaces," *Acta Biomaterialia*, vol. 9, pp. 5810-5820, 3// 2013.
- [37] J. L. Dalsin, L. Lin, S. Tosatti, J. Vörös, M. Textor, and P. B. Messersmith, "Protein Resistance of Titanium Oxide Surfaces Modified by Biologically Inspired mPEG-DOPA," *Langmuir*, vol. 21, pp. 640-646, 2005/01/01 2004.
- [38] C. Weber, C. Coester, J. Kreuter, and K. Langer, "Desolvation process and surface characterisation of protein nanoparticles," *International Journal of Pharmaceutics*, vol. 194, pp. 91-102, 1/20/ 2000.
- [39] M. J. Hawkins, P. Soon-Shiong, and N. Desai, "Protein nanoparticles as drug carriers in clinical medicine," *Advanced Drug Delivery Reviews*, vol. 60, pp. 876-885, 5/22/ 2008.
- [40] K. Langer, C. Coester, C. Weber, H. von Briesen, and J. Kreuter, "Preparation of avidin-labeled protein nanoparticles as carriers for biotinylated peptide nucleic acid," *European Journal of Pharmaceutics and Biopharmaceutics*, vol. 49, pp. 303-307, 5/2/ 2000.
- [41] A. Gomez, D. Bingham, L. d. Juan, and K. Tang, "Production of protein nanoparticles by electrospray drying," *Journal of Aerosol Science*, vol. 29, pp. 561-574, 6/1/ 1998.
- [42] M. Lundqvist, J. Stigler, G. Elia, I. Lynch, T. Cedervall, and K. A. Dawson, "Nanoparticle size and surface properties determine the protein corona with possible implications for biological impacts," *Proceedings of the National Academy of Sciences*, vol. 105, pp. 14265-14270, 2008.
- [43] E. Casals, T. Pfaller, A. Duschl, G. J. Oostingh, and V. Puntès, "Time Evolution of the Nanoparticle Protein Corona," *ACS Nano*, vol. 4, pp. 3623-3632, 2010/07/27 2010.
- [44] A. des Rieux, V. Fievez, M. Garinot, Y.-J. Schneider, and V. Pr at, "Nanoparticles as potential oral delivery systems of proteins and vaccines: A mechanistic approach," *Journal of Controlled Release*, vol. 116, pp. 1-27, 11/10/ 2006.
- [45] K. S. Soppimath, T. M. Aminabhavi, A. R. Kulkarni, and W. E. Rudzinski, "Biodegradable polymeric nanoparticles as drug delivery devices," *Journal of Controlled Release*, vol. 70, pp. 1-20, 1/29/ 2001.
- [46] W. Tan, K. Wang, X. He, X. J. Zhao, T. Drake, L. Wang, et al., "Bionanotechnology based on silica nanoparticles," *Medicinal Research Reviews*, vol. 24, pp. 621-638, 2004.
- [47] H.-H. Yang, S.-Q. Zhang, X.-L. Chen, Z.-X. Zhuang, J.-G. Xu, and X.-R. Wang, "Magnetite-Containing Spherical Silica Nanoparticles for Biocatalysis and Bioseparations," *Analytical Chemistry*, vol. 76, pp. 1316-1321, 2004/03/01 2004.
- [48] W. Lin, Y.-w. Huang, X.-D. Zhou, and Y. Ma, "In vitro toxicity of silica nanoparticles in human lung cancer cells," *Toxicology and Applied Pharmacology*, vol. 217, pp. 252-259, 12/15/ 2006.
- [49] L. Li, T. Liu, C. Fu, L. Tan, X. Meng, and H. Liu, "Biodistribution, excretion, and toxicity of mesoporous silica nanoparticles after oral administration depend on their shape," *Nanomedicine: Nanotechnology, Biology and Medicine*.
- [50] I. I. Slowing, B. G. Trewyn, and V. S. Y. Lin, "Mesoporous Silica Nanoparticles for Intracellular Delivery of Membrane-Impermeable Proteins," *Journal of the American Chemical Society*, vol. 129, pp. 8845-8849, 2007/07/01 2007.
- [51] I. I. Slowing, J. L. Vivero-Escoto, C.-W. Wu, and V. S. Y. Lin, "Mesoporous silica nanoparticles as controlled release drug delivery and gene transfection carriers," *Advanced Drug Delivery Reviews*, vol. 60, pp. 1278-1288, 8/17/ 2008.
- [52] J. L. Vivero-Escoto, I. I. Slowing, B. G. Trewyn, and V. S. Y. Lin, "Mesoporous Silica Nanoparticles for Intracellular Controlled Drug Delivery," *Small*, vol. 6, pp. 1952-1967, 2010.

- [53] T. Chen, N. Yang, and J. Fu, "Controlled Release of Cargo Molecules from Hollow Mesoporous Silica Nanoparticles Based on Acid and Base Dual-Responsive Cucurbit[7]uril Pseudorotaxanes," *Chemical Communications*, vol. 49, pp. 6555-6557, 2013.
- [54] H. Wanyika, "Sustained Release of Fungicide Metalaxyl by Mesoporous Silica Nanospheres," *Journal of Nanoparticle Research*, vol. 15, pp. 1-9, 2013/07/10 2013.
- [55] M. Lundqvist, J. Stigler, T. Cedervall, T. Berggård, M. B. Flanagan, I. Lynch, et al., "The Evolution of the Protein Corona around Nanoparticles: A Test Study," *ACS Nano*, vol. 5, pp. 7503-7509, 2011/09/27 2011.
- [56] J. S. Gebauer, M. Malissek, S. Simon, S. K. Knauer, M. Maskos, R. H. Stauber, et al., "Impact of the Nanoparticle-Protein Corona on Colloidal Stability and Protein Structure," *Langmuir*, vol. 28, pp. 9673-9679, 2012/06/26 2012.
- [57] E. Casals, T. Pfaller, A. Duschl, G. J. Oostingh, and V. F. Puntes, "Hardening of the Nanoparticle-Protein Corona in Metal (Au, Ag) and Oxide (Fe<sub>3</sub>O<sub>4</sub>, CoO, and CeO<sub>2</sub>) Nanoparticles," *Small*, vol. 7, pp. 3479-3486, 2011.
- [58] T. Cedervall, I. Lynch, S. Lindman, T. Berggård, E. Thulin, H. Nilsson, et al., "Understanding the nanoparticle-protein corona using methods to quantify exchange rates and affinities of proteins for nanoparticles," *Proceedings of the National Academy of Sciences*, vol. 104, pp. 2050-2055, 2007.
- [59] M. P. Monopoli, D. Walczyk, A. Campbell, G. Elia, I. Lynch, F. Baldelli Bombelli, et al., "Physical-Chemical Aspects of Protein Corona: Relevance to in Vitro and in Vivo Biological Impacts of Nanoparticles," *Journal of the American Chemical Society*, vol. 133, pp. 2525-2534, 2011/03/02 2011.
- [60] P. Billsten, P.-O. Freskgård, U. Carlsson, B.-H. Jonsson, and H. Elwing, "Adsorption to silica nanoparticles of human carbonic anhydrase II and truncated forms induce a molten-globule-like structure," *FEBS Letters*, vol. 402, pp. 67-72, 2/3/ 1997.
- [61] M. Lundqvist, I. Sethson, and B.-H. Jonsson, "Protein Adsorption onto Silica Nanoparticles: Conformational Changes Depend on the Particles' Curvature and the Protein Stability," *Langmuir*, vol. 20, pp. 10639-10647, 2004/11/01 2004.
- [62] M. Lundqvist, I. Sethson, and B.-H. Jonsson, "High-Resolution 2D <sup>1</sup>H-<sup>15</sup>N NMR Characterization of Persistent Structural Alterations of Proteins Induced by Interactions with Silica Nanoparticles," *Langmuir*, vol. 21, pp. 5974-5979, 2005/06/01 2005.
- [63] M. Lundqvist, I. Sethson, and B.-H. Jonsson, "Transient Interaction with Nanoparticles "Freezes" a Protein in an Ensemble of Metastable Near-Native Conformations<sup>†</sup>," *Biochemistry*, vol. 44, pp. 10093-10099, 2005/08/01 2005.
- [64] M. Tian, W.-K. Lee, M. K. Bothwell, and J. McGuire, "Structural Stability Effects on Adsorption of Bacteriophage T4 Lysozyme to Colloidal Silica," *Journal of Colloid and Interface Science*, vol. 200, pp. 146-154, 4/1/ 1998.
- [65] A. A. Vertegel, R. W. Siegel, and J. S. Dordick, "Silica Nanoparticle Size Influences the Structure and Enzymatic Activity of Adsorbed Lysozyme," *Langmuir*, vol. 20, pp. 6800-6807, 2004/08/01 2004.
- [66] S. Shrivastava, S. A. McCallum, J. H. Nuffer, X. Qian, R. W. Siegel, and J. S. Dordick, "Identifying Specific Protein Residues That Guide Surface Interactions and Orientation on Silica Nanoparticles," *Langmuir*, vol. 29, pp. 10841-10849, 2013/08/27 2013.
- [67] W. Shang, J. H. Nuffer, J. S. Dordick, and R. W. Siegel, "Unfolding of Ribonuclease A on Silica Nanoparticle Surfaces," *Nano Letters*, vol. 7, pp. 1991-1995, 2007/07/01 2007.
- [68] Z. Wang, K. Zhang, J. Zhao, X. Liu, and B. Xing, "Adsorption and inhibition of butyrylcholinesterase by different engineered nanoparticles," *Chemosphere*, vol. 79, pp. 86-92, 3// 2010.

- [69] X. Wu and G. Narsimhan, "Characterization of Secondary and Tertiary Conformational Changes of  $\beta$ -Lactoglobulin Adsorbed on Silica Nanoparticle Surfaces," *Langmuir*, vol. 24, pp. 4989-4998, 2008/05/01 2008.
- [70] S. Tenzer, D. Docter, J. Kuharev, A. Musyanovych, V. Fetz, R. Hecht, et al., "Rapid formation of plasma protein corona critically affects nanoparticle pathophysiology," *Nat Nano*, vol. 8, pp. 772-781, 10//print 2013.
- [71] S. H. D. P. Lacerda, J. J. Park, C. Meuse, D. Pristinski, M. L. Becker, A. Karim, et al., "Interaction of Gold Nanoparticles with Common Human Blood Proteins," *ACS Nano*, vol. 4, pp. 365-379, 2010/01/26 2009.
- [72] R. Cukalevski, M. Lundqvist, C. Oslakovic, B. Dahlbäck, S. Linse, and T. Cedervall, "Structural Changes in Apolipoproteins Bound to Nanoparticles," *Langmuir*, vol. 27, pp. 14360-14369, 2011/12/06 2011.
- [73] F. Bellezza, A. Cipiciani, L. Latterini, T. Posati, and P. Sassi, "Structure and Catalytic Behavior of Myoglobin Adsorbed onto Nanosized Hydrotalcites," *Langmuir*, vol. 25, pp. 10918-10924, 2009/09/15 2009.
- [74] C. Cai, U. Bakowsky, E. Rytting, A. K. Schaper, and T. Kissel, "Charged Nanoparticles as Protein Delivery Systems: A Feasibility Study Using Lysozyme as Model Protein," *European Journal of Pharmaceutics and Biopharmaceutics*, vol. 69, pp. 31-42, 5// 2008.
- [75] M. Lück, B. R. Paulke, W. Schröder, T. Blunk, and R. H. Müller, "Analysis of Plasma Protein Adsorption on Polymeric Nanoparticles with Different Surface Characteristics," *Journal of Biomedical Materials Research*, vol. 39, pp. 478-485, 1998.
- [76] M. Karlsson, J. Ekeröth, H. Elwing, and U. Carlsson, "Reduction of Irreversible Protein Adsorption on Solid Surfaces by Protein Engineering for Increased Stability," *Journal of Biological Chemistry*, vol. 280, pp. 25558-25564, 2005.
- [77] N. O. Fischer, C. M. McIntosh, J. M. Simard, and V. M. Rotello, "Inhibition of Chymotrypsin through Surface Binding Using Nanoparticle-based Receptors," *Proceedings of the National Academy of Sciences*, vol. 99, pp. 5018-5023, 2002.
- [78] C. K. Bower, S. Sananikone, M. K. Bothwell, and J. McGuire, "Activity losses among T4 lysozyme charge variants after adsorption to colloidal silica," *Biotechnology and Bioengineering*, vol. 64, pp. 373-376, 1999.
- [79] S. Manokaran, X. Zhang, W. Chen, and D. K. Srivastava, "Differential modulation of the active site environment of human carbonic anhydrase XII by cationic quantum dots and polylysine," *Biochimica et Biophysica Acta (BBA) - Proteins and Proteomics*, vol. 1804, pp. 1376-1384, 6// 2010.
- [80] A. Rajeshwari, S. Pakrashi, S. Dalai, Madhumita, V. Iswarya, N. Chandrasekaran, et al., "Spectroscopic studies on the interaction of bovine serum albumin with Al<sub>2</sub>O<sub>3</sub> nanoparticles," *Journal of Luminescence*, vol. 145, pp. 859-865, 1// 2014.
- [81] D. M. Brown, C. Dickson, P. Duncan, F. Al-Attili, and V. Stone, "Interaction between nanoparticles and cytokine proteins: impact on protein and particle functionality," *Nanotechnology*, vol. 21, pp. 215104-215112, // 2010.
- [82] P. Chen, S. A. Seabrook, V. C. Epa, K. Kurabayashi, A. S. Barnard, D. A. Winkler, et al., "Contrasting effects of nanoparticle binding on protein denaturation," *Journal of Physical Chemistry C*, vol. 118, pp. 22069-22078, 2014.
- [83] Y. Y. Syu, J. H. Hung, J. C. Chen, and H. W. Chuang, "Impacts of size and shape of silver nanoparticles on Arabidopsis plant growth and gene expression," *Plant Physiology and Biochemistry*, vol. 83, pp. 57-64, 2014.
- [84] Z. Hu, H. Zhang, Y. Zhang, R. Wu, and H. Zou, "Nanoparticle size matters in the formation of plasma protein coronas on Fe<sub>3</sub>O<sub>4</sub> nanoparticles," *Colloids and Surfaces B: Biointerfaces*, vol. 121, pp. 354-361, 2014.

- [85] D. Joshi and R. K. Soni, "Laser-induced synthesis of silver nanoparticles and their conjugation with protein," *Applied Physics A: Materials Science and Processing*, vol. 116, pp. 635-641, 2014.
- [86] G. A. Barhate, S. M. Gaikwad, S. S. Jadhav, and V. B. Pokharkar, "Structure function attributes of gold nanoparticle vaccine association: Effect of particle size and association temperature," *International Journal of Pharmaceutics*, vol. 471, pp. 439-448, 2014.
- [87] D. R. Latulippe and A. L. Zydney, "Size exclusion chromatography of plasmid DNA isoforms," *Journal of Chromatography A*, vol. 1216, pp. 6295-6302, 8/28/ 2009.
- [88] K. Farkas, A. Varsani, D. Marjoshi, R. Easingwood, E. McGill, and L. Pang, "Size exclusion-based purification and PCR-based quantitation of MS2 bacteriophage particles for environmental applications," *Journal of Virological Methods*, vol. 213, pp. 135-138, 3/1/ 2015.
- [89] R. Wang, J. Wang, J. Li, Y. Wang, Z. Xie, and L. An, "Comparison of two gel filtration chromatographic methods for the purification of Lily symptomless virus," *Journal of Virological Methods*, vol. 139, pp. 125-131, 2// 2007.
- [90] V. Raussens, J.-M. Ruysschaert, and E. Goormaghtigh, "Protein concentration is not an absolute prerequisite for the determination of secondary structure from circular dichroism spectra: a new scaling method," *Analytical Biochemistry*, vol. 319, pp. 114-121, 8/1/ 2003.
- [91] C. Louis-Jeune, M. A. Andrade-Navarro, and C. Perez-Iratxeta, "Prediction of protein secondary structure from circular dichroism using theoretically derived spectra," *Proteins: Structure, Function, and Bioinformatics*, vol. 80, pp. 374-381, 2012.
- [92] P. Satzer, F. Svec, G. Sekot, and A. Jungbauer, *Protein adsorption onto nanoparticles induces conformational changes: Particle size dependency, kinetics and mechanisms. Unpublished Work, 2015*
- [93] J. H. Kim, J. R. Bothe, T. R. Alderson, and J. L. Markley, "Tangled web of interactions among proteins involved in iron–sulfur cluster assembly as unraveled by NMR, SAXS, chemical crosslinking, and functional studies," *Biochimica et Biophysica Acta (BBA) - Molecular Cell Research*, vol. 1853, pp. 1416-1428, 6// 2015.
- [94] A. G. Kikhney and D. I. Svergun, "A practical guide to small angle X-ray scattering (SAXS) of flexible and intrinsically disordered proteins," *FEBS Letters*, vol. 589, pp. 2570-2577, 9/14/ 2015.
- [95] I. Kontro, S. K. Wiedmer, U. Hynönen, P. A. Penttilä, A. Palva, and R. Serimaa, "The structure of *Lactobacillus brevis* surface layer reassembled on liposomes differs from native structure as revealed by SAXS," *Biochimica et Biophysica Acta (BBA) - Biomembranes*, vol. 1838, pp. 2099-2104, 8// 2014.
- [96] P. M. Abuja, I. Pilz, P. Tomme, and M. Claeysens, "Structural changes in cellobiohydrolase I upon binding of a macromolecular ligand as evident by SAXS investigations," *Biochemical and Biophysical Research Communications*, vol. 165, pp. 615-623, 12/15/ 1989.

## List of figures

**Figure 1 – Typical Characterization of Nanomaterials depending on the number of nanodimensions.**

**Figure 2 – 5 nm gold nanoparticles (A [16]), 100 nm mesoporous silica nanoparticles (B [17]), 70 nm solid silica nanoparticles (C [18]), polydisperse organic polystyrene nanoparticles (D).**

**Figure 3 – Principle of a drug carrier particle, which is loaded with a cytotoxic drug and coated to protect the drug from the body and vice versa. Once the particle is at its desired destination in the body and the environment changes, the drug is released by destroying the bond between the capping agent and the drug carrier.**

**Figure 4 – Nanoparticles in a protein mixture build up a hard protein corona, which does not interact with the proteins in solution and its composition is mainly dependent on the abundance of individual proteins, and a soft protein corona, which interchanges proteins with the bulk solution by desorption and resorption and is mainly dependent on the affinity of the protein to the surface.**

**Figure 5 – Use of a full coverage protein layer to prevent hydrophobic interactions of polystyrene nanoparticles and size exclusion chromatography media (A) and the separation of bovine serum albumin covered 60 nm polystyrene (B) and 70 nm silica (C) nanoparticles from free bovine serum albumin by low salt size exclusion chromatography.**

**Figure 6 – Concentrations of 70 nm silica nanoparticles (●) and beta casein (○) in the Extract (Panel A) and Raffinate (Panel B) of the closed loop SEC-SMB [18].**

**Figure 7 – Proposed process for a continuous production of drug covered nanoparticles by the use of a simulated moving bed system for separation and a tangential flow filtration for concentration.**

**Figure 8 – Principle of ATR-FT-IR spectroscopy, showing the total reflection of the IR-beam and the evanescent field which propagates into the sample (A) spectra of bovine serum albumin showing the amide I and amide II bands, and bovine serum albumin free in solution (red curve) and adsorbed to particles (green curve) (B)**

**Figure 9 – Pulse sequences for one dimensional and two dimensional NMR**

**Figure 10 – One dimensional (A) and two dimensional (B) proton NMR spectra of beta casein. The solvent peak has been cut out in the one dimensional spectra and interesting areas in the two dimensional spectra are marked with red and green rectangles.**

**Figure 11 – Circular dichroic spectra of bovine serum albumin (A) and the principle curves behind the deconvolution of the spectra into a structural composition (B) where blue is a complete random coil protein, yellow is a complete beta sheet protein and green is a complete alpha helical protein.**

**Figure 12 – alpha helical content of myoglobin (A) and BSA (B) adsorbed on nanoparticles varying in size. The red curve shows the concentration dependent structure prediction by Lois Jeune et al [91], the black curve shows the concentration independent structure prediction by Raussens et al [90]. Horizontal lines represent the structure of the protein in solution. A clear difference between the two methods in the structure prediction for BSA is observable, whereas both methods are in excellent agreement for myoglobin. 10 individual spectra were condensed into one before structure determination. 3 of such sets were used to calculate standard deviations shown in the figure. Reproduced from [92].**

**Figure 13 – Density distribution on the surface of differently sized nanoparticles.**

# Publications

***Publication 1 - Continuous separation of protein loaded nanoparticles by simulated moving bed chromatography***

P. Satzer, M. Wellhoefer, A. Jungbauer; Journal of Chromatography A 2014, 1347, 44-49

***Publication 2 – Protein adsorption onto nanoparticles induces conformational changes: Particle size dependency, kinetics and mechanisms***

P. Satzer, F. Svec, G. Sekot, and A. Jungbauer



# Continuous separation of protein loaded nanoparticles by simulated moving bed chromatography



Peter Satzer<sup>a</sup>, Martin Wellhoefer<sup>b</sup>, Alois Jungbauer<sup>a,b,\*</sup>

<sup>a</sup> Department of Biotechnology, University of Natural Resources and Life Sciences, Vienna (BOKU), Muthgasse 18, 1190 Vienna, Austria

<sup>b</sup> Austrian Centre of Industrial Biotechnology (ACIB), Muthgasse 18, 1190 Vienna, Austria

## ARTICLE INFO

### Article history:

Received 17 February 2014

Received in revised form 11 April 2014

Accepted 28 April 2014

Available online 4 May 2014

### Keywords:

Nanoparticles

Simulated moving bed

Separation

Protein

Size exclusion chromatography

## ABSTRACT

For scale up and efficient production of protein loaded nanoparticles continuous separation by size exclusion chromatography in simulated moving bed (SMB) mode helps do reduce unbound protein concentration and increase yields for perfectly covered particles. Silica nanoparticles were loaded with an excess of beta casein or bovine serum albumin (BSA) and the loaded particles purified by size exclusion chromatography using Sephacryl300 as stationary phase in a four zone SMB. We determined our working points for the SMB from batch separations and the triangle theory described by Mazzotti et al. with an SMB setup of one Sephacryl300 26/70 mm column per zone with switch times of 5 min for BSA and 7 min for beta casein. In the case of BSA the Raffinate contained loaded nanoparticles of 63% purity with 98% recovery and the extract was essentially particle free (95% purity). We showed that the low purity of the Raffinate was only due to BSA multimers present in the used protein solution. In the case of beta casein where no multimers are present we achieved 89% purity and 90% recovery of loaded nanoparticles in the Raffinate and an extract free of particles (92% purity). Using a tangential flow filtration unit with 5 kDa cutoff membrane we proved that the extract can be concentrated for recycling of protein and buffer. The calculated space–time–yield for loaded nanoparticles was 0.25 g of loaded nanoparticles per hour and liter of used resin. This proves that the presented process is suitable for large scale production for industrial purposes.

© 2014 The Authors. Published by Elsevier B.V. This is an open access article under the CC BY-NC-ND license (<http://creativecommons.org/licenses/by-nc-nd/3.0/>).

## 1. Introduction

Large scale separation of protein loaded nanoparticles is a pending problem. Simulated moving bed (SMB) chromatography using size exclusion chromatography is a way to separate the loaded particles from residual unbound protein in solution. SMB offers a way to scale up to large scale. Moreover, at the time more sophisticated nanoparticles with different characteristics are produced with open applications to different fields ranging from agriculture such as herbicide [1,2] to medicine such as vaccines, cancer treatment and drug delivery [3–9]. At the moment the separation of protein loaded nanoparticles is mostly done by ultracentrifugation [10] if done at all [9]. Some papers reported counter current separation of different kinds or sizes of nanoparticles, but didn't account for special needs of protein-nanoparticle separation and are dependent on

specific interactions of the nanoparticle and the chromatography material [11]. However, for applications where targeting is necessary because of side effects of unbound protein, efficient separation is mandatory. Ultracentrifugation has some serious downsides, it can only be operated in batch-mode, and therefore suffers from low productivity and high buffer consumption, and it is only applicable to relatively dense particles. SEC can be used for separation of small particles from other solutes and can be operated also in a continuous mode to reduce buffer consumption and can be operated to achieve higher productivities [12].

We present a method in which only the active compound is retained by the column, and the covered nanoparticle is excluded from all volumes within the chromatographic material. Used this way, this method is applicable to a wide variety of combinations of active compounds and nanoparticles. For productivity and to be able to recycle the unbound active compound and buffer, we used a 4 zone SMB chromatography as described by Mazzotti [12] with one SEC column per zone and showed separation of nanoparticle and protein with productivities suitable for large scale production. For this proof of concept we used 70 nm sized nanoparticles because this size roughly corresponds to virus sizes (or for that matter virus

\* Corresponding author at: University of Natural Resources and Life Sciences, Vienna (BOKU), Department of Biotechnology, Muthgasse 18, 1190 Vienna, Austria. Tel.: +43476546226; fax: +43476546677.

E-mail address: [alois.jungbauer@boku.ac.at](mailto:alois.jungbauer@boku.ac.at) (A. Jungbauer).

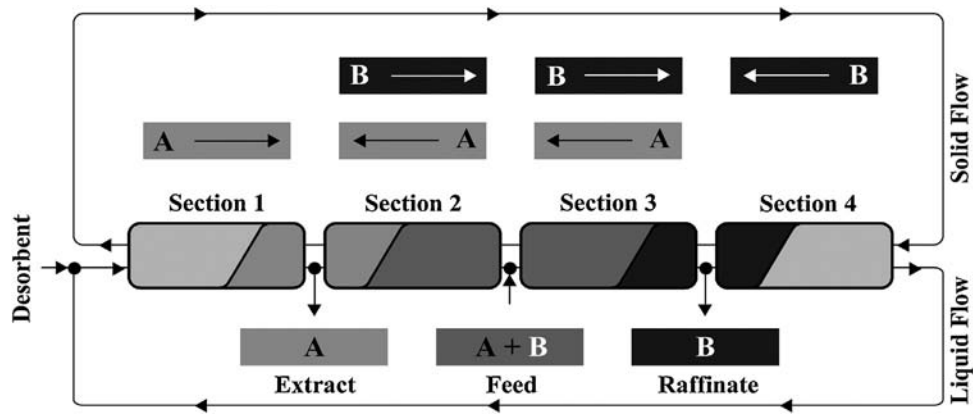


Fig. 1. Scheme representation of a four zone true moving bed.

like particles), which are commonly between 50 and 150 nm big. We think that especially the application as drug delivery vehicle and/or as vaccine are interesting routes which can benefit from special uptake mechanisms that have evolved to specifically deal with viruses efficiently.

1.1. Theory

Optimal operation conditions for an SMB system can be hard to determine empirically because of many adjustable and interconnected parameters. Different methods have been proposed to estimate suitable conditions for SMB. Ruthven and Ching [13] proposed a method later refined by Guiochon [14] which assumes linear isotherms but has to apply a safety margin on the modelled parameters to account for inaccuracy. An alternative process to find suitable parameters using equilibrium constants was presented by Storti and Mazzotti [15] and was termed triangle theory. For this model they also assumed linear adsorption isotherms, but also made the assumption that axial dispersion and mass transfer resistance are negligible. Later on, the triangle theory was refined by Mazotti et al. [12] and we based our parameters on the equation in this paper. The triangle theory works by defining a ratio for each of the four sections in the SMB, assigning different tasks to each section (Fig. 1). Zone 1 regenerates the chromatographic resin and section 4 regenerates the solvent, where section 2 and 3 are separating 2 species in a binary mixture.

According to Mazotti et al. we can formulate restrictions for each of these sections if we know the equilibrium constants of the species involved. To find this restriction one has to calculate the  $m_i$  values for each section, given by the following equation:

$$m_i = \frac{Q_i t^s - V\varepsilon}{V(q - \varepsilon)} \quad (1)$$

$Q_i$  is the volumetric flow,  $t^s$  is the switch time,  $V$  is the column volume and  $\varepsilon$  is the column porosity. Mazotti et al. showed that for complete separation these  $m_i$  values have to fulfill certain restrictions. To find this constrains one has to experimentally determine the Henry constants of the two components, preferably in the concentration range which is intended to be used in the SMB system. The first section  $m_1$  has to completely regenerate the column resin; likewise the fourth section has to completely regenerate the eluent. Therefore the following conditions can be formulated (2).

$$m_1 \geq h_1 \quad (2)$$

$$m_4 \leq h_2 \quad (3)$$

where  $h_1$  is the Henry coefficient of the more retained species and  $h_2$  is the Henry coefficient of the less retained species. Sections 2

and 3 are more critical in regards to parameter settings, as in these two sections the separation takes place. Again, we assume linear adsorption isotherms for all species involved, which lead us to the following set of restrictions for  $m_2$  (4) and  $m_3$  (5).

$$h_2 < m_2 \leq h_1 \quad (4)$$

$$h_2 \leq m_3 \leq h_1 \quad (5)$$

To find optimal parameters Mazotti et al. suggested to fix the values of  $m_1$  and  $m_4$  and to explore the  $m_2/m_3$  plane to find optimal parameters, reducing the complex problem of interconnected parameters to a 2D plot. A representation of the restrictions found by Eqs. (2)–(5) is the triangle (hence the name triangle theory) build up by the  $m_2/m_3$  plane (Fig. 2).

The zone of complete separation (triangle build up by points XYZ) is where all restrictions of Eqs. (2)–(5) are met, and the optimal production point in terms of productivity would be point X. However, this point is highly unstable as small variations in feed concentration or other parameters shift the actual working condition into Zone E or R leading to incomplete separation and loss of purity and productivity. Moreover, the triangle is only valid for strictly linear isotherms, which is rarely the case in any application. In real

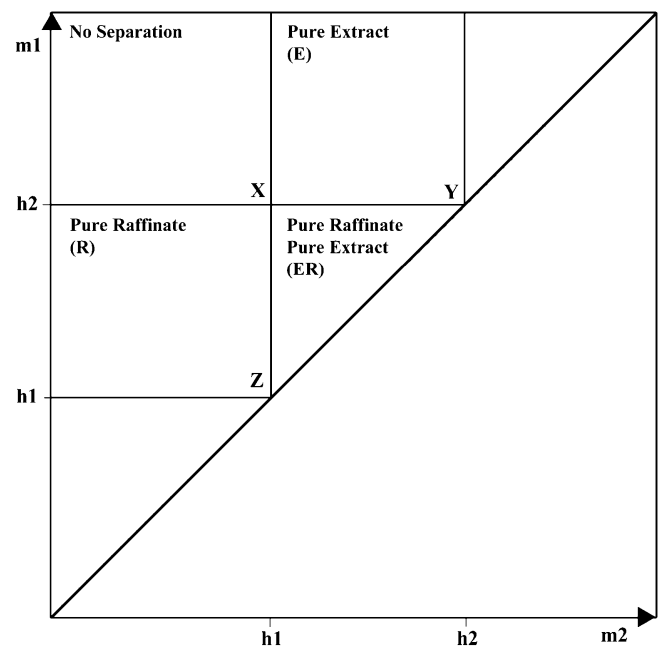


Fig. 2.  $m_2/m_3$  plane under the assumption of linear isotherms.

systems the zone of complete separation is distorted [15] which makes operation on this point  $X$  impossible. In this work we concentrated on designing a stable system for a proof of concept and therefore chose conservative values in the middle of the triangle. The productivity of the system is decreased by approaching the line of  $ZY$  because of the reduction of the feed flow rate, but this approach also diminishes the risk of failure due to non-linear isotherms in the system and due to flow fluctuations or imprecise determination of the Henry constants. For future work or real industrial applications a thorough investigation of the adsorption isotherms and the  $m_2/m_3$  is recommended for maximal productivity.

## 2. Material and methods

Chemicals without explicitly stated manufacturer were purchased from Sigma Aldrich (St Louis, USA).

### 2.1. Nanoparticles

Silica nanoparticles with amidine surface modification in the size of 30 nm, 70 nm, 200 nm and 1000 nm were purchased from Kisker (Steinfurt, Germany). The size and monodispersity was confirmed by TEM and DLS.

### 2.2. Determination of adsorption isotherm

To determine the adsorption isotherm of model proteins on nanoparticles, different concentrations of model protein were mixed with nanoparticles to obtain different protein concentrations combined with a fixed particle concentration of 2.5 mg/mL for 30 and 70 nm particles and 5.0 mg/mL for 200 and 1000 nm particles. The samples were incubated for 12 h to reach equilibrium. The concentration of model protein was determined by analytical SEC analysis as described below. No further sample preparation was necessary.

### 2.3. Analytical SEC

A Superdex 200 prep grade 10/200 GL size exclusion column (GE Healthcare, Piscaway, USA) was connected to an Agilent 1100 Series (Agilent Technologies, Santa Clara, USA) and equilibrated with SEC low salt running buffer (50 mM HEPES, pH 7.0) at 1.0 mL/min. 100  $\mu$ L of sample was injected and absorbance was monitored at 280 nm. The concentration of protein was determined by comparison to a calibration curve prepared from a standard solution of the same protein. The amount of nanoparticle was only determined relatively to the feed.

### 2.4. Preparative SEC

A Superdex 200 prep grade 10/200 GL size exclusion column (GE Healthcare) or a self-packed Sephacryl300 10/200 column (GE Healthcare) was connected to an ÄKTA-explorer system (GE Healthcare) and equilibrated with SEC low salt running buffer (50 mM HEPES, pH 7.0) at 1.0 mL/min. 200  $\mu$ L or 1000  $\mu$ L of sample was injected, the absorbance was monitored at 280 nm and the peaks were collected.

### 2.5. Simulated moving bed chromatography

The Semba System (Semba Biosciences, Madison, USA) was connected to 4 Sephacryl300 26/70 size exclusion columns (GE Healthcare) used in a 4 zone SMB mode with 1 column per zone. The flow rates used were determined through the triangle-theory model and were different for different proteins. For BSA the flow rates were: feed: 0.57 mL/min, extract: 1.70 mL/min,

Raffinate: 2.58 mL/min, recycle: 1.45 mL/min, switch time: 5 min. For beta-casein the flow rates were: feed: 0.61 mL/min, extract: 1.33 mL/min, Raffinate: 1.41 mL/min, recycle: 1.55 mL/min, switch time: 7 min. The absorbance was monitored at 280 nm for the Raffinate. Fractions were collected for the extract and Raffinate for each switch and investigated by analytical SEC for protein concentration and nanoparticle content.

### 2.6. Tangential flow filtration

The extract of one complete SEC-SMB run was collected and transferred to a Labscale TFF System (Millipore, Billerica, MA, USA) equipped with a Pellicon XL 50 Ultracel-5 PLCC Cassette with cut-off 5 kDa (Millipore). The system was operated at pressures of 10 psi transmembrane pressure for 80 min. Samples of 1 mL were collected from the Permeate and from the circulating flow of concentrated extract every 10 min and analyzed by analytical SEC for nanoparticle content and protein concentration.

## 3. Results and discussion

### 3.1. Binding of proteins to nanoparticles

To select model nanoparticles, two important factors have to be considered. The particle has to bind enough protein to be detectable by our analytical methods, and the size should be as close as possible to the size of a virus (roughly 70–150 nm). Additionally, the process parameters to ensure completely covered nanoparticles have to be found. The saturation range of protein loaded nanoparticles can be found by adsorption isotherms. To find optimal conditions for perfectly loaded nanoparticles for different sized nanoparticles, silica nanoparticles with amide functionalization in the size of 30 nm, 70 nm, 200 nm and 1000 nm were studied together with two model proteins: BSA and beta-casein (Fig. 3). The surface modification of these particles allows proteins to not only adsorb to the negatively charged silica surface, but provide additional positively charged binding opportunities. For both proteins the adsorbed amount of protein decreased with increasing particle size because of changed surface to volume ratio. This data show that our intended model of 70 nm particles adsorbs enough protein (8.14 ng/mm<sup>2</sup> for BSA and 3.11 ng/mm<sup>2</sup> of Beta Casein) to be detectable for our analytical system and is therefore a suitable model system.

Some strange behavior can be detected if we normalize the maximum amount of adsorbed protein (given by the Langmuir fit) with the available surface area (Table 1). The adsorbed amount per surface area is reasonable stable for BSA but beta-casein adsorption shows a different behavior. The amount of adsorbed beta-casein per surface area changes with different sized nanoparticles, which was unexpected. Probably the changing amount of adsorbed beta-casein per surface area as function of particle size may indicate multilayer adsorption or other complex adsorption mechanisms.

**Table 1**  
Maximum amount of bound protein estimated by a Langmuir fit or adsorption isotherms per surface area on differently sized nanoparticles for BSA and beta-casein.

Nanoparticle size (nm)	Max. adsorbed BSA [ng/mm <sup>2</sup> ]	Max. adsorbed beta-casein [ng/mm <sup>2</sup> ]
30	7.32	2.65
70	8.14	3.11
200	6.96	5.17
1000	7.40	7.00

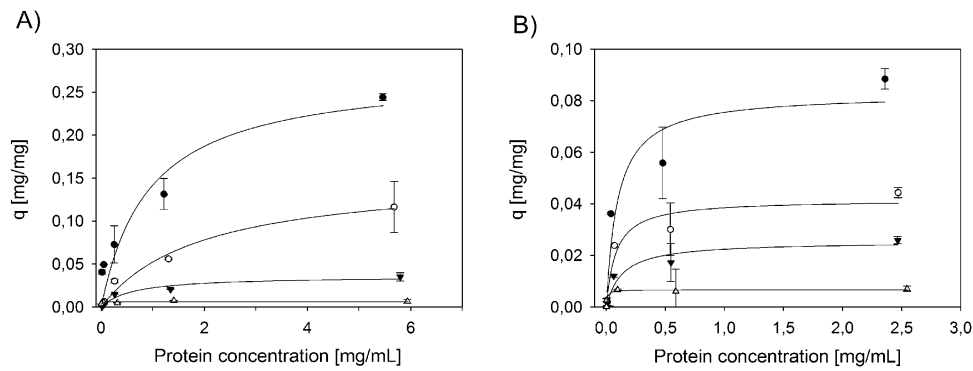


**Fig. 3.** Adsorption isotherms curves of BSA (A) and beta casein (B) on differently sized nanoparticles: (●) 30 nm, (○) 70 nm, (▼) 200 nm, (△) 1000 nm sized nanoparticles. The solid line represents a Langmuir fit of the data.

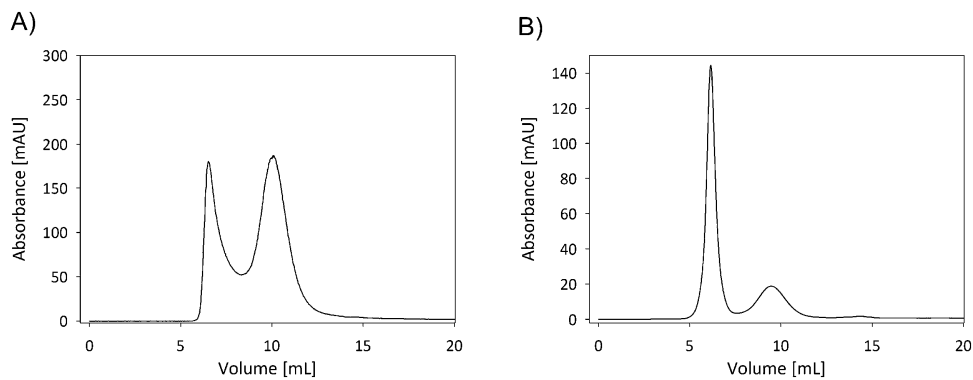


**Fig. 4.** UV280 trace of SEC chromatography of 70 nm silica nanoparticle mixed with (A) BSA and (B) beta casein.

### 3.2. SEC batch

The operating parameters of our SMB system were estimated from batch experiments. We used the triangle theory described [12] and for this purpose Henry constants and distribution coefficients are required.

70 nm silica nanoparticles loaded with BSA or beta-casein were separated from free protein (Fig. 4) by Sephacryl300 batch experiment. Protein loaded nanoparticles passed through the column and were eluted in the void fraction, but the protein was retained. The differences in the peak height of eluted nanoparticles loaded with different proteins are explained by the different molar extinction coefficients of the protein as well as the different amount of adsorbed protein. We did not achieve base line separation for BSA and protein loaded nanoparticles, but SMB does not require base line separation to yield pure fractions of a binary mixture [12].

From these chromatograms we deduced the peak moments of the substances and the distribution coefficients. Henry constants were estimated from the distribution coefficients and directly yield the constraint for  $m_1$  and  $m_4$  according to Eqs. (2) and (3). The missing constraints were calculated according to the triangle theory and Table 2 shows the process parameters we selected as well

**Table 2**

Restrictions for  $m$  values calculated by the triangle theory and selected  $m$  values for separation of 70 nm silica nanoparticles and BSA or beta-casein.

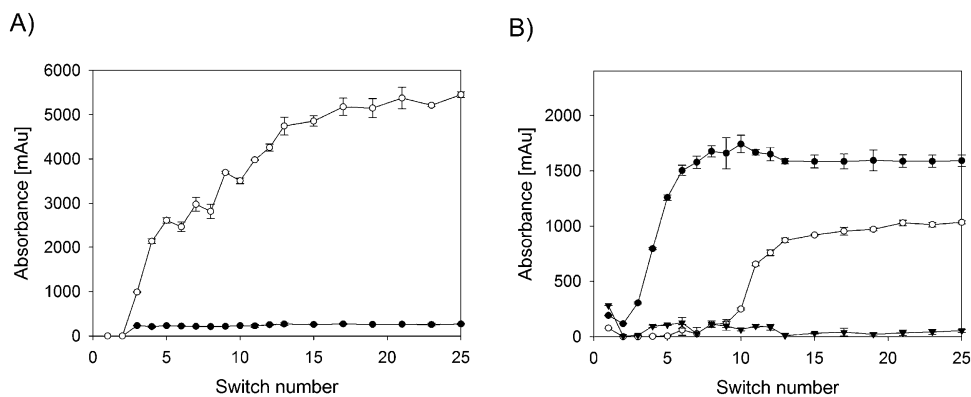
	BSA restrictions	BSA selected values	Beta-casein restrictions	Beta-casein selected values
$m_1$	$0.39 \leq m_1$	0.50	$0.41 \leq m_1$	0.50
$m_2$	$0 < m_2 \leq 0.39$	0.13	$0 < m_2 \leq 0.41$	0.09
$m_3$	$0 \leq m_3 \leq 0.39$	0.26	$0 \leq m_3 \leq 0.41$	0.28
$m_4$	$m_4 \leq 0.01$	-0.31	$m_4 \leq 0.00$	-0.15

as constraints for these parameters calculated from batch experiment data. We selected these values by an educated guess to be in the middle of the restrictions predicted by the triangle theory. The selection of the values was very conservative, being not too close to any restriction in case of non-ideal behavior of the system, to ensure a functional process and could be further optimized for an industrial process.

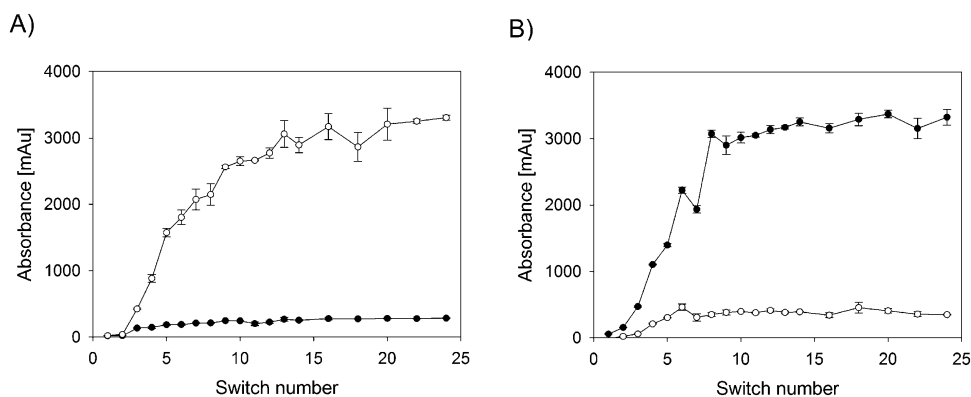
### 3.3. SMB results

Fig. 5 shows the time trace of protein concentration and particle concentration in the extract and Raffinate of the SMB separation of 70 nm protein loaded nanoparticles and free bovine serum albumin. It can be seen that the system is stable after approximately 12 switches (or 3 complete cycles). We achieved a good separation of protein and particle as the extract fraction is almost free of particles; however the Raffinate is getting contaminated with BSA multimers after 9 switches (or roughly 2 cycles). This incomplete separation can be explained by the setup of the system which was to separate BSA monomers and particles. We assumed the separation of a binary mixture when setting up the parameters according to the triangle theory, but in fact the BSA multimers add an additional third species to the system, which is not covered by the theory we used. The BSA multimer peak is between these two species and is therefore found in both fractions, extract and Raffinate. Table 3 shows the corresponding composition of feed, extract and Raffinate based on UV adsorption at 280 nm as well as the recoveries for particles and proteins. The extract is sufficiently pure of particles, but because of BSA-multimer problem the Raffinate purity is insufficient.

In comparison to BSA as model protein, beta-casein does not build up any multimers, therefore we expected no such problem



**Fig. 5.** Timetrace of the (A) extract during SMB–SEC separation of 70 nm silica nanoparticles and BSA: (●) particle and (○) protein concentration and (B) Raffinate during SMB–SEC separation of 70 nm silica nanoparticles and BSA: (●) particle, (▼) protein monomer and (○) protein dimer concentration.



**Fig. 6.** Timetrace of the (A) extract and (B) Raffinate during SMB–SEC separation of 70 nm silica nanoparticles and beta-casein: (●) particle and (○) protein concentration.

**Table 3**

Composition of feed, extract and Raffinate for SMB–SEC separation of 70 nm silica nanoparticles and BSA as well as recoveries.

	Feed (%)	Extract (%)	Raffinate (%)	Recovery (%)
Particles	16	5	63	98
BSA monomer	63	76	1	100
BSA multimer	21	19	36	

as seen for BSA. Fig. 6 shows the time traces of separation of 70 nm silica nanoparticles and beta-casein, and as expected the system is also stable after roughly 3 complete cycles with good separation of protein and particles. This system fulfils the assumption of a binary mixture, resulting in almost pure fractions of proteins and nanoparticles in the extract and Raffinate, respectively. Table 4 shows the corresponding purities and recoveries, we achieved good recovery and good purity for protein and particles around 90% and the calculated productivity was 0.25 g/L/h of purified protein loaded nanoparticle per volume of column resin, which makes this process suitable for industrial production. Chromatography and especially SMB offers great scalability advantages over Ultracentrifugation, being only restricted by the available column and pump sizes and not dependent on particle density or size. The scale up itself would be straight forward as only flow rates and column diameters have

**Table 4**

Composition of feed, extract and Raffinate for SMB–SEC separation of 70 nm silica nanoparticles and beta-casein as well as recoveries.

	Feed (%)	Extract (%)	Raffinate (%)	Recovery (%)
Particles	57	8	89	90
Beta-casein	43	92	11	96

to be adjusted to achieve the same residence time in small and large scale.

To further reduce costs and buffer consumption, this system was tested in combination with tangential flow filtration (TFF) to reuse buffer and to concentrate the protein fraction. Reusing the buffer greatly decreases buffer consumption and concentrating the protein fraction ensures that protein is not wasted during the production of protein loaded nanoparticles, which is especially interesting when the active compound is very expensive.

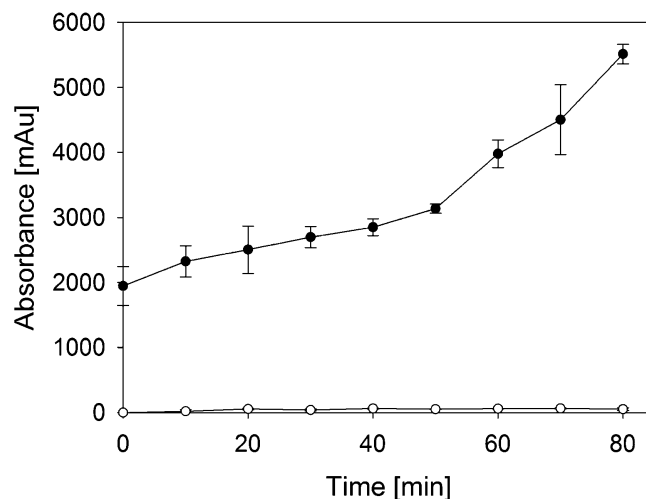


**Fig. 7.** Timetrace of (●) Retentate protein concentration and (○) Permeate protein concentration of TFF concentration of SEC–SMB extract.

To prove the applicability of TFF for concentration of protein and reuse of buffer we collected the extract of the SMB–SEC separation of 70 nm silica nanoparticles and beta-casein and concentrated it over the course of 80 min (Fig. 7). We achieved a total concentration factor of 2.8, which allows this solution to be used again for loading of nanoparticles, reaching a yield of 96%. We also proved that the resulting buffer is free of protein and ready to be used in the SMB system again (Fig. 7).

#### 4. Conclusion

We were able to prove the applicability of SEC–SMB to separate perfectly protein-covered nanoparticles from proteins resulting in high yield (>90%) and purity (>90%). The productivity achieved for the system (0.25 g/L/h of protein loaded nanoparticle) is suitable for an industrial process and can surely be further optimized as no optimization was done in this work. Cost of goods can be held low due to the demonstrated recycling of protein and buffer using TFF. The features of high purity, high recovery, and low costs due to a continuous process using recycling makes this methods highly suitable to fulfill the need of protein/nanoparticle separation not only in lab scale, but also in production scale. The generic setup of SEC chromatography allows for separation of a variety of active compound–nanoparticle combinations, even allowing to use the same parameter setup when purifying different nanoparticles, but the same protein, as the retention time for different nanoparticles is the same as long as they are unable to diffuse into the chromatographic resin. The easy scalability of the chromatographic system, as well as the TFF system by increasing either column diameter

or membrane area additionally adds to the industrial value of this process.

#### Acknowledgment

This work was supported by “Austrian Science Fund” (FWF W1224—Doctoral Program on Biomolecular Technology of Proteins—BioToP).

#### References

- [1] R. Grillo, N.Z.P. dos Santos, C.R. Maruyama, A.H. Rosa, R. de Lima, L.F. Fraceto, *J. Hazard. Mater.* 231–232 (2012) 1.
- [2] H. Wanyika, *J. Nanopart. Res.* 15 (2013) 1.
- [3] C.-M.J. Hu, L. Zhang, *Biochem. Pharmacol.* 83 (2012) 1104.
- [4] S.C. Abeylath, E. Turos, S. Dickey, D.V. Lim, *Bioorg. Med. Chem.* 16 (2008) 2412.
- [5] Y.-M. Huh, Y.-w. Jun, H.-T. Song, S. Kim, J.-s. Choi, J.-H. Lee, S. Yoon, K.-S. Kim, J.-S. Shin, J.-S. Suh, J. Cheon, *J. Am. Chem. Soc.* 127 (2005) 12387.
- [6] E. Mahon, A. Salvati, F. Baldelli Bombelli, I. Lynch, K.A. Dawson, *J. Controlled Release* 161 (2012) 164.
- [7] M. Moddarelli, M.B. Brown, Y. Zhao, S. Tamburic, S.A. Jones, *Int. J. Pharm.* 400 (2010) 176.
- [8] O. Veisoh, C. Sun, J. Gunn, N. Kohler, P. Gabikian, D. Lee, N. Bhattarai, R. Ellenbogen, R. Sze, A. Hallahan, J. Olson, M. Zhang, *Nano Lett.* 5 (2005) 1003.
- [9] T. Wang, H. Jiang, Q. Zhao, S. Wang, M. Zou, G. Cheng, *Int. J. Pharm.* 436 (2012) 351.
- [10] E. Papanikolaou, G. Kontostathi, E. Drakopoulou, M. Georgomanoli, E. Stamatidis, K. Vougas, A. Vlahou, A. Maloy, M. Ware, N.P. Anagnou, *Virus Res.* 175 (2013) 1.
- [11] C.-W. Shen, T. Yu, *J. Chromatogr. A* 1216 (2009) 5962.
- [12] A. Rajendran, G. Paredes, M. Mazzotti, *J. Chromatogr. A* 1216 (2009) 709.
- [13] D.M. Ruthven, C.B. Ching, *Chem. Eng. Sci.* 44 (1989) 1011.
- [14] G. Zhong, G. Guiochon, *Chem. Eng. Sci.* 51 (1996) 4307.
- [15] M. Mazzotti, G. Storti, M. Morbidelli, *J. Chromatogr. A* 769 (1997) 3.

## **Protein adsorption onto nanoparticles induces conformational changes:**

### **Particle size dependency, kinetics and mechanisms**

**Peter Satzer,<sup>a</sup> Frantisek Svec,<sup>b</sup> Gerhard Sekot,<sup>c</sup> and Alois Jungbauer<sup>a,c\*</sup>**

<sup>a</sup> Department of Biotechnology, University of Natural Resources and Life Sciences, Vienna (BOKU), Muthgasse 18, 1190 Vienna, Austria, <sup>b</sup> Lawrence Berkeley National Laboratory, The Molecular Foundry, Berkeley, CA 94720, USA, <sup>c</sup> Austrian Centre of Industrial Biotechnology (ACIB), Muthgasse 18, 1190 Vienna, Austria

\* Address correspondence to

[alois.jungbauer@boku.ac.at](mailto:alois.jungbauer@boku.ac.at)

Muthgasse 18, 1190 Vienna

Telephone: +43476546226

Fax: +43476546677

**Keywords:** nanoparticles, curvature, particle size, conformational change, adsorption

## **Abbreviations**

BSA Bovine Serum Albumin

CD Circular Dichroism

DLS Dynamic Light Scattering

NMR Nuclear Magnetic Resonance

PDI Polydispersity Index

TEM Transmission Electron Microscopy

## **Practical application**

Nanomaterials are under heavy investigation for medical and engineering applications but little is known about the interaction between nanoparticles and proteins. Here, we investigate nanoparticle size-dependent denaturation of adsorbed proteins and the use of CD to study such changes. Using model calculations, we showed the lacking explanatory power of commonly used theories. Furthermore, we provide the first solid data set for a variety of proteins and a whole range of nanoparticle sizes. This enables the design of nanoparticles that show low size-dependent denaturation of the adsorbed protein for various applications ranging from downstream applications and nanosensors to medical usage. In all applications where nanoparticles are used to bind protein, one has to be aware of this effect if the structure of the protein has to be preserved.

## **Abstract**

The use of nanomaterials in bio-applications demands a detailed understanding of the protein-nanoparticle interaction. It is known that proteins can undergo conformational change while adsorbing onto nanoparticles, but studies on the impact of particle size on conformational changes are scarce. We have shown that conformational changes happening upon adsorption of myoglobin and BSA are dependent on the size of the nanoparticle they are adsorbing to. Out of 8 initially investigated model proteins, two (BSA and myoglobin) showed conformational changes, and in both cases this conformational change was dependent on the size of the nanoparticle. Nanoparticle sizes ranged from 30 to 1000 nm and, in contrast to previous studies, we attempted to use a continuous progression of sizes in the range found in live viruses, which is an interesting size of nanoparticles for the potential use as drug delivery vehicles. Conformational changes were only visible for particles of 200 nm and bigger. Using an optimized circular dichroism protocol allowed us to follow this conformational change with regards to the nanoparticle size and, thanks to the excellent temporal resolution also in time. We uncovered significant differences between the unfolding kinetics of myoglobin and BSA. In this study we also evaluated the plausibility of commonly used explanations for the phenomenon of nanoparticle size dependent conformational change. Currently proposed mechanisms are mostly based on studies done with relatively small particles, and fall short in explaining the behavior seen in our studies.

# 1. Introduction

A fundamental understanding of surface curvature effects on the adsorption of biomolecules is important for the development of new surfaces and nanomaterials. These novel materials may be employed in diverse fields, from transport, where they can be used for surface modifications of ship hulls to prevent biofouling, to biomedical engineering, where they allow drug delivery to tumor cells or are used as adjuvants in vaccines [1-3]. Spherical nanoparticles also made significant contributions to new healthcare applications such as vaccination, [4] cancer treatment and imaging [5, 6]. Nanoparticles exhibit unique behavior in the human body, but there is only a limited knowledge of how nanomaterials interact with cells and proteins. Depending on the nanoparticle size and surface chemistry, proteins can form a corona at the external surface of nanoparticles, when administered to the human body [7-10]. The specific protein corona of differently functionalized or differently sized nanoparticles influence all aspects of nanoparticle-organism interaction ranging from cytotoxicity to uptake kinetics [11-13]. Nanoparticles that enter a physiological environment are covered by protein almost instantaneously. Not only the actual surface of the nanoparticle dictates its behavior *in vivo*, but also the proteins attached to the nanoparticle. Adsorbing proteins in their natural conformation, or forcing them to change their conformation upon adsorption could make the difference between an effective drug carrier and a toxic nanoparticle. Thus, understanding the specific protein-nanoparticle interactions and how or why proteins might change their conformation upon adsorption is key to comprehend how the nanoparticle surfaces behave *in vivo*. Typically, proteins can change their conformation upon binding to surfaces and this behavior is affected by the type of surface and surface geometry, in some cases these interaction might be specific for the given protein-nanoparticle interaction [14-20]. In recent years, an increasing number of studies described size dependent protein

denaturation by nanomaterials (see reviews [21-23]) but the results were not conclusive. A comprehensive list of materials, proteins and methods used in relevant sources can be found in the supporting information (Table S1). One study reports increasing conformational change on smaller particles [24]. However, most studies conclude that conformational changes are more substantial with larger particles [25-28]. One report finds stabilization of the secondary structure [29]. None of the reports give a comprehensive data set that would allow a detailed investigation of the underlying mechanisms, as they only report the behavior on up to three nanoparticle sizes. A data set so small is not able to provide sufficient data to follow the conformational changes in terms of protein size accurately. Therefore such a data set is not sufficient to test the proposed mechanisms for plausibility. Many of these reports propose as mechanism that the surface curvature itself may force bending of the protein. Alternative explanations assume that nanoparticles with less surface curvature may provide more area for interaction with the protein. Another explanation relies on the difference in the geometry dependent double layer potential that forms at the particle surface [26]. All of these studies lack the data necessary to evaluate the proposed mechanisms, because of the limited number of nanoparticle sizes used in the investigations. Compiling these results into one big picture for the evaluation of these hypotheses is impossible, since the studies present a limited number of particle sizes, different proteins and different nanoparticle materials.

In this work, we provide a data set of interactions between model proteins with a wide range of nanoparticle sizes. This conclusive data set, can in turn be used to evaluate explanations commonly offered for this phenomenon.

## **2. Material and Methods**

All chemicals and materials were purchased from Sigma Aldrich (St Louis, USA) unless indicated otherwise.

### **Nanoparticles**

Silica nanoparticles with amidine surface modification with a size of 30, 70, 100, 150, 200, 300, 500, and 1000 nm were purchased from Kisker (Steinfurt, Germany). Their size and monodispersity was confirmed by TEM and DLS. Their non-porosity was confirmed by nitrogen adsorption and the surface charges were characterized by their Zeta Potential.

### **Determination of Adsorption Isotherm**

Protein solutions of concentrations up to 4 mg/mL in 20 mM phosphate buffer, pH 7 with and without addition of 1M NaCl were mixed with a nanoparticle dispersion to reach a concentration of 2.5 mg/mL for nanoparticles smaller than 100 nm, and 5 mg/mL for nanoparticles 150 nm and larger. The mixtures were incubated for 12 h to reach equilibrium. Particles were removed by filtration through 100 kDa membranes (Merk Millipore, Billerica, USA). The concentration of residual protein in solution was determined using UV absorption at a wavelength of 280 nm. All measurements were done in triplicates.

### **Desorption of Protein**

Desorption of proteins from nanoparticles was tested by using the particles from adsorption isotherm experiments and suspending them to 20 mM phosphate buffer pH 7 either with the addition of 1 M NaCl or without the addition of salt and incubated them for 12 h. Desorbed proteins were measured after 12h of incubation using UV adsorption at a wavelength of 280 nm. Samples transferred into 20 mM phosphate buffer pH 7 without NaCl were used as a control.

## **Determination of Size, Zeta Potential and Polydispersity of Nanoparticles**

Dynamic light scattering of nanoparticle dispersions in a 20 mM phosphate buffer, pH 7 was carried out using a Zetasizer Nano S (Malvern Instruments, Malvern, GB). Particle and solution parameters (refractive index and viscosity) were obtained from the library that came with the instrument. All measurements were performed in triplicate.

## **Circular Dichroism**

All measurement were carried out using a Jasco J1100 instrument (Jasco, Easton, USA) with a quartz-cuvette and a 20 mM phosphate buffer, pH 7, with recording wavelength from 190 to 240 nm. A concentration of 1 mg/mL was used for determination of the protein structure of unbound protein. Bound protein structures were determined after coating the particles with protein at 1.5 mg/mL particle solution by using 4 mg/mL protein and subsequent removal of the unbound protein. The protein coated nanoparticles were washed 3 times with fresh buffer solution to remove any residual unbound protein. The washed protein coated nanoparticles were measured from 190 to 240 nm in a 1 mm path length cuvette. The concentration of adsorbed proteins were taken from the adsorption isotherms experiments. The spectra were blank subtracted with protein free nanoparticle solution spectra. Spectra were measured ten times and condensed into a single spectra before structure determination to reduce noise

Experiments to show differences in the structure of adsorbed protein for high and low surface coverage of the particle were done with a particle concentration of 1.5 mg/mL and either 4 mg/mL of protein or 0.01 mg/mL of protein washed and measured as described above. Time dependent CD measurements were carried out with a particle concentration of 1.5 mg/mL and protein concentration of 0.01 mg/mL. This ensures that almost all protein present in the solution is bound to the nanoparticle and a washing step can be omitted. Because of decreased signal to noise ratio this experiments were not performed for 500 or 1000 nm particles

The structure of proteins was either calculated according to Raussens [30] without using the protein concentration, or was calculated using the K2D3 software [31], using concentration values obtained from the adsorption isotherm experiments.

### 3. Results and Discussion

#### Nanoparticle Characterization

The nanoparticles used for this study were characterized thoroughly to be sure the material provided by the manufacturer is suitable for this study. Factors of interest were particle shape, surface roughness, porosity and the zeta potential. We investigated amidine modified particles of a nominal size of 30, 70, 100, 150, 200, 300, 500 and 1000 nm by transmission electron microscopy (TEM) and dynamic light scattering (DLS) to determine size and polydispersity (Figure 1 shows TEM pictures, TEM and DLS results are summarized in Table 1). Sizes determined by TEM and DLS were in good agreement to the nominal sizes. The monodispersity and spherical shape could also be confirmed.

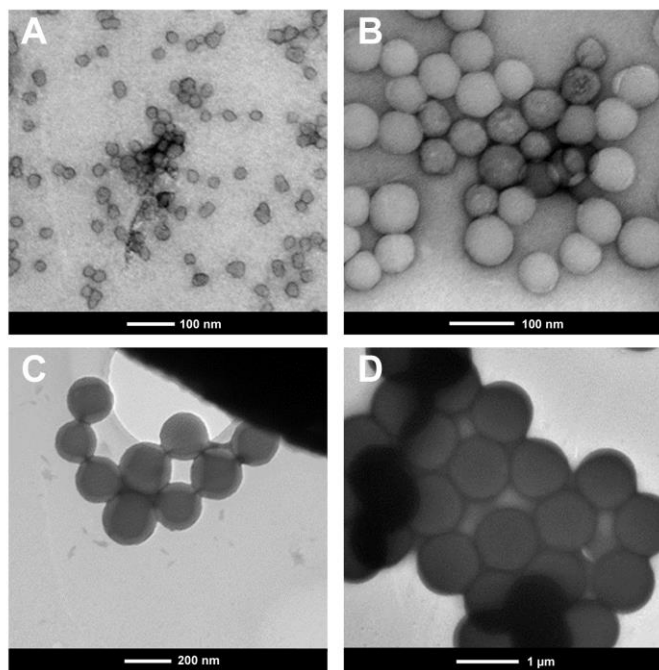


**Figure 1. Transmission electron microscopy images of spherical silica nanoparticles show monodispersity and spherical shape showing 30 nm particles (A), 70 nm particles (B), 200 nm particles (C) and 1000 nm particles (D).**

**Table 1. List of Nanoparticles Used in this Study and their Characteristics**

Particle Diameter, nm			PDI <sup>a</sup>	$\zeta$ , mV <sup>b</sup>	Surface Area, m <sup>2</sup> /g	
Nominal	TEM	DLS			Calculated	Measured
30	23.1	26.5	0.147	-46.9	130.6	ND <sup>c</sup>
70	62.9	65.1	0.025	-62.7	48.3	51.2
100	ND	110.7	0.029	-64.6	27.5	ND
150	ND	155.2	0.017	-66.2	20.1	ND
200	192.4	213.6	0.009	-70.4	18.3	20.2
300	ND	302.9	0.021	-72.1	10.0	ND
500	ND	460.8	0.041	-71.1	7.2	ND
1000	1022.2	1074.1	0.049	-70.1	3.1	3.5

<sup>a</sup> Polydispersity index obtained from DLS measurement. The lower the number, the narrower the dispersity. <sup>b</sup> Zeta potential. <sup>c</sup> Not determined.

The surface properties were assessed by measuring the zeta potential, characterizing the charges present on the surface. The results of these measurements are presented in Table 1 and all zeta potentials are highly negative and deviate only slightly from each other with the exception of very small particles. The zeta potential for particles above 150 nm can be considered as not changing at all, for smaller particles we have to keep the differences in mind, especiall for the very small particles of 30 nm.

The last property to investigate was the porosity of the particles since porosity would make our results based on the assumption of solid particles useless. We determined surface areas of 70, 200, and 1,000 nm nanoparticles through nitrogen adsorption experiments and the results are in good agreement with the theoretical surface calculated for solid spheres of the same size, indicating no porosity as well as no significant surface roughness (Table 1).

## **Protein Characterization**

We used nine proteins in the binding studies that differed in their properties as shown in supporting information Table S2. First we investigated the binding of all proteins to 70 nm nanoparticles at pH 7 in 20 mmol/L phosphate buffer (supporting information Table S2). No binding was observed for glucose oxidase and also for chymotrypsin. We continued the study using the remaining 7 model proteins and determined their structure in solution (supporting information Table S3). The structure determination was done by a simple method presented by Raussens et al [30]. The method is susceptible to systematic errors in the quantification of secondary structure elements, but remains sensitive to changes.

## **Conformational Changes of Proteins**

We determined the structural parameters of each of the proteins before and during contact with nanoparticles. Several previous studies measured the changes for protein after contact with the nanoparticle, but not in its adsorbed state [22, 32, 33]. Lunqvist et al investigated proteins by NMR bound to very small nanoparticles with 2 different proteins and we attempted to build onto and expand this work, especially to nanoparticle sizes similar to that of viruses [32-35]. NMR is not applicable for large particles, and as such an alternative method was sought out. CD spectroscopy was found to be applicable for the structural prediction required in this study. To counter-act the additional noise introduced by nanoparticles obstructing the light path, we chose to measure the CD spectra at very high concentrations of adsorbed protein. We removed unbound proteins by washing the particles, and enhanced the signal by condensing ten individual spectra into one measurement for structure determination (a representative CD spectra used for structure determination can be seen in supporting information Figure S1). The protein concentration on the

particles was not determined in these first experiments and structures were estimated by the use of a concentration independent method [30]. Since this method has its limitations, it was only used for a fast screening of our model proteins.

We observed that the 7 model proteins can be grouped in three categories: (i) proteins that do not reveal any conformational change, (ii) proteins for which the conformational change was unclear due to signal/noise, and (iii) proteins that exhibit clear conformational change.

The first group included lysozyme,  $\beta$  casein and ribonuclease A. These proteins showed no conformational change after adsorption on nanoparticles of any size (supporting information Figure S2). This result was expected as two of the proteins are very stable (ribonuclease A and lysozyme) and one of them lacks a very pronounced secondary structure ( $\beta$  casein).

The second category of proteins included cytochrome C and ovalbumin. The data we collected is not sufficient to judge the unfolding of the protein upon adsorption (supporting information Figure S3). Our data may indicate a change in the  $\alpha$  helical content in the protein structure depending on the nanoparticle size. However, the experimental error of the method used is too big to make any reliable conclusions.

The proteins which showed clear conformational changes were myoglobin and bovine serum albumin, both alpha helical rich proteins. We determined adsorption isotherms for all nanoparticle sizes for these two proteins to estimate the amount of bound protein (supporting information Figure S4). Concentrations taken from these curves were used to determine the secondary structure composition by the K2D3 software [36]. Both proteins show a decrease in alpha-helical structure once adsorbed to relatively large particles above 150nm in size (Figure 2).

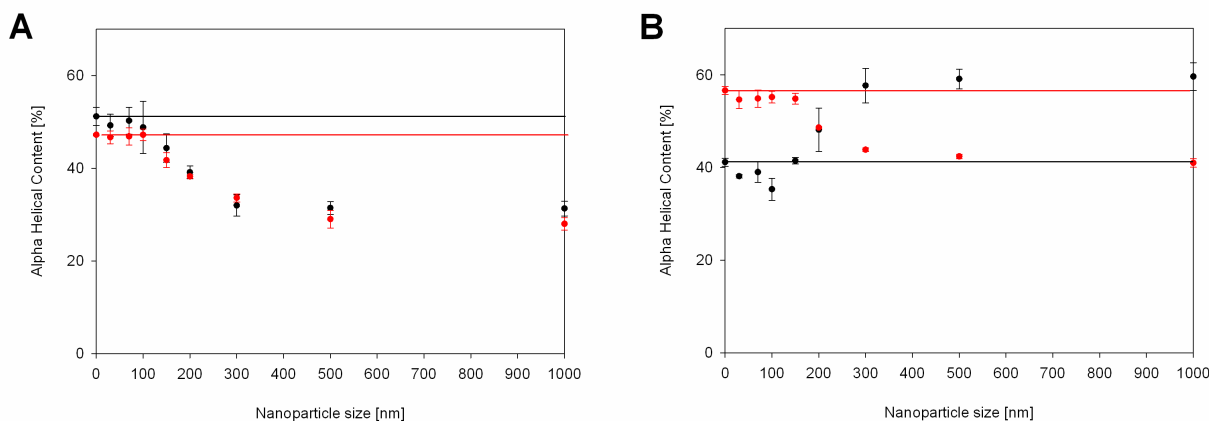


**Figure 2.  $\alpha$ -helical content of myoglobin (A) and BSA (B) adsorbed on nanoparticles varying in sizes. The red curve shows the concentration dependent structure prediction by Louis-Jeune et al. [31], the black curve shows the concentration independent structure prediction by Raussens et al [30]. Horizontal lines represent the structure of the protein in solution. A clear difference between the two methods in the structure prediction for BSA is observable, whereas both methods are in excellent agreement for myoglobin. 10 individual spectra were condensed into one before structure determination. 3 of such sets were used to calculate standard deviations shown in the error bars of the figure.**

Interestingly the structure prediction given by the concentration independent method predicted an increase in alpha helical structure of BSA on larger particles, rather than a decrease. This clearly demonstrates the limitation of concentration independent structure determination, as it is sensitive to changes, but does not give exact values. In fact, in this case it inversed the observed trend.

To be sure we are dealing with significant differences between the small and large particles we performed a t-test including all measurements from 0-100 nm into one group and all measurements from 300 to 1000 nm into another group and tested if the two populations are significantly different. For myoglobin and for BSA the resulting p-value is below 0.0001, meaning the difference is of very high statistical significance.

A very interesting detail is the sigmoidal shape of the curve in both cases, which gives the opportunity to investigate proposed mechanisms for this denaturation. Something has to change significantly between the particle size of 100 nm and the particle size of 300 nm. Looking at this

window we can exclude that the different zeta potentials found in our particle analysis (Table 1) as driving factor for the conformational change. If the zeta-potential would be the driving force, we would expect a difference between 30 nm particles and the rest as well as no change above 150 nm particle size

To quantify the effect of concentration dependent changes of conformation we calculated the protein load per surface area for the particles in this experiment (Table 2). We can clearly see that the protein load on this particles rises between 30 and 70 nm particle size, stays relatively stable in the region of 70 to 200 nm and then again rises as the particles grow bigger. Such a trend of increased BSA adsorption onto less curved surfaces was also recently shown by experiment and simulation in the case of carbon nanotubes [37].

**Table 2. Adsorbed Protein Amount for Myoglobin and Bovine Serum Albumin at a Protein Concentration of 4 mg/mL**

Particle Size, nm	Adsorption Capacity, g/m <sup>2</sup>	
	Myoglobin	Bovine Serum Albumin
30	0.60	0.76
70	0.98	1.13
100	0.80	1.70
150	0.98	1.74
200	1.08	1.80
300	1.83	3.51
500	2.51	3.88
1000	5.48	6.02

Rough calculations using as protein size 2 and 4 nm for myoglobin and BSA respectively show that on all particle sizes the adsorption is a thick multilayer. The calculated coverage ranged from 700 to 7000 % of the available surface area. We do not know why the multilayer increases with the nanoparticle size, but the unfolding of the protein may be a driving force for building up huge multilayers. This might expose hydrophobic regions at the surface where other protein molecules

might attach. To test for concentration dependent conformational changes we measured the structure of adsorbed proteins at very low and very high surface concentration on 300 nm nanoparticles. The normalized spectra (Figure 3) show no difference in the spectra for high and low concentration for BSA, but show a small change in the spectra for myoglobin corresponding to a change in alpha helical content of 3 %.

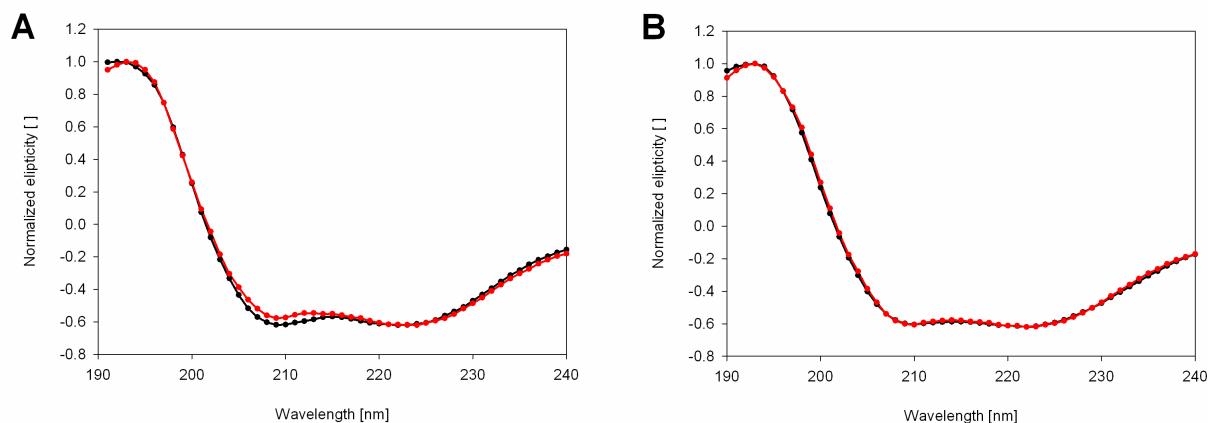


**Figure 3. Normalized spectra of myoglobin (A) and BSA (B) adsorbed at low concentration (black line) and high concentration (red line). A small concentration dependent conformation change is visible in myoglobin, but not in BSA.**

## Kinetics of adsorption and conformational change

We used CD spectroscopy to follow the conformational change of myoglobin and BSA because we wanted to know if the unfolding or the adsorption is the rate limiting step. To get reasonable results we had to modify the previous experimental set up. The washing and dissolution steps used before require an extra hour of sample handling, which of course makes it impossible to measure kinetics. To overcome this limitation we used a low protein concentration set up that does not require a washing step. To further increase the signal/noise ratio we only investigated the smallest particles that showed significant structural changes in previous experiments: 200 nm particles for myoglobin and 300 nm particles for BSA. Adsorption kinetic experiments showed the adsorption of protein in both cases to be a relatively fast process. The adsorption was finished in 30 minutes (Figure 4).

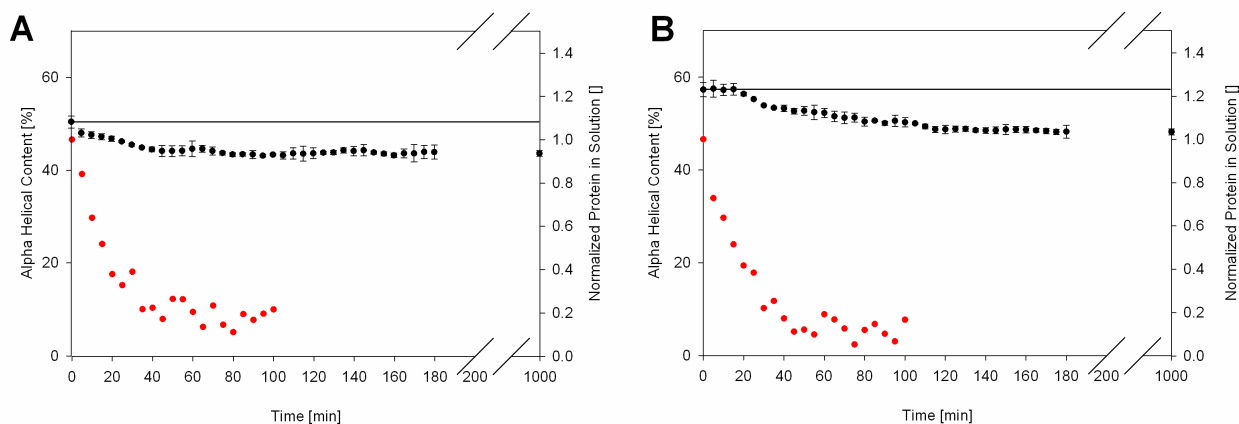


**Figure 4. Kinetics of adsorption kinetic (red) and conformational changes after adsorption (black); myoglobin on 200 nm silica nanoparticles (A) and bovine serum albumin on 300 nm silica nanoparticles (B). Kinetics of adsorption and conformational change happen simultaneously for myoglobin, but not for BSA. 10 individual spectra were collected and used to calculate standard deviations shown in the error bars of the figure.**

Figure 4 shows the time trace of the alpha helical structure of myoglobin (panel A) and BSA (panel B) determined by the K2D3 software. Myoglobin seems to undergo a fast conformational change, finished in about the same duration as the adsorption, whereas BSA takes longer to change its conformation. Looking at these results we can conclude that myoglobin contradicts the usual assumption that conformational changes are a slow process compared to adsorption. Myoglobin adsorbs and almost immediately changes its conformation. BSA follows the classical principle as the rate limiting step is the conformational change. While adsorption takes about 30 minutes, the conformational changes happens over 180 minutes.

One of the theories discussed in the literature deals explicitly with charges on the surface of the nanoparticle, as well as the charge of the protein. We therefore had to check if the interaction of protein and nanoparticle is driven purely by electrostatic interaction, or by other factors as well. To test this we made adsorption experiments in the presence of salt, which should interrupt electrostatic interaction between protein and particle and result in lower binding. The addition of 1M salt into the buffer prior to the adsorption experiment resulted for myoglobin in a decrease of binding capacity down to 46 +/- 8 %. This shows that electrostatic interaction is not the only force, but contributes a very significant portion to the overall force between myoglobin and the nanoparticle. BSA shows hydrophobic interaction with the nanoparticle as the adsorption capacity increased to 126 +/- 22 % when adding salt to the mixture. Interestingly both proteins show different interaction mechanism (mixed mode for myoglobin and hydrophobic for BSA) but show the same pattern regarding the size dependency of the conformational change.

We also performed desorption experiments of adsorbed protein, but were not able to desorb any protein after the adsorption and conformational change of the protein, even under high salt conditions. Unfortunately our method did not allow to desorb the proteins before they changed

conformation due to the handling time of samples. We can conclude from these experiments that there is an additional hydrophobic contribution of binding energy once the protein changes its conformation on the surface. Whether this additional hydrophobic binding energy is the driving force of the conformational change or rather a consequence of the unfolding is impossible to tell with the currently available data.

## **Evaluation of common theories**

A number of theories have been proposed to explain the particle size dependent conformational change of proteins after adsorption. The most accepted explanation is that the curvature of the particle itself leads to a change in either interaction area of protein and particle, or to a bending of the protein to accommodate the curvature of the particle. This explanation is usually used for very small particles and may be a factor on very small scales, but has to be re-evaluated to see if it can explain the conformational changes seen in this study.

Another explanation was based on the electrostatic interaction between protein and nanoparticle. The double layer potential build up at the interface of particle and solution is geometry dependent and therefore dependent on the particle size. We calculated the implications of these models and tried to find something that was able to explain the pattern we saw in our experiments: no change between 30 and 100 nm particle size, significant change between 100 and 300 nm size, and no change between 300 and 1000 nm particle size.

## **Calculation of Interaction Area Based on Nanoparticle Size**

We defined the interaction area of nanoparticle and protein to be the portion of the protein surface which is closer than 0.4 nm to the surface of the particle, which is a typical interaction range of electrostatic interaction [26]. For the case of hydrophobic interaction there is no

interaction area to be calculated with this model, as hydrophobic interaction acts only on contact. Equations for calculation and figures for explanations can be seen in the supporting information. Longer interaction ranges than 0.4 nm would be a case of electrostatic interaction in a solution of lower conductivity. Shorter interaction would represent Van der Waals interactions, hydrophobic interactions have no range by themselves, but typically act on a range of 0.1 nm or lower through the exclusion of water.

The interaction area on the protein given in  $\text{nm}^2$  dependent on the nanoparticle size is presented in Figure 5 Panel A for the case of 0.4 nm interaction range (equations and additional interaction ranges can be found in the supporting information Figure S5).

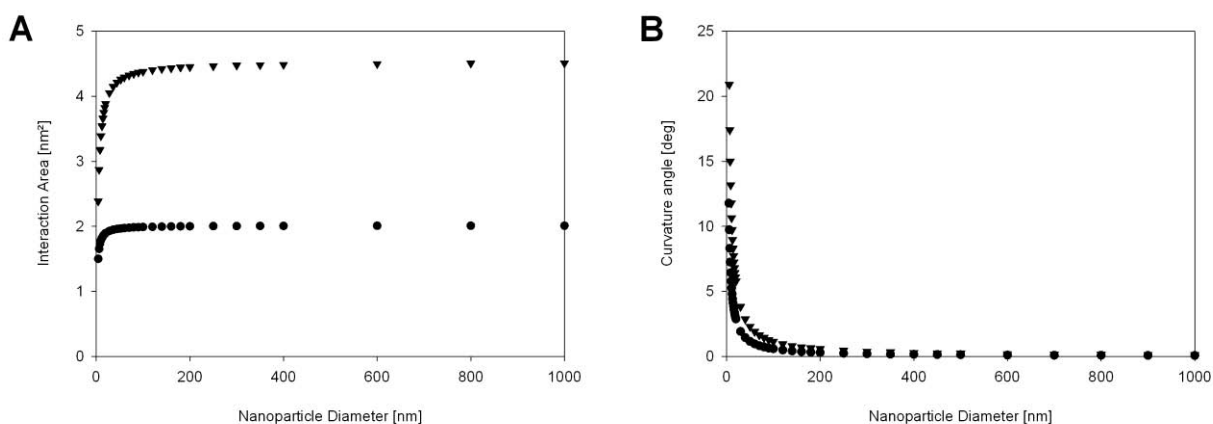


**Figure 5 – Interaction Area calculated for 2 differently sized theoretical proteins, 2 (●) and 4 nm (▼) (A), and the angle of this interaction (B). No significant change in interaction area or angle of interaction is visible for particles bigger than 150 nm.**

From this graph we can see that the interaction area is steeply increasing for smaller particle sizes and no significant change is observed for particles larger than 100 nm for both a model protein of 2 nm size and a model protein of 4 nm size. We conclude that the size dependency of the interaction area might have a large impact on very small particles below 50 but the effect is negligible for particles above 100 nm.

## **Calculation of an Angle of Interaction Based on Nanoparticle Size**

Another hypothesized explanation for the direct influence of the curvature on the conformation of the adsorbed protein is that the protein has to bend to accommodate the curved surface. This explanation is typically used in studies presenting an inverse dependency of size and conformational change of the adsorbed proteins. We calculated the angle between the point at which the two spheres touch and the point on the particle circumference corresponding to the projected area (the shadow) of the protein. Equations and figures for explanation can be seen in the supporting information Figure S6. Figure 5 Panel B shows the calculated angle in relation to the particle size for two sizes of protein (2 nm and 4 nm). The angle is steeply decreasing for very small particles and might be an explanation for changes seen in this particle range, but does not significantly change for particles above 100 nm.

## **Calculation of Double Layer Potential Based on Nanoparticle Size**

An indirect influence of the surface curvature, hypothesized as reason for size dependent denaturation by Vertegel et al.[26], is the geometry dependent double layer potential. This potential builds up at the interface between the solid particle and the liquid buffer and is dependent on the size of the particle, increasing with the particle diameter. Larger particles could lead to a stronger electrostatic force and this could result in conformational changes in the protein. Figure 6 shows the potential in mV calculated by the equations presented by Vertegel et al.

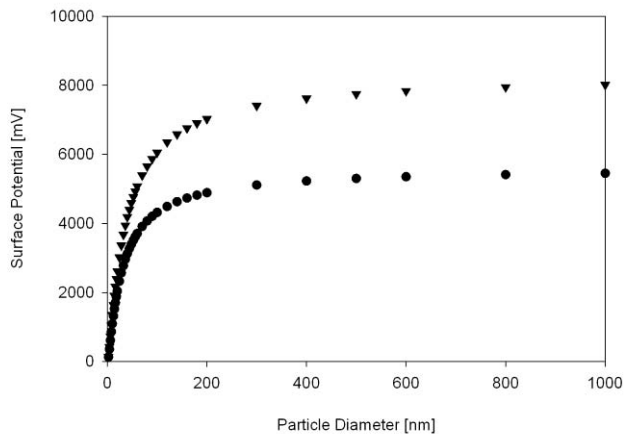


**Figure 6 – Surface potential calculated for hypothetical proteins of 2 (●) and 4 nm (▼) in diameter.**

As in the other proposed theories we see a steep increase for small particles, but a shallower curve. The change in double layer potential is quite significant for smaller particles than 100 nm and might therefore not be distinguishable from other factors such as interaction area and curvature. This change in double layer potential is negligible above a particle size of 300 nm. This leaves a window of 100 to 300 nm particle size where the direct contributions of the surface (curvature and interaction) is negligible, and the potential is still changing. We expect that any change seen in this size range might be at least partially attributed to the change in the double layer potential.

## 4. Concluding remarks

We studied the interaction of nanoparticles with nine proteins and demonstrated conformational changes for myoglobin and BSA upon adsorption to nanoparticles. The susceptibility of proteins to conformational changes upon adsorption varies substantially for different protein-nanoparticle combinations and might be specific for any combination. All proteins that showed conformational change (myoglobin and BSA) did this in a nanoparticle size dependent manner. Both proteins showed conformational changes on nanoparticle sizes bigger than 150 nm, but no significant change in conformation for any smaller size. Although the interaction mechanism and the kinetics of the conformational change is different for both proteins (mixed mode for myoglobin and hydrophobic for BSA) they show the same pattern of conformational change. Using model calculations we excluded surface curvature as the major driving force for the size ranges in which conformational changes occurred in this study (above 100 nm). Geometry dependent double layer potentials may still play a significant role for the denaturation of myoglobin, as it interacts in a mixed mode. For the binding of BSA the double layer potential should be insignificant as it is interacting purely hydrophobic. This interesting result still asks the question if some of the behaviors are universal, or may be specific for these two proteins. It also asks the question if we are missing a mechanism completely that might explain the behavior of both BSA and myoglobin. For both proteins the conformational change was particle size dependent. It would be interesting if this is universally true for all proteins susceptible to denaturation on these particles, or if proteins exist which show denaturation, but not in a particle size dependent way. If all proteins that do show conformational change show the same pattern, regardless of the specific protein or of the interaction force between them, we might be able to construct a new theory to explain this phenomenon.

***Acknowledgment.*** This work was supported by Austrian Science Fund (FWF W1224—Doctoral Program on Biomolecular Technology of Proteins—BioToP). Some experimental and characterization work was performed at the Molecular Foundry, Lawrence Berkeley National Laboratory supported by the Office of Science, Office of Basic Energy Sciences, Scientific User Facilities Division of the U.S. Department of Energy, under Contract No. DE-AC02-05CH11231. Gerhard Sekot was financed by acib. acib is supported by the Federal Ministry of Economy, Family and Youth (BMWFJ), the Federal Ministry of Traffic, Innovation and Technology (bmvit), the Styrian Business Promotion Agency SFG, the Standortagentur Tirol and ZIT - Technology Agency of the City of Vienna through the COMET-Funding Program managed by the Austrian Research Promotion Agency FFG. We would like to thank Dr. Nico Lingg for his critical review of the manuscript. The authors have declared no conflicts of interest.

## REFERENCES

1. Dvir, T., et al., *Nanotechnological strategies for engineering complex tissues*. Nat Nano, 2011. **6**(1): p. 13-22.
2. Dobrovolskaia, M.A. and S.E. McNeil, *Immunological properties of engineered nanomaterials*. Nat Nano, 2007. **2**(8): p. 469-478.
3. Auffan, M., et al., *Towards a definition of inorganic nanoparticles from an environmental, health and safety perspective*. Nat Nano, 2009. **4**(10): p. 634-641.
4. Wang, T., et al., *Enhanced Mucosal and Systemic Immune Responses Obtained by Porous Silica Nanoparticles Used as an Oral Vaccine Adjuvant: Effect of Silica Architecture on Immunological Properties*. International Journal of Pharmaceutics, 2012. **436**(1-2): p. 351-358.
5. Hu, C.-M.J. and L. Zhang, *Nanoparticle-based Combination Therapy Toward Overcoming Drug Resistance in Cancer*. Biochemical Pharmacology, 2012. **83**(8): p. 1104-1111.
6. Huh, Y.-M., et al., *In Vivo Magnetic Resonance Detection of Cancer by Using Multifunctional Magnetic Nanocrystals*. Journal of the American Chemical Society, 2005. **127**(35): p. 12387-12391.
7. Dell'Orco, D., et al., *Delivery Success Rate of Engineered Nanoparticles in the Presence of the Protein Corona: A Systems-Level Screening*. Nanomedicine: Nanotechnology, Biology and Medicine, 2012. **8**(8): p. 1271-1281.
8. Lesniak, A., et al., *Serum Heat Inactivation Affects Protein Corona Composition and Nanoparticle Uptake*. Biomaterials, 2010. **31**(36): p. 9511-9518.
9. Natte, K., et al., *Impact of polymer shell on the formation and time evolution of nanoparticle-protein corona*. Colloids and Surfaces B: Biointerfaces, 2013. **104**(0): p. 213-220.
10. Wang, F., et al., *The biomolecular corona is retained during nanoparticle uptake and protects the cells from the damage induced by cationic nanoparticles until degraded in the lysosomes*. Nanomedicine: Nanotechnology, Biology and Medicine, (0).
11. Hata, K., et al., *Evaluation of silica nanoparticle binding to major human blood proteins*. Nanoscale Research Letters, 2014. **9**(1): p. 1-7.
12. Saptarshi, S.R., A. Duschl, and A.L. Lopata, *Interaction of nanoparticles with proteins: relation to bio-reactivity of the nanoparticle*. Journal of Nanobiotechnology, 2013. **11**: p. 26-26.
13. Walkey, C.D. and W.C. Chan, *Understanding and controlling the interaction of nanomaterials with proteins in a physiological environment*. Chem Soc Rev, 2012. **41**(7): p. 2780-99.
14. Barbucci, R. and A. Magnani, *Conformation of Human Plasma Proteins at Polymer Surfaces: The Effectiveness of Surface Heparinization*. Biomaterials, 1994. **15**(12): p. 955-962.
15. Benesch, J., et al., *Fluorescence Probe Techniques to Monitor Protein Adsorption-induced Conformation Changes on Biodegradable Polymers*. Journal of Colloid and Interface Science, 2007. **312**(2): p. 193-200.
16. Shao, Q., et al., *Graphene oxide-induced conformation changes of glucose oxidase studied by infrared spectroscopy*. Colloids and Surfaces B: Biointerfaces, 2013. **109**(0): p. 115-120.

17. Jiang, X., et al., *Effect of electrode surface microstructure on electron transfer induced conformation changes in cytochrome c monitored by in situ UV and CD spectroelectrochemistry*. *Spectrochimica Acta Part A: Molecular and Biomolecular Spectroscopy*, 2005. **61**(5): p. 943-951.
18. Ghosh, G., et al., *Counter ion induced irreversible denaturation of hen egg white lysozyme upon electrostatic interaction with iron oxide nanoparticles: A predicted model*. *Colloids and Surfaces B: Biointerfaces*, 2013. **103**(0): p. 267-274.
19. Bragdon, B., et al., *Semiconductor Nanoparticle Uptake and Toxicity Correlates with Particle Size and Core Degradation*. *Nanomedicine: Nanotechnology, Biology and Medicine*, 2006. **2**(4): p. 318.
20. Mayer, A., et al., *The Role of Nanoparticle Size in Hemocompatibility*. *Toxicology*, 2009. **258**(2-3): p. 139-147.
21. Nel, A.E., et al., *Understanding biophysicochemical interactions at the nano-bio interface*. *Nature Materials*, 2009. **8**(7): p. 543-557.
22. Lynch, I., et al., *The Nanoparticle-Protein Complex as a Biological Entity; A Complex Fluids and Surface Science Challenge for the 21st Century*. *Advances in Colloid and Interface Science*, 2007. **134-135**(0): p. 167-174.
23. Shemetov, A.A., I. Nabiev, and A. Sukhanova, *Molecular Interaction of Proteins and Peptides with Nanoparticles*. *ACS Nano*, 2012. **6**(6): p. 4585-4602.
24. Wang, Z., et al., *Adsorption and inhibition of butyrylcholinesterase by different engineered nanoparticles*. *Chemosphere*, 2010. **79**(1): p. 86-92.
25. Lacerda, S.H.D.P., et al., *Interaction of Gold Nanoparticles with Common Human Blood Proteins*. *ACS Nano*, 2009. **4**(1): p. 365-379.
26. Vertegel, A.A., R.W. Siegel, and J.S. Dordick, *Silica Nanoparticle Size Influences the Structure and Enzymatic Activity of Adsorbed Lysozyme*. *Langmuir*, 2004. **20**(16): p. 6800-6807.
27. Bellezza, F., et al., *Structure and Catalytic Behavior of Myoglobin Adsorbed onto Nanosized Hydrotalcites*. *Langmuir*, 2009. **25**(18): p. 10918-10924.
28. Fenoglio, I., et al., *Multiple Aspects of the Interaction of Biomacromolecules with Inorganic Surfaces*. *Advanced Drug Delivery Reviews*, 2011. **63**(13): p. 1186-1209.
29. Cukalevski, R., et al., *Structural Changes in Apolipoproteins Bound to Nanoparticles*. *Langmuir*, 2011. **27**(23): p. 14360-14369.
30. Raussens, V., J.-M. Ruyschaert, and E. Goormaghtigh, *Protein concentration is not an absolute prerequisite for the determination of secondary structure from circular dichroism spectra: a new scaling method*. *Analytical Biochemistry*, 2003. **319**(1): p. 114-121.
31. Louis-Jeune, C., M.A. Andrade-Navarro, and C. Perez-Iratxeta, *Prediction of protein secondary structure from circular dichroism using theoretically derived spectra*. *Proteins: Structure, Function, and Bioinformatics*, 2012. **80**(2): p. 374-381.
32. Lundqvist, M., I. Sethson, and B.-H. Jonsson, *High-Resolution 2D 1H-15N NMR Characterization of Persistent Structural Alterations of Proteins Induced by Interactions with Silica Nanoparticles*. *Langmuir*, 2005. **21**(13): p. 5974-5979.
33. Lundqvist, M., I. Sethson, and B.-H. Jonsson, *Transient Interaction with Nanoparticles "Freezes" a Protein in an Ensemble of Metastable Near-Native Conformations†*. *Biochemistry*, 2005. **44**(30): p. 10093-10099.

34. Lundqvist, M., I. Sethson, and B.-H. Jonsson, *Protein Adsorption onto Silica Nanoparticles: Conformational Changes Depend on the Particles' Curvature and the Protein Stability*. *Langmuir*, 2004. **20**(24): p. 10639-10647.
35. Lundqvist, M., et al., *Nanoparticle size and surface properties determine the protein corona with possible implications for biological impacts*. *Proceedings of the National Academy of Sciences*, 2008. **105**(38): p. 14265-14270.
36. Caroline, L.-J., A.-N. A., and Perez-IratxetaCarol, *Prediction of protein secondary structure from circular dichroism using theoretically derived spectra*. 2011.
37. Gu, Z., et al., *Surface Curvature Relation to Protein Adsorption for Carbon-based Nanomaterials*. *Scientific Reports*, 2015. **5**: p. 10886.

## Supporting Information

### *Protein adsorption onto nanoparticles induces conformational changes: Particle size dependency, kinetics and mechanisms*

Peter Satzer,<sup>a</sup> Frantisek Svec,<sup>b</sup> Gerhard Sekot,<sup>c</sup> and Alois Jungbauer <sup>a,c \*</sup>

<sup>a</sup> Department of Biotechnology, University of Natural Resources and Life Sciences Vienna

(BOKU), Muthgasse 18, 1190 Vienna, Austria, <sup>b</sup> Lawrence Berkeley National Laboratory, The

Molecular Foundry, Berkeley, CA 94720, USA, <sup>c</sup> Austrian Centre of Industrial Biotechnology

(ACIB), Muthgasse 18, 1190 Vienna, Austria

\* Address correspondence to

[alois.jungbauer@boku.ac.at](mailto:alois.jungbauer@boku.ac.at)

Muthgasse 18, 1190 Vienna

Telephone: +43476546226

Fax: +43476546677

## Relevant publications dealing with denaturation of proteins upon adsorption to nanoparticles – Supporting Information Table S1

List of some relevant publications for the topic of particle size dependent denaturation of proteins upon adsorption and if they indicated size dependency and/or conformational change.

Type	Dimension	Protein	Material	Conformational Change?	Size dependency	Group	Methods	Reference
Particle	9 nm	Lysozyme	Silica	Yes	ND	1998, Tian	Circular dichroism	[1]
Particle	5-100 nm	Histone, albumin, insulin, globulin, fibrinogen	Gold	Yes	Yes	2009, Lacerda	Circular dichroism, Fluorescence	[2]
Particle	25 nm	Apolipoprotein, HDL, HAS	Polystyrene	Yes	ND	2011, Cukalevski	Circular dichroism, Fluorescence, Limited proteolysis	[3]
Crystal	unknown	Myoglobine	Hydrotalcite (NiAl)	Yes	Yes	2009, Bellezza	FT-IR, Fluorescence, Raman, Activity	[4]
Particle	100-200 nm	Lysozyme	Polystyrene +polylactic acid	ND	ND	2008, Cai	TEM, SEM, AFM, DSC	[5]
Particle	20, 30 nm	butyrylcholinesterase	Silica	Yes	Yes	2010, Wang	Activity	[6]
Particle	10-60 nm	butyrylcholinesterase	Metal	Yes	Yes	2010, Wang	Activity	[6]
Particle	60-600 nm	Blood plasma proteins	Polystyrene	ND	Yes	1998, Lück	2D-DIGE	[7]
Particle	90 nm	Beta-lactoglobulin	Silica	Yes	ND	2008, Wu	Fluorescence, FTIR, CD	[8]
Surface	-	Human carbonic anhydrase II	Functionalized thiols	Yes	ND	2005, Karlsson	Surface plasmon resonance	[9]
Particle	35, 120, 140 nm	Blood plasma proteins	Silica	ND	Yes	2013, Tenzer	SDS-PAGE,	[10]
Particle	4, 15 nm	Ribonuclease A	Silica	Yes	Yes	2007, Shang	Circular Dichroism	[11]
Particle	4, 20, 100 nm	Lysozyme	Silica	Yes	Yes	2004, Vertegel	Circular Dichroism, Activity	[12]
Particle	4, 15 nm	Acylphosphatase	Silica	Yes	Yes	2013, Shrivastava	Activity, Circular dichroism, NMR	[13]
Particle	6, 9, 15 nm	Human carbonic anhydrase I and II	Silica	Yes	Yes	2004, Lundqvist	Circular dichroism, NMR	[14]
Particle	9 nm	Human carbonic anhydrase II	Silica	Yes	ND	1997, Billsten	Circular dichroism, Fluorescence	[15]
Particle	9 nm	Human carbonic anhydrase I	Silica	Yes	ND	2005, Lundqvist	NMR	[16]
Particle	6, 9 nm	Human carbonic anhydrase I and II	Silica	Yes	No	2005, Lundqvist	NMR	[17]
Particle	6 nm	Chymotrypsin	Functionalized gold	Yes	ND	2002, Fischer	Circular dichroism, Activity	[18]
Particle	9 nm	Lysozyme	Silica	Yes	ND	1999, Bower	Circular dichroism, Activity	[19]
Particle	4.5 nm	Human carbonic anhydrase XII	Quantum dot	Yes	ND	2010, Manokaran	Fluorescence, Activity	[20]
Particle	<50nm	Bovine serum albumin	Al <sub>2</sub> O <sub>3</sub>	Yes	ND	2014, Rajeshwari	FT-IR, Circular dichroism, Fluorescence, UV-VIS	[21]
Particle	15, 260nm	TNF- $\alpha$ , IL-8	Carbon black	ND	Yes	2010, Brown	Cellular uptake	[22]
Particle	10 kDa	Lysozyme, IgG	Fullerol	Yes	ND	2014, Chen	Circular Dichroism, Fluorescence, DSC	[23]
Particle	8, 45 nm	Plants	Silver	ND	Yes	2014, Syu	Plant growth	[24]
Particle	30. 200. 400 nm	Blood plasma proteins	Fe <sub>3</sub> O <sub>4</sub>	ND	Yes	2014, Hu	2D DIGE	[25]
Particle	5-50	Ovalbumin	Silver	Yes	ND	2014, Joshi	UV-VIS, Raman Spectroscopy	[26]
Particle	20, 40, 80 nm	Tetanus Oxois	Gold	Yes	Yes	2014, Barhate	Circular Dichroism, Thermodynamic studies	[27]

## Protein Characteristics - Supporting Information Table S2 and Table S3

In our study we investigated 9 model proteins, which are presented in supporting information Table S2. We used a variety of different model proteins to cover a wide range of different protein characteristics, namely size ranging from 11 kDa to 160 kDa, a pI ranging from 4.2 to 11.0 and different stabilities represented by different melting temperatures ranging from 44 °C to 85 °C. Two of this model proteins did not show significant binding: chymotrypsin and glucose oxidase and so they were excluded from further studies. All other proteins were investigated for their structural composition (supporting information Table S3).

**Table S2 – List of Proteins Used in this Study and their Characteristics**

<b>Protein</b>	<b>MW, kDa<sup>a</sup></b>	<b>pI<sup>b</sup></b>	<b>T<sub>m</sub>, °C<sup>c</sup></b>	<b>binds to 70 nm nanoparticles</b>
lysozyme	11	11.0	73	Yes
cytochrome c	12	10.3	85	Yes
ribonuclease A	13	9.6	64	Yes
myoglobin	17	6.8	80	Yes
β casein	25	4.7	70	Yes
ovalbumin	42	4.7	84	Yes
bovine serum albumin	66	4.7	62	Yes
chymotrypsin	25	8.7	44	No
glucose oxidase	160	4.2	56	No

<sup>a</sup> Molecular weight of the protein, <sup>b</sup> Isoelectric point, <sup>c</sup> Melting point representing thermal stability.

**Table S3 – Structural Composition of Proteins Determined by Circular Dichroism and concentration independent Structure Prediction**

<b>Protein</b>	<b>content of structures, %</b>		
	<b>α-helical</b>	<b>β-sheet</b>	<b>random-coil</b>
lysozyme	32.6 +/- 0.5 %	13.8 +/- 0.5 %	34.1 +/- 0.1 %
cytochrome c	28.2 +/- 0.4 %	15.5 +/- 0.6 %	33.2 +/- 0.1 %
ribonuclease a	17.6 +/- 0.3 %	25.9 +/- 0.5 %	36.2 +/- 0.1 %
myoglobin	55.2 +/- 0.9 %	4.2 +/- 0.2 %	26.9 +/- 0.1 %
β casein	7.1 +/- 0.4 %	31.8 +/- 0.4 %	41.2 +/- 0.1 %
ovalbumin	42.9 +/- 1.0 %	13.9 +/- 0.4 %	29.3 +/- 0.2 %
bovine serum albumin	42.3 +/- 0.3 %	12.01 +/- 0.2 %	30.6 +/- 0.2 %

## CD Measurement Raw Data - Supporting Information Figure S1

Using our method of compiling 10 individual CD spectra to one spectra before using it for structure determinations we were able to obtain high quality CD spectra despite the unavoidable fact of signal loss due to the particles in solution. Figure S1 shows such a spectra from BSA bound 200 nm particles. We can see that using 10 individual measurements condensed to one for further investigation results in good quality spectra without additional smoothing of the spectra.

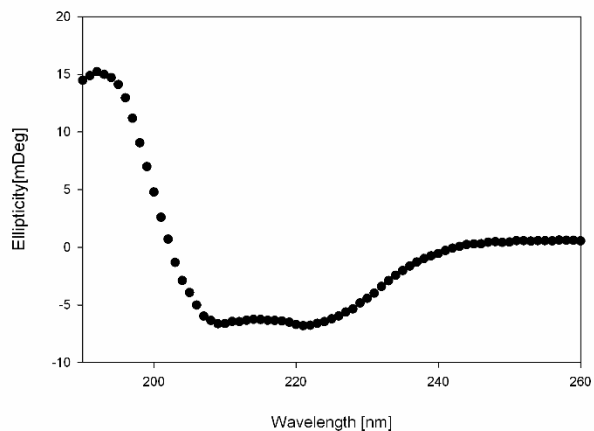


**Figure S1 CD-spectra of BSA adsorbed onto 200 nm silica nanoparticles.**

## Protein Adsorption to Nanoparticles - Supporting Information Figure S2 and Figure S3

From the model proteins we investigated, 3 did not show any significant change in secondary structure upon adsorption to nanoparticles (supporting information Figure S2), namely beta casein, lysozyme and ribonuclease A. These 3 proteins were not further studied. For 2 model proteins we saw a trend in the data (supporting information Figure S3) but the standard deviations from the measurements are too big to draw a final conclusion about whether there is a change in structure or not.

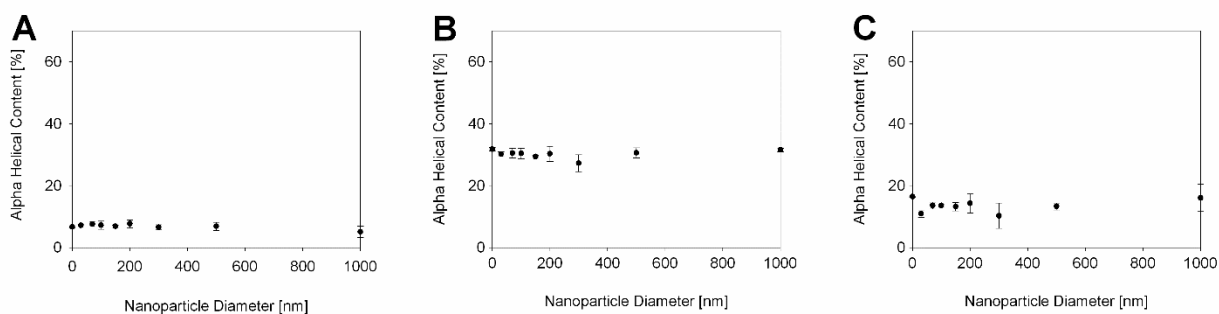


**Figure S2**  $\alpha$ -Helical content of  $\beta$  casein (A), lysozyme (B) and ribonuclease A (C) adsorbed on nanoparticles varying in sizes. The point at 0 nm nanoparticle diameter is the structure of the protein in solution with no nanoparticles. 10 individual spectra were condensed into one before structure determination. 3 of such sets were used to calculate standard deviations shown in the error bars of the figure.

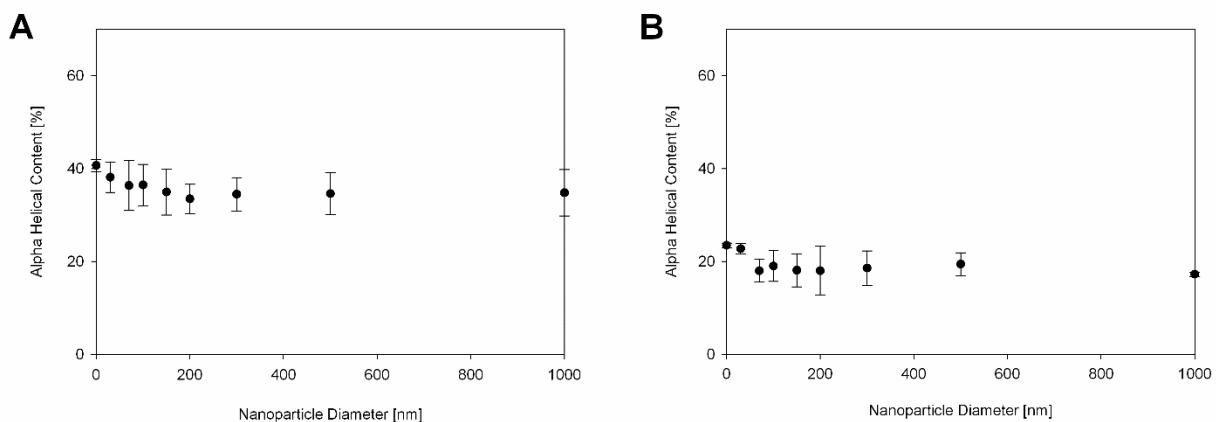


**Figure S3.**  $\alpha$ -Helical content of ovalbumin (A) and cytochrome C (B) adsorbed on nanoparticles varying in sizes. The point at 0 nm nanoparticle diameter is the structure of the protein in solution with no nanoparticles. 10 individual spectra were condensed into one before structure determination. 3 of such sets were used to calculate standard deviations shown in the error bars of the figure.

## Adsorption Isotherms of all Particle Sizes for Myoglobine and BSA. Supporting Information Figure S4

We determined the adsorption isotherms for all particles by simple adsorption experiments done in triplicates, curves of 30, 100, 300 and 1000 nm are shown (Figure S4). This curves were only used for determining the protein amount on the particle.

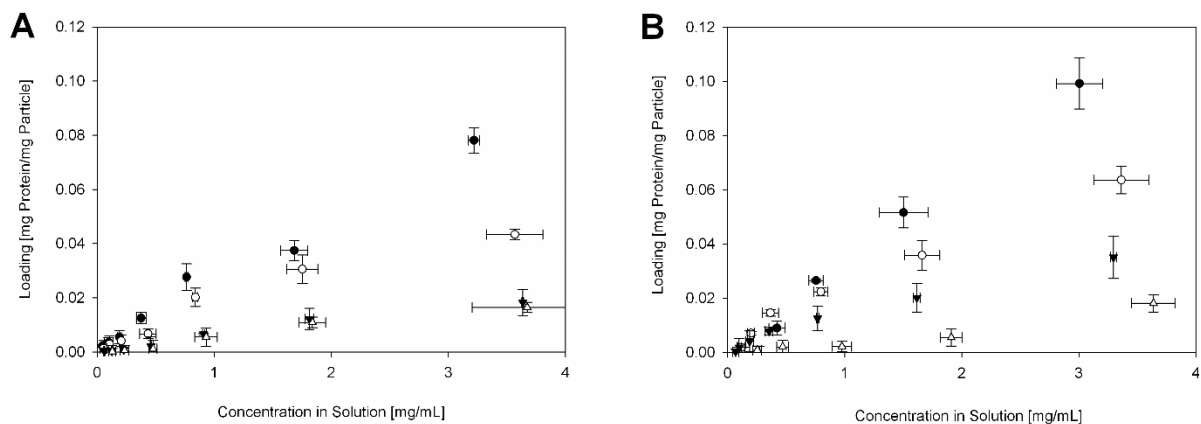


**Figure S4 Adsorption isotherms of myoglobin (A) and bovine serum albumin (B) on 30 (●), 100 (○), 300 (▼) and 1000 nm (△) silica nanoparticles. We present mean values and standard deviations from three independent measurements.**

## Determination of available surface for interaction between protein and nanoparticle – Supporting information Figure S5

For evaluation of the curvature based theory we calculated the cross-section available for interaction between protein and nanoparticle using an interaction cutoff of 0.4 nm, a usual penetration length of electrostatic forces in buffered solutions. We calculated this cross-section for differently sized nanoparticles and two different sizes of proteins, 2 nm and 4 nm sized spherical proteins. Equations (1) to (3) allow the calculation of the radius of the interaction area  $r$  which directly gives the interaction area using  $A = \pi r^2$ .

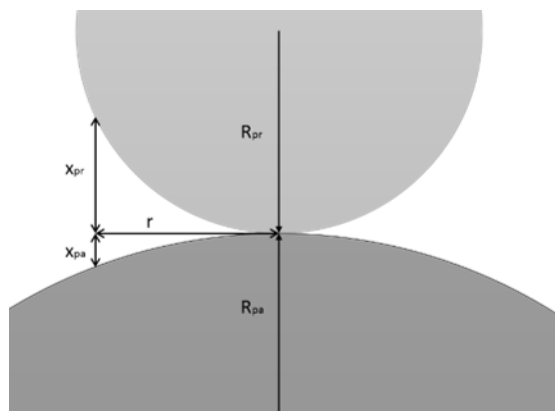


**Figure S5a – Graphical representation of two touching spheres and the important system defining lengths used in Equation (1) to (3) to calculate the radius of the interaction area.**

$$x_{pa} + x_{pr} = 0.4 \quad (1)$$

$$R_{pa}^2 = r^2 + (R_{pa} - x_{pa})^2 \quad (2)$$

$$R_{pr}^2 = r^2 + (R_{pr} - x_{pr})^2 \quad (3)$$

The calculations were done with an interaction range of 0.1 nm, 0.4 nm (as shown in the equations) and 0.8 nm (Figure S5b Panel A-C). The different interaction ranges do not show any significant impact on the shape of the curve.

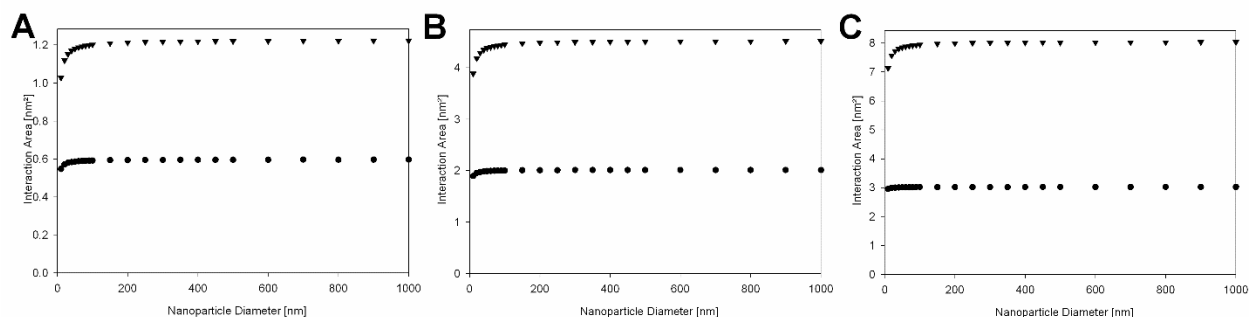


**Figure S5b – Interaction area of two touching spheres with an interaction range of 0.1 nm (Panel A), 0.4 nm (Panel B) and 0.8 nm (Panel C) calculated by the equations (1) to (4).**

### **Determination of surface curvature as seen by a protein sitting on top of a nanoparticle – Supporting information Figure S6**

A second method for determining the curvature seen by the protein adsorbed to the nanoparticle is to calculate the angle at which the protein would have to bend to accommodate the surface presented to the protein. We calculated this angle for small and large proteins (2 nm and 4 nm) size as depicted in Figure S2 and the corresponding Equations (4) to (5).

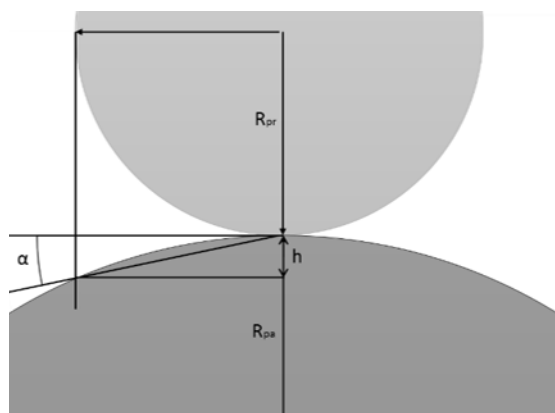


**Figure S6 – Graphical representation of two touching spheres and the important system defining lengths used in Equation (4) to (5) to calculate the angle at which the protein would have to bend to accommodate the surface.**

$$R_{pa} = \frac{4h^2 + (2R_{pr})^2}{8h} \quad (4)$$

$$\tan \alpha = \frac{h}{R_{pr}} \quad (5)$$

## References

1. Tian, M., et al., *Structural Stability Effects on Adsorption of Bacteriophage T4 Lysozyme to Colloidal Silica*. Journal of Colloid and Interface Science, 1998. **200**(1): p. 146-154.
2. Lacerda, S.H.D.P., et al., *Interaction of Gold Nanoparticles with Common Human Blood Proteins*. ACS Nano, 2009. **4**(1): p. 365-379.
3. Cukalevski, R., et al., *Structural Changes in Apolipoproteins Bound to Nanoparticles*. Langmuir, 2011. **27**(23): p. 14360-14369.
4. Bellezza, F., et al., *Structure and Catalytic Behavior of Myoglobin Adsorbed onto Nanosized Hydroxalrites*. Langmuir, 2009. **25**(18): p. 10918-10924.
5. Cai, C., et al., *Charged Nanoparticles as Protein Delivery Systems: A Feasibility Study Using Lysozyme as Model Protein*. European Journal of Pharmaceutics and Biopharmaceutics, 2008. **69**(1): p. 31-42.
6. Wang, Z., et al., *Adsorption and inhibition of butyrylcholinesterase by different engineered nanoparticles*. Chemosphere, 2010. **79**(1): p. 86-92.
7. Lück, M., et al., *Analysis of Plasma Protein Adsorption on Polymeric Nanoparticles with Different Surface Characteristics*. Journal of Biomedical Materials Research, 1998. **39**(3): p. 478-485.
8. Wu, X. and G. Narsimhan, *Characterization of Secondary and Tertiary Conformational Changes of  $\beta$ -Lactoglobulin Adsorbed on Silica Nanoparticle Surfaces*. Langmuir, 2008. **24**(9): p. 4989-4998.
9. Karlsson, M., et al., *Reduction of Irreversible Protein Adsorption on Solid Surfaces by Protein Engineering for Increased Stability*. Journal of Biological Chemistry, 2005. **280**(27): p. 25558-25564.
10. Tenzer, S., et al., *Rapid formation of plasma protein corona critically affects nanoparticle pathophysiology*. Nat Nano, 2013. **8**(10): p. 772-781.
11. Shang, W., et al., *Unfolding of Ribonuclease A on Silica Nanoparticle Surfaces*. Nano Letters, 2007. **7**(7): p. 1991-1995.
12. Vertegel, A.A., R.W. Siegel, and J.S. Dordick, *Silica Nanoparticle Size Influences the Structure and Enzymatic Activity of Adsorbed Lysozyme*. Langmuir, 2004. **20**(16): p. 6800-6807.
13. Shrivastava, S., et al., *Identifying Specific Protein Residues That Guide Surface Interactions and Orientation on Silica Nanoparticles*. Langmuir, 2013. **29**(34): p. 10841-10849.
14. Lundqvist, M., I. Sethson, and B.-H. Jonsson, *Protein Adsorption onto Silica Nanoparticles: Conformational Changes Depend on the Particles' Curvature and the Protein Stability*. Langmuir, 2004. **20**(24): p. 10639-10647.
15. Billsten, P., et al., *Adsorption to silica nanoparticles of human carbonic anhydrase II and truncated forms induce a molten-globule-like structure*. FEBS Letters, 1997. **402**(1): p. 67-72.
16. Lundqvist, M., I. Sethson, and B.-H. Jonsson, *Transient Interaction with Nanoparticles "Freezes" a Protein in an Ensemble of Metastable Near-Native Conformations<sup>†</sup>*. Biochemistry, 2005. **44**(30): p. 10093-10099.
17. Lundqvist, M., I. Sethson, and B.-H. Jonsson, *High-Resolution 2D 1H-15N NMR Characterization of Persistent Structural Alterations of Proteins Induced by Interactions with Silica Nanoparticles*. Langmuir, 2005. **21**(13): p. 5974-5979.
18. Fischer, N.O., et al., *Inhibition of Chymotrypsin through Surface Binding Using Nanoparticle-based Receptors*. Proceedings of the National Academy of Sciences, 2002. **99**(8): p. 5018-5023.
19. Bower, C.K., et al., *Activity losses among T4 lysozyme charge variants after adsorption to colloidal silica*. Biotechnology and Bioengineering, 1999. **64**(3): p. 373-376.

20. Manokaran, S., et al., *Differential modulation of the active site environment of human carbonic anhydrase XII by cationic quantum dots and polylysine*. *Biochimica et Biophysica Acta (BBA) - Proteins and Proteomics*, 2010. **1804**(6): p. 1376-1384.
21. Rajeshwari, A., et al., *Spectroscopic studies on the interaction of bovine serum albumin with Al<sub>2</sub>O<sub>3</sub> nanoparticles*. *Journal of Luminescence*, 2014. **145**(0): p. 859-865.
22. Brown, D.M., et al., *Interaction between nanoparticles and cytokine proteins: impact on protein and particle functionality*. *Nanotechnology*, 2010. **21**(21): p. 215104-215112.
23. Chen, P., et al., *Contrasting effects of nanoparticle binding on protein denaturation*. *Journal of Physical Chemistry C*, 2014. **118**(38): p. 22069-22078.
24. Syu, Y.Y., et al., *Impacts of size and shape of silver nanoparticles on Arabidopsis plant growth and gene expression*. *Plant Physiology and Biochemistry*, 2014. **83**: p. 57-64.
25. Hu, Z., et al., *Nanoparticle size matters in the formation of plasma protein coronas on Fe<sub>3</sub>O<sub>4</sub> nanoparticles*. *Colloids and Surfaces B: Biointerfaces*, 2014. **121**: p. 354-361.
26. Joshi, D. and R.K. Soni, *Laser-induced synthesis of silver nanoparticles and their conjugation with protein*. *Applied Physics A: Materials Science and Processing*, 2014. **116**(2): p. 635-641.
27. Barhate, G.A., et al., *Structure function attributes of gold nanoparticle vaccine association: Effect of particle size and association temperature*. *International Journal of Pharmaceutics*, 2014. **471**(1-2): p. 439-448.